Title

From legacy contamination to watershed systems science: a review of scientific insights and technologies developed through DOE-supported research in water and energy security

Journal

Environmental Research Letters, 17(4)

ISSN

1748-9318

Authors

Dwivedi, Dipankar
Steefel, Carl I
Arora, Bhavna
et al.

Publication Date

2022-04-01

DOI

10.1088/1748-9326/ac59a9

Peer reviewed

ENVIRONMENTAL RESEARCH
LETTERS

ACCEPTED MANUSCRIPT • OPEN ACCESS

From legacy contamination to watershed systems science: a review of scientific insights and technologies developed through DOE-supported research in water and energy security

To cite this article before publication: Dipankar Dwivedi *et al* 2022 *Environ. Res. Lett.* in press https://doi.org/10.1088/1748-9326/ac59a9

From Legacy Contamination to Watershed Systems Science: A Review of Scientific Insights and Technologies Developed through DOE-Supported Research in Water and Energy Security

Dipankar Dwivedi[1], Carl I. Steefel[1], Bhavna Arora[1], Jill Banfield[2], John Bargar[3], Maxim I. Boyanov[4], Scott C. Brooks[5], Xingyuan Chen[6], Susan S. Hubbard[1], Dan Kaplan[7], Kenneth M. Kemner[4], Peter S. Nico[1], Edward J. O'Loughlin[4], Eric M. Pierce[5], Scott L. Painter[5], Timothy D. Scheibe[6], Haruko M. Wainwright[1], Kenneth H. Williams[1], and Mavrik Zavarin[8]

[1]Lawrence Berkeley National Laboratory, [2]University of California, Berkeley, [3]SLAC National Accelerator Laboratory, [4]Argonne National Laboratory, [5]Oak Ridge National Laboratory, [6]Pacific Northwest National Laboratory, [7]Savannah River Ecology Laboratory, [8]Lawrence Livermore National Laboratory

Abstract

Water resources, including groundwater and prominent rivers worldwide, are under duress because of excessive contaminant and nutrient loads. To help mitigate this problem, the United States Department of Energy (DOE) has supported research since the late 1980s to improve our fundamental knowledge of processes that could be used to help clean up challenging subsurface problems. Problems of interest have included subsurface radioactive waste, heavy metals, and metalloids (e.g., uranium, mercury, arsenic). Research efforts have provided insights into detailed groundwater biogeochemical process coupling and the resulting geochemical exports of metals and nutrients to surrounding environments. Recently, an increased focus has been placed on constraining the exchanges and fates of carbon and nitrogen within and across bedrock to canopy compartments of a watershed and in river–floodplain settings, because of their important role in driving biogeochemical interactions with contaminants and the potential of increased fluxes under changing precipitation regimes, including extreme events. While reviewing the extensive research that has been conducted at DOE's representative sites and testbeds (such as the Oyster Site in Virginia, Savannah River Site in South Carolina, Oak Ridge Reservation in Tennessee, Hanford in Washington, Nevada National Security in Nevada, Riverton in Wyoming, and Rifle and East River in Colorado), this review paper explores the nature and distribution of contaminants in the surface and shallow subsurface (i.e., the critical zone) and their interactions with carbon and nitrogen dynamics. We also describe state-of-the-art, scale-aware characterization approaches and models developed to predict contaminant fate and transport. The models take advantage of DOE leadership-class high-performance computers and

are beginning to incorporate artificial intelligence approaches to tackle the extreme diversity of hydro-biogeochemical processes and measurements. Recognizing that the insights and capability developments are potentially transferable to many other sites, we also explore the scientific implications of these advances and recommend future research directions.

Keywords: DOE Science; subsurface; contaminant; groundwater; critical zone; reactive transport models; redox; hot spots and hot moments

1 Introduction

Water security is critical for food and energy production, economic development, and national security. Yet water security is under severe duress globally because of climate change, growing population, and human activities (Alley et al., 2002; Heathwaite, 2010; Famiglietti, 2014; Rodell et al., 2009). A recent study projected that more than 65% of the human population ($\sim$ 5 billion people) live in water-insecure regions (Vörösmarty et al., 2010). Exacerbating the problem, the demand for freshwater ($<$ 3% of all water on Earth) is increasing, challenging our ability to meet food and energy needs globally. Although future technologies may allow us to increase clean water supplies, it is imperative to protect the available freshwater resources from numerous threats, such as a range of chemicals, including metals, metalloids, radionuclides, and nutrients that reduce usable supply.

Increasing contamination of freshwater poses a serious problem to both surface water and groundwater (e.g., Brender et al., 2013; Dwivedi et al., 2013, 2016b; Varol and Şen, 2012), particularly because most of the world's prominent rivers, supporting several million people, are under threat and experiencing contamination from a variety of chemicals, including uranium (U), chromium (Cr), arsenic (As) and excessive amounts of nutrients (e.g., Tripathi et al., 2016; Brown and Halweil, 1998; Lu et al., 2018; Paddison, 2016; Dodds, 2006; Gross, 2017). To understand the behavior and reactivity of a plethora of contaminants and nutrients, the United State Department of Energy (DOE) has funded extensive research across several sites in the United States of America (USA) for several decades now (`https://www.energy.gov/`). Below, we provide how scientific progress has evolved through these efforts (Figure 1).

The DOE's mission is "to ensure America's security and prosperity by addressing its energy, environmental and nuclear challenges through transformative science and technology solutions." The DOE was created in 1977, succeeding various energy-related programs previously dispersed throughout various federal agencies, including the Manhattan Project effort to develop the atomic bomb during World War II. Over fifty years of nuclear weapons production, testing, and energy research generated a vast volume of legacy contamination and created contaminated soil and water across the USA. The DOE has supported research and cleanup associated with several challenging subsurface problems since the late 1980s, such as treating radioactive waste (e.g., U, plutonium (Pu)) and heavy metals and metalloids (e.g., Cr, mercury (Hg), As) in the subsurface. Notably, since its inception in 1989, the DOE's Environmental Management (EM) and Environmental Remediation (ER) programs have been responsible for the restoration of as many as 107 sites across the country—an area equal to Rhode Island and Delaware combined (Figure 2). Within the DOE's Office of Science, the Biological and Environmental Research (BER) program has led the fundamental science research associated with water and energy security at the watershed, continental, and global scales through various projects and programs. The DOE-BER, its predecessors, and other related programs have significantly contributed to the progress of environmental sciences, setting the stage for this paper's thematic organization (Figure 1).

Next, we briefly describe the history of various DOE programs that have supported water-security-research. The DOE-BER pioneered genomics, system biology, and biotechnology research through the Human Genome Project in 1986. In the late eighties, the Subsurface Science program initiated biological and co-contaminant geochemistry research through its deep microbiology and later bacterial transport projects. The Natural

and Accelerated BIoRemediation (NABIR) program subsequently pioneered the "bio" part of biogeochemistry (e.g., metal-reducing bacteria, in-silico modeling). The Subsurface Biogeochemical Research (SBR) program then continued that linkage, emphasizing the interplay between transport and biogeochemistry. Within the DOE's Office of Science, the Advanced Scientific Computing Research (ASCR) brings together researchers from various fields to tackle some of the most challenging scientific problems, leveraging DOE's leadership-class supercomputers and developing high-end computational science. In the environmental sciences, the ASCR's Scientific Discovery Through Advanced Computing (SciDAC) program has boosted subsurface research like multiscale science and reactive transport modeling. We use "DOE research" and "DOE-supported science" interchangeably to broadly reflect scientific advances pioneered through BER–SBR, their predecessors, and other related programs (e.g., EM, ASCR). This review paper follows the evolution of DOE research in this context, focusing primarily on the subsurface environmental sciences from the nineties to recent times.

Research efforts during the 1990s and early 2000s led to significant developments in our understanding of microbial communities, metals geochemistry, and co-contaminant interactions. These included the development of novel techniques for sampling and cultivating subsurface microbial communities (Ghiorse and Wobber, 1989; Phelps et al., 1989), identification of colloids as an important mechanism for mobilizing low solubility metals and radionuclides (e.g., Kersting et al., 1999; Santschi et al., 2002; Suzuki et al., 2002), understanding of the influence of natural organic matter (NOM) on metal speciation and sorption on mineral surfaces (Gu et al., 1994, 1995), application of synchrotron-based x-ray absorption spectroscopies to elucidate the nature of metal and organic matter complexes on mineral surfaces (e.g., Bargar et al., 2000) and bacterial cells (Kelly et al., 2002; Boyanov et al., 2003), computational approaches to understanding the fundamental properties of natural minerals as metal sorbents (e.g., Felmy and Rustad, 1998; Steefel et al., 2003; Zachara et al., 1995), examination of microbial impacts on metal immobilization (e.g., Fredrickson et al., 2000; Labrenz et al., 2000; Kemner et al., 2004), and implementation of mechanistic processes in reactive transport codes to simulate transport behavior (e.g., Steefel et al., 2005).

At the same time, it was realized that natural and accelerated bioremediation held great potential for solving a wide spectrum of contamination problems (Lovley and Phillips, 1992). These research efforts led to significant advances in natural and active stabilization of metals in the subsurface (Lovley, 2003; Bender et al., 2000). Coupled hydrological and biogeochemical processes such as reactive, colloidal, and advective–dispersive transport were investigated within the view of biological availability, transformation, and movement of radionuclides and metals (Wang et al., 2003). Some notable examples include the abiotic (O'Loughlin et al., 2003a) and microbially mediated reductive precipitation and stabilization of U, iron (Fe) reduction, Pu surface-mediated reduction (Powell et al., 2005), and the influence of NOM (McCarthy et al., 1998), and other competing processes that can limit metal immobilization in the subsurface (Brooks et al., 2003). Subsequent studies (e.g., Tokunaga et al., 2008; Wan et al., 2005; Zheng et al., 2003) questioned whether the microbially mediated redox changes resulting in radionuclide immobilization were sustainable.

Motivated by the potential of natural and accelerated bioremediation as an effective cleanup strategy for DOE, the Oyster Virginia Subsurface Bacterial Transport Project was initiated in 1999 as the first large, team-based, multidisciplinary, multi-institutional, DOE-supported scientific project that was specifically tied to a field research testbed.

Through iterative integration of information gained through lab experiments, field characterization, field experiments, and numerical modeling associated with the seminal South Oyster Site, the project greatly advanced a predictive understanding of bacterial transport in physically, chemically, and biologically heterogeneous aquifers. The project led to several scientific firsts, including the first:

(a) Estimation of shallow subsurface moisture content (Hubbard et al., 2001), hydraulic conductivity (Hubbard et al., 2001), and Fe geochemistry (Chen et al., 2004) using high-resolution geophysical data,

(b) Use of geophysically-obtained estimates, field experimental datasets, and numerical models to document how even mild heterogeneity influenced transport (Scheibe et al., 2006; Hubbard et al., 2001),

(c) Documentation of scale effects and relative controls of physical and geochemical heterogeneity on bacterial transport using numerical models (Scheibe et al., 2006; Scheibe and Chien, 2003), and

(d) Development of new methods for microbial enumeration and strain selection (DeFlaun et al., 2001; Fuller et al., 2000; Johnson et al., 2001) and new insights regarding microbial attachment and transport (Dong et al., 2002a,b; Mailloux et al., 2003).

As summarized by Scheibe et al. (2011), not only has the body of literature resulting from the Oyster Site research been widely cited, but the project has served as a model for subsequent DOE-supported team-based research using data from highly-instrumented field testbeds with model-guided experimental design (Scheibe et al., 2001). Many such representative DOE sites and testbeds are described below (Section 3), together with advanced characterization and simulation modeling approaches to advance predictive understanding of complex hydro-biogeochemical phenomena and water security research.

In the late 2000s, much emphasis was placed on linking the interplay between transport and biogeochemistry (e.g., diffusion-limited mass transfer, kinetic sorption-desorption). Indeed, this was the time when a paradigm shift ensued in multiscale, multiphysics science, and reactive transport modeling (e.g., Steefel et al., 2005; White and Oostrom, 2000, 2003; Pruess, 2004; Hammond et al., 2007). These advances subsequently paved the way for fully exploiting the DOE's unique computational capabilities in high-performance computing. In unison, subsurface environmental simulation capabilities were enhanced by explicitly representing multiphase, multicomponent process dynamics, and by code parallelization.

Up until the past decade, the investigations of small-scale (molecular to millimeter) processes had been a primary focus. This small-scale process understanding was used to upscale and predict behavior at the field scale by deriving scaling laws and mathematical models. Although this reductionist (bottom-up) approach was remarkable in advancing basic research, it was inadequate for addressing scaling behavior in the presence of a range of complex as well as coupled processes, nonlinearity, and a wide range of landscape heterogeneity. Consequently, large uncertainties existed in predictions that lacked a holistic, unifying approach to capture large-scale responses. There was a need to link small-scale process understanding with the larger-scale responses systematically (i.e., treating several ecosystem subsystems, components, and compartments, from the bedrock to the canopy, as a complex system). This perspective aims to comprehensively couple and model key

processes across the critical zone (National Research Council, 2001), and to link these processes to deep hydrological flow paths and atmospheric circulation systems.

To address this need, at the beginning of the last decade, researchers associated with DOE fate and transport challenges recommended new approaches that melded select strengths of mechanistic, bottom-up approaches that were prevalent at the time with top-down approaches, with an aim to improve characterization and prediction of complex hydro-biogeochemical behavior across scales (DOE-Complexity, 2009). New emphasis was placed on actively linking sub-compartments of the Earth system, including atmospheric and biospheric processes, from the bedrock to the canopy. Multiple aspects of the system, such as hydrologic and carbon (C) cycles as well as microbiological and geochemical processes, were explicitly represented, linked, and allowed to interact with each other. This approach encouraged researchers to recognize scale transitions in a hierarchical subsurface system, link local and regional chemical fluxes, and investigate collective system behavior.

Subsequently, a more holistic system science approach evolved through active contaminant remediation-type studies. The system science approach tackles questions such as how watersheds respond to changes over the long term (e.g., Hubbard et al., 2018). These include developing insights into the surface–subsurface hydrology; groundwater–surface water interactions; C, nutrient, and trace element transformations; ecosystem disturbances and resilience; impacts on earth systems, Earth System Models development, and pioneering interdisciplinary community science (e.g., Hubbard et al., 2020; Stegen and Goldman, 2018; Arora et al., 2019b).

Here we summarize the important findings developed from several decades of research work at DOE sites that have contributed to our understanding of contaminants and nutrient cycling and their transport in the environment. These DOE sites have been heavily tracked, monitored, and investigated for legacy contamination and have subsequently served as testbeds for exploring the exchange of materials between terrestrial and aquatic ecosystems—and how this exchange influences element export at river-basin scales. Therefore, these sites and their associated scientific discoveries provide an opportunity for us to review the nature and distribution of legacy contamination and their coupled interactions with C, nitrogen (N), and sulfur (S) dynamics, as well as the timescales of biogeochemical exports. Finally, with this article, we expect to raise awareness of the water-security problems arising from the dispersal of a range of chemicals in the environment and to provide a rich body of literature to address these problems.

2 An Outline of DOE-Supported Science

A central focus of the DOE-supported science has been identifying the dominant biogeochemical processes controlling the migration of metals and radionuclides in the environment. Given the interrelationships between metals' behaviors and the presence of other elements (e.g., C, N, Fe, S), investigations into the geochemistry of metals and radionuclides have necessarily evolved to include detailed studies into the behavior of a broader range of elements that impact water quality (e.g., C, N). In the past decade, detailed mechanistic studies of metals geochemistry have included both laboratory and field investigations. Particular focus was initially placed on elements such as U (e.g., Rifle, Hanford, Oak Ridge), Hg (e.g., Oak Ridge), Pu (e.g., Savannah River Site, Nevada National Security Site), and metal co-contaminants (e.g., Rifle, Hanford), which later expanded to a broader set of biogeochemically complex elements, such as C and N, that are relevant to the ecosystem's health and water security at a national scale. Although it is

not possible to capture all the scientific progress made at the DOE offices and associated sites in the past several decades, our goal is to provide a broad understanding from all the contaminated sites in the past that lead to current ecosystem science.

We first describe the salient features of the DOE's representative sites used to achieve important successes in subsurface environmental sciences over the past two decades in Section 3. Section 4 chronicles scientific progress in subsurface microbiology, geochemistry and biogeochemistry, and hydro-biogeochemistry over the past two decades. We primarily discuss the water security issues concerning the fate and transport of legacy contaminants, critical elements, and nutrients at representative DOE sites.

We then describe the capability development achieved while making many scientific advancements in Section 5. We choose Hg as a use case to describe watershed biogeochemical processes holistically in Section 6. Hg is emblematic in its complexity, unique to DOE challenges, and is particularly sensitive to extreme events that are increasingly expected in the future.

Then Section 7 briefly reviews a few constructs such as multiscale, multiphysics, hybrid modeling approaches, hot spots and hot moments (HSHMs), and functional zonation that evolved over the years to transfer knowledge across sites. We then review legacy contamination and their coupled interactions with C, N, and S dynamics in the backdrop of the HSHM construct. After that, in Section 8, we identify the current ecosystem science, eco-hydro-biogeochemistry, that links ecology, hydrology, and biogeochemistry. Following this, we highlight global water security issues and offer possible solutions in Section 9. Finally, Section 10 discusses the implications of scientific advances in ecosystem science and provides concluding thoughts and future research directions.

3 Description of the DOE's Representative Sites

To summarize the broad understanding that has emerged from DOE research, we choose seven DOE representative sites or testbeds: Savannah River Site in South Carolina, Oak Ridge Reservation in Tennessee, Hanford in Washington, Nevada National Security in Nevada, Riverton in Wyoming, and Rifle and East River in Colorado (Figure 2). The Savannah River Site, Oak Ridge Reservation, Hanford, and Nevada National Security are DOE-EM sites. The Riverton and Rifle sites have been managed by the Office of Legacy Management (LM), which was established in 2003 to manage the remaining legacy of World War II (i.e., radioactive and chemical waste, contaminants, and hazardous material) at over 100 sites across the country. The East River is not associated with any DOE historical contamination, but represents evolution of DOE research toward broader watershed systems science. In addition, all of these sites were later funded by the SBR program to study ecosystem function, thereby providing an excellent opportunity to learn how near-surface and subsurface legacy contaminant transport is modified by terrestrial and aquatic ecosystems.

The Savannah River Site, Oak Ridge Reservation, Hanford, Nevada National Security, and Riverton are respectively located in the South Atlantic-Gulf Region, Tennessee, Pacific Northwest, Lower Colorado regions, and Missouri regions. The Rifle and East River sites are located in the Upper Colorado River Basin, the principal water source in the southwestern USA. The Colorado River, one of the major rivers in the region, supplies water for 40 million people in seven states: Arizona, California, Colorado, Nevada, New Mexico, Utah, and Wyoming. These sites span across a wide range of hydro-climatic and geologic conditions. Table 1 describes contrasts in climate, geology, hydrogeology, surface water bodies, and groundwater depths across the representative sites.

Although several other DOE-funded testbeds have advanced the environmental sciences, they were not included in this review to keep the discussion manageable. This was particularly the case for sites with an extensive focus on aboveground processes, while this contribution's primary focus is to review the progress in understanding belowground processes and ecosystem function.

3.1 Savannah River Site

The Savannah River Site, located in south-central South Carolina, near Aiken, is an 800 square kilometer area where facilities were constructed in the early 1950s to produce special radioactive isotopes (e.g., Pu and tritium (^{3}H)) for the Department of Defense nuclear weapons stockpile. The major facilities constructed included production reactors, chemical processing plants, and solid and liquid waste storage sites. It is estimated that the Savannah River Site has approximately 172×10^6 m^3 of groundwater, soil, and debris contaminated with metals, radionuclides, and organics (National Research Council, 2000). Contamination of the environmental resources is the result of disposal practices conducted on-site. For example, the F-Area Seepage Basins (located in the north-central portion of Savannah River Site) consists of three unlined, earthen surface impoundments that received approximately 7.1 billion liters of acidic low-level radioactive (e.g., U, iodine (I)) waste solutions.

3.2 Oak Ridge Reservation Site

The Oak Ridge Reservation (formerly known as Clinton Engineer Works) was established in the early 1940s as part of the Manhattan Project on 239 square kilometers of land in eastern Tennessee, approximately 40 kilometers west of Knoxville, Tennessee. Its original missions, conducted at three large facilities, included U isotope enrichment, construction, and operation of the world's first continuously operating nuclear reactor to demonstrate Pu production and separation, and radiochemical research and development. Today, the Oak Ridge Reservation covers an area of approximately 134 square kilometers and includes three major DOE complexes: the Oak Ridge National Laboratory (ORNL), the East Tennessee Technology Park, and the Y-12 National Security Complex (Y-12 NSC). Over the past 70 years, historical activities have resulted in significant releases of contaminants into the environment on the Oak Ridge Reservation, contaminating soils, sediments, groundwater, surface water, and biota. Waste disposal areas, unlined infiltration pits, trenches, and spills and leaks have created extensive subsurface contamination. Additionally, from 1950 through 1963, lithium (Li) isotope separation processes at the Y-12 NSC resulted in the release of about 212,000 kg of Hg into the environment, of which about 108,000 kg were estimated to have been lost to the East Fork Poplar Creek (EFPC). Both historical and ongoing Hg releases continue to negatively impact downstream waters, including many kilometers of the river–reservoir system outside the Oak Ridge Reservation.

3.3 Hanford Site

The Hanford Site, located in southeastern Washington State, was established by the federal government to conduct defense-related nuclear research, development, and weapons production activities. As a result of activities at the Pu production complex and processing facilities (chemical separations plants and solid–liquid disposal and waste storage sites), it is estimated that the 1517 square kilometer area has approximately 1400 $\times10^6$ m^3 of groundwater, soil, and debris contaminated with metals, radionuclides, and or-

ganics (National Research Council, 2000). Contamination of the sites' environmental resources occurred as a result of 1.3 trillion liters of wastewater from chemical processing operations being intentionally discharged into the ground through settling ponds and other subsurface drainage structures (DOE, 1997). Additionally, DOE estimates that 67 of the 177 underground high-level radioactive waste storage tanks have leaked 3.8 million liters or more of the highly radioactive waste into the subsurface (DOE, 1997). Most of Hanford's subsurface contamination is concentrated in two locations: the Columbia River Corridor (100 Area and 300 Area) and the Central Plateau (200 Area). The 544 square kilometer Columbia River Corridor contained the production reactors, several waste burial sites, and major research facilities (DOE, 1996). The 194 square kilometer Central Plateau, near the middle of the Hanford Site, contained the chemical processing facilities for extracting U and Pu from irradiated reactor fuel, associated waste storage facilities (18 tank farms), and waste disposal facilities (i.e., surface settling basins and underground drainage cribs) (DOE, 1996). It is estimated that more than 220 square kilometers of groundwater at the Hanford Site is contaminated above current standards, mostly from operations in the 100 and 200 Areas. Section 5 briefly discusses the modeling of U contamination in the Hanford 300 Area and cesium (Cs) migration at the Hanford 200 Area.

3.4 Nevada National Security Site (formerly Nevada Test Site)

The Nevada National Security Site (NNSS), located in southern Nevada, was the primary site for USA's underground nuclear testing. It led to the deposition of substantial quantities of 43 different radionuclides into the environment (Smith et al., 2003). While ^{3}H is the most abundant anthropogenic radionuclide deposited in the Nevada National Security Site subsurface from an activity standpoint, Pu is the most abundant anthropogenic element by mass. Between 1951 and 1992, 828 underground nuclear tests (and 100 aboveground tests) were performed, and approximately 2.8 metric tons of Pu remains in the NNSS subsurface (DOE, Nevada Operations Office, 2000). The site is approximately $\sim$ 145 km northwest of Las Vegas, Nevada, and covers approximately 3500 square kilometers. The DOE-EM program has been developing a monitoring strategy that involves identifying contaminant boundaries, restricting access to contaminated groundwater, and implementing a long-term monitoring program.

3.5 Riverton Site

The Riverton, Wyoming DOE legacy site is a riparian floodplain that was the location of a U and vanadium (V) ore processing mill that conducted operations between 1958 to 1963 (DOE-LM, 1998). It is situated at $\sim 1,500$ m elevation along the gravel bed of Little Wind River and has a semiarid to arid climate (25 cm mean annual precipitation). Temperatures exceed 0 °C 154 days per year. The floodplain is vegetated with steppe flora, including sagebrush, grasses, and willows. Roots are relatively abundant, and robust upward solute transport through evapotranspiration has resulted in extensive evaporite mineralization of unsaturated soils (Dam et al., 2015). The upper 2.5 m of soil is predominantly loam with abundant clay lenses, deposited abruptly over the underlying gravelly–cobbly–sandy alluvial bed. Groundwater contains persistent U, molybdenum (Mo), and sulfate ($SO_4{}^{-2}$) contamination from an upgradient legacy U ore processing facility. Soils are loamy, but clay layers and sand lenses are present above and within the unconfined shallow sandy–gravelly aquifer (2.5 m to 3 m below the ground surface). The site experiences intense seasonal redox activity triggered by rising and ebbing water

tables and frequent flood events. Clay lenses exhibit molecular oxygen (O_2) depletion upon water saturation and the establishment of reducing conditions (including iron sulfide (FeS) precipitation). Significantly, reducing conditions extend into the surrounding sandy aquifer and persist in proximity to clay lenses.

3.6 Rifle Site

The Rifle, Colorado DOE legacy site is a riparian floodplain that was the location of a former U and V ore processing facility that operated from 1924 through 1958 (DOE-LM, 1998). The Rifle site is approximately 750 m in length along the Colorado River shore and 250 m at the widest point. The former processing facility contained large piles of mill tailings on-site, from which residual U and other associated contaminants leached into the subsurface. All surface structures and contaminated soil were subsequently removed, and the site was capped with fill material and vegetated. However, the potential for infiltration of groundwater contaminants remained until that time (Long et al., 2012; Williams et al., 2011). Site-specific investigations revealed that the groundwater contained dissolved U at the micromolar concentration level. Other contaminants of concern were identified as As, selenium (Se), and V. Groundwater at the site flows through alluvial flood plain deposits, which are 6 m to 7 m thick and underlain by the relatively impermeable Wasatch formation. Groundwater enters the alluvial aquifer from upgradient sources above the floodplain and exits into the Colorado River.

Given this background, earlier research was focused on *in situ* immobilization of contaminants. More recently, an increased focus was placed on constraining the exchanges and fates of different forms of C and N in river–floodplain settings because of their important roles in driving biogeochemical interactions with contaminants. More broadly, efforts were dedicated to developing a fundamental understanding of microbial communities and how they mediate biogeochemical cycles in the terrestrial subsurface. More than 15 years of focused investigations at the site have created a rich legacy of understanding subsurface contaminant transport and provided transferable insights.

3.7 East River Site

The East River Watershed, located in western Colorado, is a mountainous headwater testbed for exploring how climatic perturbations impact downgradient water availability and quality. The East River Watershed is located approximately 160 kilometers southeast of the Rifle Site and covers approximately 300 square kilometers. The East River is a pristine watershed. The Berkeley Lab's Scientific Focus Area (SFA; `https://watershed.lbl.gov/`) is examining the contribution to the riverine budgets of C and N that were neglected in previous assessments of contaminated sites like Rifle. The East River testbed began operation in 2014. Since then, it has enhanced process understanding of watershed dynamics and developed new approaches (such as monitoring strategies using sensor networks and scale-adaptive approaches) to improve watershed-dynamics simulation (Hubbard et al., 2018; Arora et al., 2020).

4 Advances and Innovations through DOE Science in the Last 20 Years

DOE research has evolved in scale and complexity, beginning with fundamental microbiology and geochemistry, and then linking them into biogeochemistry. Further, this research expanded to hydro-biogeochemistry (Figure 3) in unison with characterization

and monitoring strategies. A detailed description of these is highlighted below.

4.1 Advances in Subsurface Microbiology

It is widely understood that microbial communities, not individual microbes, are the drivers of most subsurface biogeochemical cycles (Figure 3A). Yet, in the early period of biological research at the Rifle site, the focus was primarily on one family of bacteria, the *Geobacteraceae*, which have a laboratory-demonstrated capacity for U reduction (Gorby and Lovley, 1992). This body of work motivated *in situ* acetate injection experiments to test the potential of a *Geobacter*-based bioremediation strategy at the Rifle site (Anderson et al., 2003). Proteomics of subsurface-derived cells (metaproteomics) were attempted to assay for *Geobacter*-specific proteins in amended aquifer groundwater. The only reference protein sequences available for this analysis were from *Geobacter* isolate genomes (Wilkins et al., 2009). Thus, the effectiveness of protein identification was limited because the aquifer *Geobacter* genotypes differed from those in pure cultures.

The first proteomics experiment motivated one of the first cultivation-independent genomics (metagenomic) analyses of groundwater to improve the representation of *Geobacter* protein sequences. DNA from a *Geobacter* isolate not present at the Rifle site provided an internal standard that was used to verify the accuracy of the recovered sequences. The experiment uncovered the very substantial microbial diversity of groundwater microbiomes. Draft genomes were reconstructed for over 80 bacteria, most of which were from previously unsampled or unknown lineages. Approximately half were from a group of novel bacteria whose gene content suggested they were symbionts of other microorganisms (Wrighton et al., 2012). These groups were subsequently deeply sampled in a larger acetate injection experiment at the site and from unamended groundwater, and are now recognized as essentially ubiquitous in groundwaters worldwide (He et al., 2021). The lineages share a common ancestry, so they were described as the Candidate Phyla Radiation (CPR) and were shown to comprise a substantial fraction (15 % to ∼50 %) of all bacterial diversity (Brown et al., 2015; Hug et al., 2016). The uniformly small genomes for CPR bacteria (Wrighton et al., 2012; Kantor et al., 2013) predicted their small cell size and thus potential to pass through the filters routinely used for cell recovery. Imaging of cells from the smallest filtrate fraction from acetate-amended groundwater revealed that the cells are around the theoretical minimum size for life (Luef et al., 2015).

Also first detected in Rifle groundwater were novel archaea with genomic features reminiscent of CPR bacteria. These diverse archaea, now part of the DPANN group, substantially extended the breadth of known archaeal diversity (Castelle et al., 2013). Given that both CPR bacteria and DPANN archaea are generally predicted to grow as surface-attached symbionts of other cells, it has been inferred that they have the potential to impact biogeochemical cycles through their impacts on host cells as well as via their own capacities for C, H, N, and S compound transformations. Subsequent research identified numerous bacteriophages (phages), the virus of bacteria, in subsurface communities (Al-Shayeb et al., 2020), bringing them into focus as important contributors to C compound turnover.

Sampling of subsurface microbial communities from pumped pore fluids overlooks particle-associated cells. This motivated the study of sediment-associated consortia and uncovered very significant microbial diversity (Castelle et al., 2013). One of the first applications of long-read sequencing to complex microbiomes revealed the presence of thousands of different organisms, most of which are at similar, very low abundance levels in Rifle sediments (Sharon et al., 2015). Metagenomic analyses of saturated whole

sediment samples recovered from 4, 5, and 6 m depths identified numerous new lineages, one of which is the bacterial phylum Zixibacteria. From a complete, curated genome, Zixibacteria were predicted to have an incredible diversity of metabolic capacities that enable growth despite shifts in conditions and the available aquifer resources (Castelle et al., 2013). Another study targeting sediment-associated Chloroflexi revealed, among other traits, an unexpected pathway for carbon dioxide (CO_2) fixation that brings into focus the potential for this process in C cycling in the aquifer (Hug et al., 2013).

A study that utilized groundwater and sediment metagenomes sampled from below and above the water table indicated that microbial cohorts consistently establish across the aquifer (Hug et al., 2015). This, along with the desire to develop models for integrated microbial community function (Zhuang et al., 2011), motivated a major genomes recovery effort. Genomes from over 2000 different microbial community members were analyzed simultaneously (an unprecedented effort). The major conclusion from this study was that biogeochemical cycles are attributed not to single organisms with capacities for specific pathways but to consortia whose metabolisms are interlinked by handoffs of pathway intermediates (Anantharaman et al., 2016). This ecosystem structure probably confers resilience and has since been documented by genomics-based studies in other ecosystems, including soil (Diamond et al., 2019).

Important limitations of the Rifle research site were its comparatively small size, lack of access to undisturbed soil and riparian zone sediments, and limited vegetation, slope, and aspect types. Thus, methods developed at the Rifle site were scaled up to tackle the challenge of watershed ecosystem-scale microbial biogeochemical process analyses that incorporate genome-derived information. Initial studies focused on the soils surrounding the meanders of the East River Site in Colorado. Motivated by the need to link micron-scale microbial analyses to a transect that is many kilometers in length, it was hypothesized that soils within the arcs of successive meanders would represent a system representative of meanders along the river length.

Metagenomic datasets were generated from a sampling grid at three sites in the river's upper, middle, and lower reaches. Extensive genome recovery enabled documentation of biogeochemically important capacities across each site. A core floodplain microbiome was identified and found to be enriched in capacities for aerobic respiration, aerobic carbon monoxide oxidation, and thiosulfate oxidation. Metatranscriptomic data revealed that the most highly transcribed genes were *amoCAB* and *nxrAB* (for nitrification). Low soil organic C correlates with the high activity of genes involved in methanol, formate, sulfide, hydrogen, and ammonia oxidation, nitrite oxidoreduction, and nitrate and nitrite reduction. Overall, it was concluded that the meander-bound regions serve as scaling motifs that predict aggregate capacities for biogeochemical transformations in floodplain soils (Carnevali et al., 2021). Similar research has addressed patterns of organism distribution and function across hillslopes and under four different vegetation types.

4.2 Advances in Geochemistry and Biogeochemistry

DOE's research in water and energy security arose from its historical and present-day need to resolve the many environmental management issues across its vast nuclear facilities, and its responsibility to develop a long-term solution to the USA's growing nuclear waste stockpile associated primarily with civilian nuclear energy production. The range of radiologic contaminants quite literally spans the entire periodic table: from ^{3}H to the short-lived heavy elements (e.g. curium-244 (^{244}Cm)) (Kurosaki et al., 2014). More traditional contaminants of concern include Cr, Hg (discussed in Section 6), and highly

radioactive Cs and radioactive U (discussed in Section 5.2), and more recently C and nutrients, including N and phosphorus (P). Below, we briefly describe DOE advancements in understanding the biogeochemical processes impacting contaminant fate and transport, as well as the major elements and nutrients (i.e., C, N, Fe, S, and manganese (Mn)) that drive subsurface biogeochemistry.

4.2.1 Contaminant biogeochemistry in redox-dynamic environments

U is a major risk driver at many of DOE's legacy waste sites, and DOE-funded programs have made major contributions to our knowledge of molecular species and processes controlling the movement of U in natural waters. The mobility of U in the DOE legacy waste sites is largely controlled by its speciation. The speciation includes dissolved, adsorbed, and mineralized species, predominantly in the +4 or +6 valence states. U^{V} is generally unstable and disproportionates to U^{VI} and U^{IV} (O'Loughlin et al., 2011); however, U^{V} has been detected in environmentally relevant systems (Ilton et al., 2005; Nico et al., 2009b), and stable U^{V} associated with Fe^{II}-containing clays has been reported (Boyanov et al., 2017a, 2016). Hexavalent U is stable and soluble under oxic conditions as the uranyl cation (UO_2^{2+}) (Ragnarsdottir et al., 2000). Tetravalent U is stable and sparingly soluble under reducing conditions, but can be mobilized as complexes with organic or inorganic C (Frazier et al., 2005; Luo and Gu, 2009; Stoliker et al., 2013).

U^{VI} can be reduced by microbial organisms (Wall and Krumholz, 2006, and references therein) and structural Fe^{II} in minerals (O'Loughlin et al., 2003a; O'Loughlin et al., 2010; Ilton et al., 2005; Ithurbide et al., 2009; Veeramani et al., 2011; Latta et al., 2012b; Singer et al., 2012; Boyanov et al., 2017a). These reactions generally produce amorphous U^{IV} products (Kelly et al., 2008; Sharp et al., 2011; Latta et al., 2012a; Bargar et al., 2013; Wang et al., 2014a; Morin et al., 2016; Bone et al., 2017a; Stetten et al., 2018; Bone et al., 2020, 2017b). For example, adsorbed U^{IV} was found to be the dominant form of U in naturally reduced sediments at legacy DOE sites across the Upper Colorado River Basin (Noël et al., 2017b,a). NOM functional groups, phosphate or phosphoryl groups, and high-affinity titanium (Ti)- or Fe-based binding sites in minerals have been cited as important ligands for U^{IV} in natural systems (Bone et al., 2020, 2017b; Fletcher et al., 2010; Boyanov et al., 2011; Sivaswamy et al., 2011; Veeramani et al., 2011; Stylo et al., 2013; Latta et al., 2014; Wang et al., 2015; Boyanov et al., 2017b). U redox cycling also can lead to the production of U^{V} in Fe^{III} oxyhydroxides (Kerisit et al., 2011; Massey et al., 2014; Dewey et al., 2020). The finding that sorbed species are a major mode of occurrence of U^{IV} was initially unexpected and has subsequently informed the development of reactive transport models (Yabusaki et al., 2017).

Oxidation of U^{IV} by O_2 has been studied extensively for uraninite (Gu et al., 2005; Boyanov et al., 2007; Senko et al., 2007; Ulrich et al., 2009; Lezama-Pacheco et al., 2015). Oxidation of UO_2 by Fe^{III} oxides and clays has also been documented within the DOE programs (Sani et al., 2005; Ginder-Vogel et al., 2006; Senko et al., 2007; Stewart et al., 2013). Oxidation of non-uraninite U^{IV} species by O_2 has also been investigated to a limited extent, producing mixed results regarding their stability relative to uraninite (Sharp et al., 2011; Cerrato et al., 2013; Bi et al., 2016; Latta et al., 2016). Another recent finding is that the presence of reduced C and Fe phases inhibits oxidative release of non-uraninite U^{IV} (Newsome et al., 2015; Bone et al., 2017a).

Unlike U, which is regulated at picomolar concentrations, many radionuclides are regulated at femtomolar concentrations (e.g., The United States Environmental Protection Agency (EPA) Maximum Contaminant Levels for drinking water of 6.4×10^{-16}, 1.7×10^{-14},

and 3.7×10^{-15} mol/L for strontium-90 (^{90}Sr), ^{137}Cs, and ^{238}Pu, respectively) (Deblonde et al., 2020). The body of environmental radiochemistry research supported by the DOE is much too vast to summarize here; however, we have selected a few examples to highlight key advances in this area. Much of DOE's research in environmental radiochemistry has focused on a process-level understanding of radionuclide reactive transport. Examination of colloid-facilitated Pu transport revealed the importance of both organic (Zhao et al., 2011; Xu et al., 2008) and inorganic colloids (Zhao et al., 2020), the nature of these colloid associations (Powell et al., 2011), the importance of redox cycling (Pan et al., 2021), and the sorption–desorption kinetics that limit colloid-facilitated transport (Begg et al., 2017, 2018). A combination of molecular dynamics simulations revealed the importance of Cs interaction with minerals via ion exchange (Zaunbrecher et al., 2015) along with experiments that determined the retardation properties controlling its migration (Durrant et al., 2018; Steefel et al., 2003; Zachara et al., 2002; Steefel et al., 2005). The complex chemistry and reactive transport of I were found to be controlled by a combination of redox chemistry and organic matter associations (Neeway et al., 2019). Indeed, the importance of redox conditions in the transport behavior of radionuclides is a theme that spans across several radionuclides of concern to the DOE (^{129}I, technetium (Tc), U, neptunium (Np), Pu) (O'Loughlin et al., 2011). Section 5.2 describes the reactive migration of U and Cs at the Hanford and Rifle sites further illustrating the importance of redox conditions and demonstrating the comprehensive and rigorous treatment of geochemistry in contamination modeling, as part of the simulation capability development.

In addition to U and other radionuclides, Cr is a contaminant of concern at many DOE legacy waste sites. Cr is a naturally occurring, redox-active transition metal that can exist in a range of oxidations states, with Cr^{III} and Cr^{VI} being the most stable in environmental systems. Furthermore, Cr^{VI} is one of the most mobile forms of Cr, which is transported in surface and subsurface waters as a negatively charged oxyanion. Although hexavalent Cr is generally more soluble, mobile, and toxic, Cr^{III} is significantly less soluble than Cr^{VI} and is an essential micronutrient. At DOE sites, such as the Hanford 100 Area (near reactor D, see `https://www.hanford.gov/page.cfm/100Area`), sodium dichromate was used during reactor operations to retard corrosion in reactor cooling systems. Consequently, Cr was released to the environment by spills and/or leaks from pipes, resulting in Cr^{VI} contamination in the vadose zone and groundwater adjacent to the Columbia River. For over two decades, DOE has performed groundbreaking research on factors that control Cr fate and transport at the Hanford 100 Area. For example, researchers investigated Cr interactions with sediments (Zachara et al., 1988, 1987; Beller et al., 2014) and the use of various forms of Fe and biostimulation to convert Cr^{VI} to Cr^{III} (Hazen and Tabak, 2005; Powell et al., 1995; Mayes et al., 2000; Jardine et al., 1999; Fendorf and Li, 1996), illustrating techniques for transforming mobile Cr^{VI} to immobile Cr^{VI} in subsurface systems.

The fate and mobility of As in a heterogeneous redox environment are difficult to predict because it is influenced by mineralogy, chemical speciation, and biological processes. Arsenic has five oxidation states (-III, -I, 0, III, V), with As^{III} and As^{V} being the most prevalent oxidation states in surface and groundwater, where it typically is present as oxyanion (arsenate and arsenite) and thioanion species. Thioarsenic can dominate in sulfidic environments that contain large amounts of reduced S, such as organic-rich surface water and groundwater (Kumar et al., 2020a; Stucker et al., 2014; Boye et al., 2017). Stucker et al. (2014, 2013) observed the presence of thioarsenic species under SO_4^{-2}-reducing conditions while conducting a biostimulation experiment at the Rifle site

in Colorado to treat the U-contaminated groundwater plume. NOM is also an important consideration in understanding As fate and mobility in environmental systems, such as wetlands, riparian areas, and groundwater aquifers, where redox conditions vary over space and time. This type of redox heterogeneity can have an outsized influence on As speciation, release, and retention. Recently, Kumar et al. (2020a) showed that As release and retention in natural aquifer sand is governed by the presence of thin organically rich clay lenses, which generate redox heterogeneities in sediments and thus alter the relative concentrations of Fe and S and promote the formation of mobile thioarsenate species.

4.2.2 Biogeochemical critical elements that mediate contaminant behavior

Mn is one of the most abundant trace metals in soils, sediments, and natural waters. Its complex redox chemistry, consisting of three commonly occurring oxidation states of Mn^{II}, Mn^{III}, and Mn^{IV}. The Mn^{II} state is highly soluble, while the Mn^{III} and Mn^{IV} states are sparingly soluble and occur most frequently as mixed hydr(oxides). While oxidation of Mn^{II} by O_2 is highly thermodynamically favorable, it is kinetically limited, leading to significant concentrations of dissolved Mn in many natural waters and leading control of Mn oxidation by a number of key processes. The most dominant of these is biological Mn oxidation, in which microorganisms including both bacterial and fungi catalyze the oxidation of Mn^{II} to Mn^{III}/Mn^{IV} (Geszvain et al., 2012; Santelli et al., 2011; Spiro et al., 2010). These organisms oxidize Mn directly through enzymes such as multicopper oxidase as well as indirectly through the production of reactive oxygen species (ROS)(Hansel et al., 2012). ROS produced abiotically, e.g., through photochemistry or Fenton chemistry, also provide an abiotic pathway to Mn^{II} oxidation (Learman et al., 2011; Nico et al., 2002; van Genuchten and Peña, 2016). The strong coupling of the Mn cycle with the ROS cycle is also thought to protect organisms from ROS-driven oxidative damage (Spiro et al., 2010).

The oxidation of Mn^{II} can produce a wide variety of Mn (hydr)oxides with different structures and reactivity (Bargar et al., 2009; Droz et al., 2015; Ling et al., 2020; Tan et al., 2010). Given the ubiquitous nature of Mn (hydr)oxides, they play important roles at DOE sites. Some of the most common Mn (hydr)oxides have layered type structures consisting predominantly of MnO_6 octahedra, but also contain multiple vacancies and defects, including inclusions of Mn^{III} centers (Bargar et al., 2009; Ilton et al., 2005; Spiro et al., 2010). The domain particle size is frequently on the nanoscale, making them natural nanoparticulate materials (Bargar et al., 2009). Overall, Mn (hydr)oxides are both powerful oxidants of other elements and strong, high surface area adsorbents. In terms of sorption behavior, they have been shown to strongly sorb other key elements, including cobalt (Co), zinc (Zn), nickel (Ni), Mn, copper (Cu), Cr, cadmium (Cd), lead (Pb), and U (van Genuchten and Peña, 2016; Wang et al., 2013a; Duckworth et al., 2009; Fuller and Bargar, 2014; Kwon et al., 2009, 2013; Peña et al., 2015; Simanova et al., 2015). This sorption behavior is frequently associated with vacancy sites within the oxides and can also include sorption at edges and structural incorporation. Mn (hydr)oxides frequently act as oxidants of other environmentally important metals and metalloids, including As, Cr, S, U, Tc, Co (Duckworth et al., 2014; Fan et al., 2014; McClain et al., 2017; Nico et al., 2009a; Plathe et al., 2013; Tang et al., 2014; Wang et al., 2013a,b, 2014a,b). The oxidation of these species by Mn hydr(oxides) is important in the efficacy of contamination remediation approaches focused on reductive immobilization of critical elements. In the case of Cr, Mn (hydr)oxides appear to be the critical pathway by which Cr^{VI} is generated in natural systems (Hausladen and Fendorf, 2017; Keiluweit

et al., 2015; McClain et al., 2017; Plathe et al., 2013; Wang et al., 2013b, 2014b). More recently, Mn has been shown to play an important role in natural C cycling both in waters as well as soils and sediments, whereby either through direct reaction with Mn (hydr)oxides or by biological utilization of an Mn complex, organic material is oxidatively decomposed into smaller molecules (Estes et al., 2017; Jones et al., 2018, 2020; Keiluweit et al., 2015). Microorganisms can directly utilize Mn (hydr)oxides as terminal electron acceptors, thereby coupled with C and other elemental redox cycles.

Fe oxides and Fe-bearing clay minerals are common constituents of soils and sediments at DOE sites. The biogeochemistry of Fe in most aquatic and terrestrial environments is driven largely by microbial activity, particularly in Fe-rich soils and sediments where Fe redox cycling by microorganisms is a significant component of C cycling and energy flux (Nealson and Saffarini, 1994; Roden and Wetzel, 1996; Lovley, 2000). As a group, dissimilatory iron-reducing bacteria (DIRB) can use a wide range of Fe^{III} forms as terminal electron acceptors for anaerobic respiration, including soluble Fe^{III} complexes, Fe^{III} oxides, and clay minerals containing varying amounts of structural Fe^{III} (Fredrickson et al., 1998; Zachara et al., 1998; Kukkadapu et al., 2001; O'Loughlin et al., 2021). DIRB activity can yield a suite of Fe^{II} species including soluble Fe^{II} complexes, Fe^{II} complexes with the surfaces of organic and inorganic solid phases, and a host of mineral phases containing structural Fe^{II} (Lovley et al., 1987; O'Loughlin et al., 2013, 2019; Dong et al., 2020). Many of these Fe^{II} species effectively reduce a wide range of organic and inorganic contaminants of concern at DOE sites, including chlorinated hydrocarbons, nitrate, Cr^{VI}, U^{VI}, Tc^{VII}, Np^{V}, and Pu^{V} (Bond and Fendorf, 2003; O'Loughlin et al., 2003a,b; Kelly et al., 2002; Kemner et al., 2004; Fredrickson et al., 2004; Peretyazhko et al., 2008; Wiatrowski et al., 2009; Felmy et al., 2011; Veeramani et al., 2011; Latta et al., 2012a; O'Loughlin et al., 2020). Finally, Fe^{II} (bio)oxidation can result in the formation of a variety of Fe^{III}-bearing minerals, depending on geochemical conditions.

Because of the relative insolubility of most Fe-bearing minerals in typical aquatic and terrestrial environments (i.e., circumneutral pH), their use for respiration by DIRB and iron-oxidizing bacteria (IOB) as terminal electron acceptors and donors, respectively, requires different mechanisms for electron transfer relative to soluble terminal electron acceptors/donors that are easily transported into the cell (e.g., O_2, NO_x^-, SO_4^{-2}). DOE-funded research has advanced understanding of extracellular electron transfer to solid-phase electron acceptors. Some DIRB such as *Geobacter* and *Shewanella* can transfer electrons directly to Fe^{III} oxide surfaces by means of reductases located on their outer cell membrane (Shi et al., 2009) or via electrically conductive pili or nanowires (Reguera et al., 2005; Gorby et al., 2006). The need for physical contact between Fe^{III} oxide minerals and microbial cells, however, can be readily overcome. The dissolution of Fe^{III} oxides is promoted by exogenous and endogenous ligands, and the resulting soluble Fe^{III} complexes can diffuse away and be reduced by DIRB at a distance (Nevin and Lovley, 2002; Taillefert et al., 2007). Likewise, the transfer of electrons from the cell to external electron acceptors (e.g., Fe^{III} oxides) can be facilitated by soluble electron shuttles, i.e., compounds that can be reversibly oxidized and reduced, which include a wide variety of endogenous and exogenous organic and inorganic compounds, including quinones, flavins, humic substances, and reduced S species (Nevin and Lovley, 2000, 2002; Royer et al., 2002; O'Loughlin, 2008; Roden et al., 2010; Flynn et al., 2014).

Although S is often less abundant than Fe in soils and sediments at DOE sites, its biogeochemical transformations are more complex because of the variety of S oxidation states (VI, V, IV, III, II, I, 0, -I, and –II). In oxic environments S^{VI} (e.g., SO_4^{2-}) is

typically the most thermodynamically stable valence state, while S^{-II} (e.g., H_2S and metal sulfides) is the most stable in anoxic environments. Unlike Fe^{III}, S^{VI} as SO_4^{2-} is a highly soluble anion found commonly in groundwater, as a consequence of the dissolution of SO_4^{-2} minerals or as a product of the oxidation of iron sulfide minerals (e.g., pyrite). Like DIRB, dissimilatory sulfate-reducing bacteria (DSRB) and archaea are anaerobes that can obtain energy by coupling the oxidation of organic compounds or molecular H_2 with the reduction of SO_4^{-2} to sulfide. This process is a key component of S and C cycles in anoxic soils and sediments (Megonigal et al., 2004). In addition, sulfide generated by DSRB can reduce Fe^{III} oxides (Kwon et al., 2014a,b; Johnson et al., 2021), resulting in the oxidation of sulfide, primarily to elemental S (as molecular S^0 and polysulfides) with minor amounts of thiosulfate. These pathways are important links coupling Fe and S biogeochemical cycles (Howarth et al., 1992; Lovley, 1993; Nealson and Saffarini, 1994; Flynn et al., 2014; Hansel et al., 2015).

4.2.3 C and N biogeochemistry

C biogeochemistry in soils is linked with redox reactions (e.g., aerobic respiration, denitrification, methanogenesis) in a simplified manner by conceptualization of a single solid phase soil organic matter (SOM) that provides a sustained supply of dissolved organic carbon (DOC). However, DOC availability that drives redox reactions is not unlimited and is also influenced by SOM dynamics. The traditional modeling approach for belowground C cycling does not explicitly consider the primary underlying processes and agents (e.g., microbes, aggregation) important for SOM cycling. Instead, SOM is classified into multiple C pools based on their degradability and is qualitatively named—for instance, recalcitrant versus labile or active pools. An emergent modeling approach recognizes that SOM comprises many complex molecules (Schmidt et al., 2011; Dwivedi et al., 2019) and that SOM decomposition is a function of a wide range of ecosystem properties and mechanisms such as temperature, thermodynamics, redox status, moisture content, exoenzyme production, decomposition, organo-mineral interactions, microbial necromass, ecology of belowground biota, and root contributions, as well as the mobilization of nutrients (as shown in Figure 3C, Keiluweit et al., 2016; Schmidt et al., 2011; Boye et al., 2017; Dwivedi et al., 2019, and references therein). As a result, the DOC supply that drives redox reactions varies significantly in space and time, and has implications for redox processes.

Motivated by this emerging understanding, Riley et al. (2014) developed a complex reaction network of SOM, including above- and belowground organic inputs, multiple DOC species, and heterotrophic microbes. They captured vertical SOM variability reasonably well. However, they did not include explicit organo-mineral interactions in their reaction network, and used a Langmuir isotherm to represent sorption (Riley et al., 2014), which does not adequately account for the suite of minerals present in the subsurface. Dwivedi et al. (2017a) later enhanced this reaction network by including a Surface Complexation Model (SCM) and demonstrated controls exerted by plant roots and mineral surface area on availability and persistence of DOC in the soil.

Maggi et al. (2008) developed a reaction network primarily consisting of ammonia oxidation and denitrification to examine N cycling in near-surface soil. Maggi et al. (2008) did not consider other redox species, like Fe and S, in their reaction network as their investigation was limited to N cycling for an agricultural field. However, Arora et al. (2016b) developed a reaction network representing a redox staircase for the Rifle site, where redox species (e.g., Fe, S) and naturally reduced sediments were predominantly

present. Dwivedi et al. (2018a) subsequently used this reaction network at the Rifle site and investigated the N dynamics in a floodplain environment. They demonstrated that, although the Rifle site experiences little precipitation (being in an arid climate), short and episodic summer rain events led to the formation of HSHMs of N species due to nitrification resulting from the percolation of oxic water. Yabusaki et al. (2017) also examined N biogeochemistry at the Rifle site; however, they did not explicitly consider nitrification processes and instead focused on the reductive pathways. Moving away from a contaminated site, Dwivedi et al. (2018b) also examined N biogeochemistry within intra-meander regions of the East River site. The East River, a pristine watershed, is low in nitrate. N cycling in the East River is primarily linked with snowmelt, vegetation, and atmospheric deposition (Newcomer et al., 2021).

4.2.4 Coupling of contaminant and nutrient redox cycles

Redox-active U in natural sediments is coupled to the C cycle through metabolic oxidation of organic matter by microbes to CO_2. Electrons released from this process are transferred to U^{VI}, reducing it to U^{IV} (see Section 4.2.1). This process is the basis for stimulated bio-reduction, in which exogenous DOC is injected into groundwater, stimulating the reduction of U^{IV} and resulting in net attenuation of dissolved U (Long et al., 2012; Williams et al., 2011). Another mode by which contaminant and nutrient cycles interact is via complexation reactions with functional groups produced via metabolic and anabolic processes. For example, NOM coatings, abundant on clay and other minerals, strongly complex U^{IV} (see Section 4.2.1). As pointed out elsewhere in this paper, methyl groups are profoundly important as complexing ligands Hg in natural waters, and organic functional groups containing reduced S are important as complexing agents for As (see Section 4.2.1) and Hg (see Section 6).

Nitrate-facilitated oxidation of U^{VI} has been extensively investigated and provides numerous examples of strong coupling between the U and N cycles, as well as of the impacts of the Fe and S cycles on U-N redox coupling. Researchers have noted that when groundwater enriched in nitrate is amended with DOC (e.g., acetate) U^{VI} will not be reduced until nitrate has been consumed, and metal reduction or SO_4^{-2} reduction commences (Finneran et al., 2002; Istok et al., 2004; Senko et al., 2002). Furthermore, U^{VI} can be recovered from aquifer sediments that have previously been reduced when groundwater is amended with nitrate (Finneran et al., 2002; Istok et al., 2004; Wu et al., 2010). There are multiple pathways through which nitrate reduction can lead to U^{IV} oxidation. It has been suggested that some bacteria can couple denitrification to U^{IV} oxidation (Finneran et al., 2002; Beller, 2005). However, nitrate-dependent microbial oxidation of U^{IV} may be slower than abiotic oxidation of U^{IV} under nitrate-reducing conditions (Senko et al., 2005b); for instance, U^{IV} is oxidized more quickly by nitrite formed during denitrification (Senko et al., 2002). U^{IV} is oxidized most rapidly by Fe^{III} oxides that are produced by the oxidation of Fe^{II} by nitrite (Senko et al., 2005a). The extent (Ginder-Vogel et al., 2006) of U^{IV} oxidation by Fe^{III} (hydr)oxides depends strongly on the type of Fe^{III}(hydr)oxide; nanocrystalline/amorphous Fe^{III} oxides may react rapidly with U^{IV} due to high surface areas (Senko et al., 2005a). In support of these conclusions, recent studies performed under diffusion-limited conditions suggest that denitrification occurs rapidly in soils and aquifers that host reduced U and is unlikely to overwhelm the reducing capacity of sediments that resides in the form of Fe^{II}, sulfide, and other reduced species.

Although O_2 can oxidize U^{IV}, nitrate-dependent U^{IV} oxidation has been shown to

occur much more rapidly (Moon et al., 2007, 2009). Using sediments from the background area of the Rifle site, Moon et al. (2007, 2009) demonstrated that slower oxidation of U^{IV} under oxic conditions was due to O_2 reacting quickly with numerous other reduced sediments species. In contrast, nitrate was less reactive towards the reduced species and could travel farther into the sediments and reach a greater total amount of U^{IV}. In fact, O_2 breakthrough did not occur for several weeks, whereas nitrate- breakthrough occurred within hours (Moon et al., 2007, 2009). Furthermore, in the presence of FeS, only 1 % of U in the sediment columns was solubilized in the presence of O_2 over the same time period as 11 – 60 % U was solubilized in the presence of nitrate (Moon et al., 2009). Buffering of U^{IV} against oxidation by reduced species including Fe^{II}, S^{-II}, and organic C has been suggested by several other researchers (e.g., N'Guessan et al., 2010; Abdelouas et al., 1999; Spycher et al., 2011).

4.3 Advances in Hydro-biogeochemistry

Hydro-biogeochemistry is essential for tracking and monitoring contaminants and nutrients that affect river water quality through subsurface geochemical fluxes. The subsurface geochemical behavior of contaminants and nutrients differs across sites due to distinct environmental, geological, and hydroclimatic conditions (Neeway et al., 2019; Zachara et al., 2013). In particular, sediments, mineral composition, geology, and hydroclimatic conditions give rise to contrasting mechanisms controlling plume persistence in the subsurface and riparian corridors. For example, several studies have demonstrated that the effect of mineral surfaces and sediments is important for the transformation and export of geochemical species (Allard and Gallard, 2013; Keppler et al., 2000; Cumberland et al., 2016; Maher et al., 2013; Fox et al., 2012; Dwivedi et al., 2019, 2017a), while hydrology plays a critical role in mobilizing contaminants (Jemison et al., 2020; Li et al., 2010; Dangelmayr et al., 2017; Flores Orozco et al., 2011; Williams et al., 2013).

In a comparative study, Zachara et al. (2013) outlined key differences in the geochemical nature of residual contaminant U at the Rifle and Hanford 300 Area sites. They suggested that the major differences between the sites and the kinetic processes influencing the U distribution in space primarily resulted from the spatial geochemical heterogeneity of detrital organic matter and the magnitude of groundwater hydrologic dynamics controlled by river stage fluctuations.

At DOE sites, including the Rifle and Columbia River Corridor at Hanford, it was found that the interplay between groundwater dynamics and river stage oscillations may result in gradient reversal, changes in flow velocities, redox zonation, and alterations in groundwater composition (Greskowiak et al., 2010; Yabusaki et al., 2011; Dwivedi et al., 2018a; Noël et al., 2019; Lezama-Pacheco et al., 2015). The relative variations in groundwater levels and river stages can alter the mixing zone's extent, where groundwater meets the surface waters and exchanges solutes (Ellis et al., 2007; Fritz and Arntzen, 2007). The mixing zone may span over distances of the meter- to kilometer scales (Dwivedi et al., 2018b; Zachara et al., 2020; Dwivedi et al., 2017b). For example, Dwivedi et al. (2018a); Arora et al. (2016b), and Yabusaki et al. (2017) demonstrated that the subsurface geochemical exports, and thus river water quality, were influenced by the spatial geochemical heterogeneity of detrital organic and temporal variability in groundwater flow direction at the Rifle site. Similarly, the Columbia River Corridor site at Hanford also experiences frequent hydrologic gradient reversals, primarily due to dam operations and distinct subsurface hydrogeology control (Shuai et al., 2019). Overall, the gradient reversal at sites like Rifle and Hanford can result in episodic oxic and anoxic conditions in the subsur-

face (Chen et al., 2020; Dwivedi et al., 2018a; Yabusaki et al., 2011; Lezama-Pacheco et al., 2015). Consequently, changes in the oxic environment due to groundwater mixing and microbially mediated sequential biogeochemical processes can lead to distinct redox gradients through a succession of electron acceptors.

4.3.1 Influence of hyporheic exchange flows and water-table fluctuations on mobilizing contaminants

The hyporheic zone, an active dynamic ecotone where nutrient-rich groundwater and oxic river water interact, extends below the saturated sediments adjacent to the flowing channels of streams and rivers and signifies the elevated reaction rates for nutrients and contaminants (e.g., Mulholland et al., 2008; Dwivedi et al., 2018b). The hyporheic exchange flows, referring to the water movement between hyporheic zones and river channels, are important controls on contaminant and nutrient transformations and ultimately export to downstream surface water bodies. To illustrate this further, the dynamic redox behavior in the hyporheic zone influences the fate and transport of Cr, a common contaminant in the subsurface and surface water. Liu et al. (2017) investigated Cr behavior in the Columbia River hyporheic zone at the Hanford site. They found that the hyporheic zone acts as a natural redox barrier for reductively immobilizing Cr under dynamic hydrological conditions.

In the Upper Colorado River Basin, seasonal water-table elevations can vary by up to 2 m over the course of the year (Tolar et al., 2020; Noël et al., 2019). During wet spring conditions, invasion of water into sediment pore space displaces air (and O_2), allowing reducing conditions to develop in shallow sediments that can persist into late summer in fine-grained clay-rich sediments (Tolar et al., 2020). Subsequently, drainage of water from sediments in late summer allows air to perfuse in, facilitating re-oxidation of U^{IV}, as well as Fe^{II} and sulfides (Lezama-Pacheco et al., 2015; Noël et al., 2019; Lefebvre et al., 2019). Under repeated annual cycles, complex patterns of U, as well as S and Fe redox cycles, overlap, creating distinctive signatures of redox conditions (Noël et al., 2017b,a).

4.3.2 Influence of hydro-climatic conditions on contaminant and nutrient dynamics

Hydro-climatic conditions specific to precipitation and evapotranspiration are equally important from the contaminant and nutrient dynamics standpoint. Frequent and intense rainfall in subtropical and humid climates like the Savannah River Site leads to prolonged flooding and stormwater infiltration (O'Reilly et al., 2012). Changing hydro-climatic and geochemical conditions and wet-dry redox cycles exert significant controls on contaminant cycling and mobilization–immobilization in the subsurface (Noël et al., 2017b; Song et al., 2018). For example, redox processes such as nitrification can be significant for mobilizing contaminants (e.g., U), particularly when oxic river water or rainwater infiltration alters the redox gradients (Dwivedi et al., 2018a; Bone et al., 2017a; Tolar et al., 2020; Cardarelli et al., 2020). Noël et al. (2019) showed that U accumulated as U^{IV} in shallow riparian floodplain sediments at the contaminated DOE Shiprock Disposal Site in New Mexico under water-saturated spring conditions, but was oxidized and precipitated as U^{VI} carbonates or silicates during summer drought.

Climate change is causing precipitation to decrease and evapotranspiration to increase in the Upper Colorado River Basin (Christensen and Lettenmaier, 2007; Prein et al., 2016), leading to decreasing water tables and exposure of reduced sulfidic sediments to oxygenated conditions. It is thus plausible that climate change will drive regional remobilization of accumulated U and other metals. In support of this conclusion, Janot

et al. (2016) estimated that oxidative release of U from a single moderate-sized naturally reduced zone at the Rifle, Colorado site could sustain a U plume at the regulatory concentration limit (0.044 mg_U/L) for hundreds if not thousands of years.

Developing insights into the interplay of hydrology, geochemistry, and biology requires developing insights into processes controlling the cycling of contaminants, nutrients, and elements such as oxygen (O), Fe, S, C, and N in the groundwater and floodplain. High-fidelity multicomponent reactive transport modeling has been found to advance a robust predictive understanding of this interplay across the DOE representative sites (Yabusaki et al., 2011; Dwivedi et al., 2018a; Li et al., 2017; Steefel, 2019). Significant progress has been made in modeling complex multidirectional flow processes and their biogeochemistry interactions using these DOE representative sites. We describe these modeling developments in greater detail in Section 5.

4.4 Characterization and Monitoring Strategies

Over the last several decades, there have been significant advances in the characterization of above- and belowground properties and dynamics necessary to parameterize, calibrate, and validate reactive transport models. At the point and single-borehole scales, there have been rapid advances in *in situ* sensors to measure groundwater and surface qualities, such as soil moisture, pH, water table, and electrical conductivity. These sensors are typically placed inside wells to continuously monitor groundwater or surface water.

Geophysical methods—including electrical resistivity, seismic, and radar—have been increasingly used to characterize the subsurface in a noninvasive manner (e.g., Hubbard and Rubin, 2005; Binley et al., 2015). Geophysics can bridge the gap in sparse wellbore locations by providing high-resolution and spatially extensive information in a minimally invasive manner. It can image subsurface contaminant plumes (e.g., Johnson et al., 2010, 2012; Dafflon et al., 2011), as well as map flow and biogeochemical properties that are important for predictive modeling and understanding (e.g., Johnson et al., 2010, 2012; Dafflon et al., 2011; Wainwright et al., 2014). In particular, geophysics has been powerful in identifying biogeochemical hot spots (Wainwright et al., 2016a). For the watershed or regional scale, airborne geophysics—particularly airborne electromagnetic surveys—was originally developed for mineral exploration, but is now increasingly used for water-resources applications (e.g., Barfod et al., 2018; Ball et al., 2020). While a number of different field experiments have demonstrated the feasibility of such subsurface imaging techniques (e.g., Johnson et al., 2015), real-time monitoring was still challenging until recently. In particular, autonomous electrical resistivity and phase tomography (ERT) monitoring have the potential to achieve rapid and automated detection and identification of changes in the subsurface (Johnson et al., 2015; Dafflon et al., 2011).

In parallel, recent advances in remote sensing have revolutionized how we characterize and monitor ecosystem and watershed dynamics. A high-resolution digital elevation model (DEM) derived from the Light Detection and Ranging (LiDAR) method is increasingly available across the USA, which has been applied to understand better the relationship between geomorphology and hydrology (Prancevic and Kirchner, 2019), as well as to measure snow depths and snow-water-equivalent (SWE) over a basin scale (Painter et al., 2016b). Because LiDAR data has been shown to inform near-surface soil properties (Patton et al., 2018; Gillin et al., 2015), hydrological connectivity (Jencso et al., 2009) and biogeochemical hot spots (Duncan et al., 2013) in the literature, it is being increasingly used in several DOE sites, including the East River (Hubbard et al., 2018) and Columbia River Corridor site at Hanford (Chen et al., 2020). Similarly, hyper-

spectral remote sensing is used extensively in DOE- and non-DOE supported research to map plant traits (e.g., Asner et al., 2015), leaf water contents (e.g., Colombo et al., 2008), leaf chemistry (e.g., Feilhauer et al., 2015) and other properties, which are also proxies for soil biogeochemistry (e.g., Madritch et al., 2014). The East River is making use of these methods to characterize a range of properties, including leaf area, wet, and dry weights for leaf sample, strait models developed independently for needle and non-needle leaf species (Chadwick et al., 2020a,b,c). For capturing the spatiotemporal heterogeneity, time-lapse images from satellites have enabled the monitoring of vegetation dynamics associated with hydrological disturbances (e.g., Wainwright et al., 2020). The remote sensing images are available at increasingly high resolution and high frequencies (Falco et al., 2018; Devadoss et al., 2020).

Representativeness and quality of collected environmental datasets (e.g., groundwater, precipitation) impact accuracy and precision of climate, hydrological, and biogeochemical analyses and predictions. Often, these are incomplete and may contain unspecified or missing entries due to unavoidable reasons, such as unfavorable weather conditions or delays in collecting sensor data. Several statistical and machine learning-based methods have been developed to render Quality Assurance (QA)/Quality Control (QC) and address related issues using datasets at the East River (Dafflon et al., 2020; Dwivedi et al., 2022; Faybishenko et al., 2021; Mital et al., 2020).

5 Simulation Capability Developments (HPC, RTM and Other Advances)

With the evolution of research on the DOE sites, several important advances have been made, and new computational capabilities have been developed that enable a more robust predictive understanding of the complex processes at work. A more detailed description of these processes is presented below.

5.1 Developments in Hydrological and Reactive Transport Modeling Tools

The need to understand and predict contaminant transport and the export of nutrients and other important constituents has driven the development of much-improved modeling tools for multiphase (variably saturated) hydrological flow, such as TOUGH (Pruess, 2004, 1987; Jung et al., 2018; Finsterle et al., 2014; Sonnenthal et al., 2021), STOMP (White and Oostrom, 2000, 2003), PFLOTRAN (Lichtner et al., 2015; Hammond et al., 2014, 2007), and reactive transport such as Crunch (Steefel et al., 2005, 2015), ToughReact (Sonnenthal et al., 2021), PFLOTRAN (Lichtner et al., 2015; Hammond et al., 2014, 2007). In turn, the availability of the new and evolving software has made it possible to address many scientific and engineering issues quantitatively at levels that were not possible previously.

5.1.1 Multiphase hydrology software

The multiphase (variably saturated) hydrological flow software developed for the DOE sites has historically been intended primarily for simulation of subsurface processes based on continuum formulations for porous media Darcy flow. Several hydrological codes such as HP1/HPx (Jacques et al., 2012; Jacques and Simunek, 2005; Jacques et al., 2006, 2013),PHT3D (Appelo and Rolle, 2010; Greskowiak et al., 2010), OpenGeoSys (Nagel et al., 2013; Kolditz et al., 2012), MIN3P (Mayer et al., 2002), and HYDRUS (Šimůnek

et al., 2006; Šimůnek et al., 2008; Šimůnek and van Genuchten, 2008) have been developed globally since the late 1980s and early 1990s. However, many of the multiphase codes for variably saturated flow were developed within the DOE Laboratory system, including the TOUGH family of codes (Finsterle et al., 2014), PFLOTRAN (Hammond et al., 2012), STOMP (White et al., 2012), NUFT (Hao et al., 2012), FEHM (Zyvoloski et al., 1997a; Dempsey et al., 2012; Zyvoloski et al., 1997b), and Amanzi–Advanced Terrestrial Simulator (ATS) (Garimella et al., 2014; Coon et al., 2016, 2020). Variably saturated flow has been represented by the Richards equation, which assumes a passive gas phase, as well as with a full multiphase treatment in which multiple phases are subject to gradients and allowed to flow. Enhancements over the years have focused on improving the numerical stability of the Richards or multiphase flow simulations, which are notoriously difficult because of the nonlinearity of the problems they address. In addition, implementation of massively parallel computer architectures has been the focus of much of the effort (e.g., Hammond et al., 2012; Jung et al., 2017; Garimella et al., 2014), although the details of this effort are beyond the scope of this review.

In order to extend beyond the subsurface so as to consider integrated surface and subsurface water, as required for analyzing terrestrial systems that consist of watersheds and river basins, much additional effort has been required. DOE-supported researchers have made important advancements to the state of the art in these integrated surface–subsurface hydrological models, with a focus on highly parallel open-source community codes. For example, extensions (Wu et al., 2021) of PFLOTRAN (Hammond et al., 2014) to include surface water and recent updates (Kuffour et al., 2020) to the integrated surface–subsurface hydrology model PARFLOW (Kollet et al., 2010; Kollet and Maxwell, 2008) were supported by DOE projects. The Amanzi–ATS code (Coon et al., 2016, 2020) was initiated as subsurface flow and reactive transport code (Amanzi) to support work at DOE legacy sites, and then extended as Amanzi–ATS to include surface flow and reactive transport processes to support research across DOE's network of watershed research testbeds.

The state of the art with respect to reactive transport modeling was summarized recently in Steefel et al. (2015). In this summary of a special issue on benchmarking of reactive transport software for environmental applications emphasizing continuum formulations, such codes as PHREEQC, TOUGHReact, OpenGeoSys, PFLOTRAN, MIN3P, eStomp, HydroGeochem, and CrunchFlow were described. The first of these benchmarking workshops was supported by DOE-BER, although at a bare-bones level. The codes were shown to be capable of achieving similar or identical results for a range of complex environmental problems that required numerical solutions, i.e., those with nonlinear or coupled processes that are well beyond what can be described with analytical solutions subject to many simplifying assumptions. A significant portion (but not all) of this software development was undertaken with funding from the DOE, while the applications of the software were motivated in many cases by environmental problems on DOE lands and later by the desire to understand and predict biogeochemical cycling in ecosystems.

The development of biogeochemical reaction capabilities that could be used in reactive transport codes has followed a somewhat separate path. These efforts have followed closely the fundamental scientific work on understanding the role of microbes in surface and subsurface environments, particularly as they contribute to contaminant retardation through their control of the redox environment (NABIR, 2006). Thus, the focus in reactive transport development here has been on incorporating arbitrarily complex biogeochemical reaction networks mediated by one or more competing or collaborating

microbial communities. The microbial communities mediate rates that depend on the local environmental conditions and thermodynamics and contribute to reaction pathways that affect contaminant sorption (and thus retardation) and mineral dissolution + precipitation, as well as gas exchange. One example of such a biogeochemical reaction network with multiple microbially mediated pathways is shown in Figure 4 (Arora et al., 2016b).

As might be expected for complex environmental problems like those facing the DOE Hanford site, where several processes come into play over a large spatial extent, massively parallel computing for reactive transport is now playing an important role. Arguably the first parallel code for reactive transport was the MCTracker code described and verified in Yabusaki et al. (1998). Following this by a few years was the parallel software PFLOTRAN (Hammond et al., 2012) that built on many of the capabilities found in FLOTRAN. The power of this new code and its application to the real-world environmental problem of U contamination in the Hanford 300 Area was highlighted in Hammond and Lichtner (2010), discussed below (Figure 5). As part of the DOE **A**dvanced **S**imulation **C**apability for EM (ASCEM) program, the high-performance computing code Amanzi was developed to simulate subsurface flow and transport. This Amanzi framework was later integrated into the ATS code to bring in surface processes like freeze and thaw (Painter et al., 2016a), overland flow, and river flow (Coon et al., 2020).

5.1.2 Integrated surface–subsurface reactive transport software

Although spatially distributed models that fully integrate surface and subsurface flow representations are increasingly available (e.g., Paniconi and Putti, 2015), extensions to include reactive transport in surface and subsurface water are relatively rare, Amanzi–ATS includes the capability for integrated surface–subsurface transport and accesses mature biogeochemical reaction capabilities in PFLOTRAN or CrunchFlow (see Dwivedi et al., 2016a) through an Application Programming Interface called Alquimia (`github.com/LBL-EESA/alquimia-dev`). This relatively new reactive transport capability for integrated surface water-groundwater systems is an important complement to observational studies, with significant potential for aiding in the interpretation of field observations.

Reactive transport in the integrated surface water–groundwater system is important for understanding transport and biogeochemical transformation in river corridors. The hyporheic zone often contains biogeochemical hot spots where many biogeochemical transformations occur. However, the open channel is the primary pathway for downstream movement and allows for O_2 exchange with the atmosphere, emphasizing the importance of an integrated modeling capability. Integrated surface–subsurface reactive transport models have great potential for helping understand the field-scale implications of relatively small-scale hydrologic and geochemical processes occurring in the hyporheic zone. However, it is first necessary to address the mismatch between the native spatial and temporal scales of fundamental hydrologic and biogeochemical processes, and the systems that they impact (e.g., watersheds). For example, locally anoxic conditions within an otherwise O_2-rich environment are important for nutrient and trace-metal processing in stream corridors, but bringing that fundamental understanding into field-scale models remains challenging. DOE-funded researchers have recently introduced multiscale models that confront that scale mismatch by using relatively coarse discretization for the channel network, with subgrid models for hyporheic zone transport and reactions. Painter (2018), and Painter (2021) introduced the ADELS (Advection Dispersion Equation with Lagrangian Subgrid) model, which associates a one-dimensional advection-reaction subgrid model with each channel grid cell to represent the ensembles of streamlines that

are diverted from the channel into the biogeochemically active hyporheic zone before returning to the channel. The computationally challenging simulations are made tractable by formulating the subgrid models in stochastic Lagrangian form, with hyporheic age replacing travel distance. Key model inputs—hyporheic exchange rates and hyporheic lifetime distributions—can be inferred from nonreacting tracer tests (Rathore et al., 2021) or synthesized data products (Gomez-Velez and Harvey, 2014). The ADELS model is implemented in Amanzi–ATS (Jan et al., 2021). Motivated by similar considerations, Fang et al. (2020) implemented a multirate transient storage model in PFLOTRAN. In contrast to the advection-based conceptualization of the ADELS model, the multirate transient storage model (mTSM) considers the hyporheic zone to be a collection of well-mixed reactors that are each coupled to the channel but not to each other. The ADELS and mTSM models have been shown to be mathematically equivalent for nonreacting tracers but yield very different results for reactive transport, because of the different conceptualization of hyporheic exchange (Painter, 2021). These model developments clearly demonstrate that field-scale models that honor fine-scale understanding are possible and have significant potential, but the identified differences in field-scale reactive transport also underscore the importance of the observational studies afforded by DOE's network of watershed research testbeds.

5.2 Advances in Contaminant Transport modeling

Modern reactive transport methods have made significant contributions to the topic of contaminant transport in recent years, and many of these applications are to DOE legacy sites or to sites where DOE contributed funding (e.g., Naturita, Colorado). The contributions can be broadly divided into two important themes:

1. The comprehensive and rigorous treatment of geochemistry in contaminant transport models, and

2. The role of aquifer heterogeneity in transport and mixing rates.

The second of these topics is not considered further here, since it is primarily the purview of hydrology and transport disciplines and is beyond the scope of this review paper. We focus here on the geochemical and mineralogical aspects of the problem.

The starting point for contaminant hydrogeology has always been the linear distribution coefficient (or K_d) models for sorption, which have the advantage of being easily incorporated into transport equations without rendering them nonlinear. It has also been asserted that they have an advantage in that the data required for the implementation is minimal, or at least less than that required by the multicomponent models discussed below. However, it should be pointed out that the K_d models, while potentially being as simple as the determination of the sorbed and aqueous concentration under a set of environmental conditions, typically require unique constraints for each and every site to which they are applied. In addition, as will be apparent from the discussion below, such K_d models may not even apply to a single site where conditions (temperature, salinity, competing ion concentrations, sorption site density) change over time and space. In other words, there is no real generality in the case of linear distribution coefficients, in contrast to the more rigorous ion exchange and surface complexation models (like that of metals on Fe-hydroxides) that can be applied quite widely.

The use of linear K_d coefficients came under strong attack when it became apparent that ^{137}Cs had migrated further than expected as a result of highly saline tank leaks in

the Hanford 200 tank farm (Zachara et al., 2002; Steefel et al., 2003, 2005). To address this issue, multicomponent ion exchange and surface complexation models were then considered in the context of reactive transport. Below, we briefly review them.

5.2.1 Ion exchange and Cs migration at Hanford 200 Area

The problem of understanding and predicting ^{137}Cs migration was made more complicated as a result of the multiple exchange sites that occur in sediments below the Hanford 200 tanks (Zachara et al., 2002; Steefel et al., 2003). In the Hanford case, the effective K_d depends on the Cs^+ concentration in addition to the competing sodium ion (Na^+) concentration (Figure 6A), since the ion exchange sites with a very high preference for Cs^+ are present in only low concentrations in the sediment. The low concentration of the high affinity exchange sites means that they could be completely filled, resulting in a reliance on relatively lower affinity sites for the ^{137}Cs sorption.

An example 2D reactive transport simulation was presented in Steefel et al. (2005) to demonstrate the effect of the competing sodium nitrate ($NaNO_3$) (a major component of the leaking tank fluids) concentration. This simulation was carried out using ion exchange selectivities and site concentrations determined from Hanford bulk sediment (Steefel et al., 2003). Figure 6B shows the transport of the nonreactive nitrate, with the plume extending over the entire domain size considered. The fractional migration of ^{137}Cs at 1M $NaNO_3$ is significantly less, in keeping with the expectation that some retardation of this contaminant will occur (although still more than would be the case for ^{137}Cs in a typically dilute soil or vadose zone water). At 5 M $NaNO_3$, the migration of the ^{137}Cs is significantly farther, even if still retarded relative to the nitrate. The enhanced ^{137}Cs observed below many of the Hanford 200 tanks can thus be explained largely by a classical ion exchange model that accounts for the competing $NaNO_3$ concentrations in the plume, and by the elevated concentrations of Cs^+ that exceed the number of high affinity sites that are available for strong sorption. The model also suggests that as leaking of highly concentrated $NaNO_3$ tank fluids ceases, further migration of the ^{137}Cs is unlikely. This is because infiltration by more normal rainwater is not capable of displacing the ^{137}Cs presently sorbed on the Hanford sediment. In any case, the use of constant linear K_d to describe the transport fails completely, so either the more rigorous ion exchange models need to be used, or at minimum, a model that accounts for environmental condition-dependent sorption (i.e., a "smart K_d").

5.2.2 Surface complexation and U migration

Perhaps an even more convincing demonstration of the inadequacy of the classical K_d models is provided by reactive transport analyses of metal and radionuclide migration influenced by surface complexation on Fe-hydroxides. In fact, an entire generation of geochemists has investigated the surface complexation behavior of metals on ferric hydroxides over many years (Dzombak and Morel, 1990; Davis et al., 2004, 1998), but only more recently has the use of surface complexation models been demonstrated convincingly in reactive transport frameworks at the field scale.

Most likely, the first successful demonstration of the use of surface complexation models to describe field-scale reactive transport was presented by Davis and co-workers for the DOE-LM U-contaminated site at Naturita, Colorado (Curtis et al., 2004, 2006; Davis et al., 2004). Davis et al. (2004) used both electrostatic and nonelectrostatic surface complexation models to describe U sorption on the Naturita sediment, but finally settled on the nonelectrostatic models because of their flexibility in treating natural and complex multimineralic sediments (Figure 7A). In order to match the pH dependence of sorption,

in particular, it was necessary to use a three-site SCM consisting of weak, strong, and very strong sites. Figure 7B shows the match with the experimental data at a variety of CO_2 partial pressures, an important variable because of the strong competition between U carbonate complexes in solution and the surface complexes developed on the Naturita sediment surfaces (Hsi and Langmuir, 1985; Prikryl et al., 2001; Davis et al., 2004). Calcium uranium carbonate complexes in solution can further reduce the sorption of U, especially $Ca_2UO_2(CO_3)_{3aq}$ (Bernhard et al., 2001; Brooks et al., 2003; Fox et al., 2006).

Curtis et al. (2006) used the nonelectrostatic surface complexation model presented in Davis et al. (2004) to investigate field-scale transport at the Naturita, Colorado site (Figure 7B). They demonstrated that the surface complexation model accurately reproduced the available data when combined with the realistic flow and transport parameters for the aquifer. They also demonstrated the inadequacy of a constant K_d model (Figure 7B).

Many other studies have been carried out that demonstrate the ability of the surface complexation models to describe field-scale behavior, including those at the Rifle Colorado U-contaminated site (Zachara et al., 2013; Yabusaki et al., 2007), and at the contaminated Savannah River site (Arora et al., 2018).

5.2.3 Modeling of microbially mediated reaction effects on U migration at the Rifle site

The fundamental studies of biogeochemistry mediated by microbial communities undertaken as part of the DOE research portfolio over the last 10-15 years have contributed to a much improved ability to model redox processes in the subsurface. This is a key development for predicting the dependence of redox-sensitive contaminants like U and Tc in the subsurface. The redox state of the subsurface depends on the classical sequence of electron acceptor-donor microbially mediated pathways from aerobic respiration under oxidizing conditions to methanogenesis under reducing conditions. The redox state of the subsurface can be manipulated with the injection of a suitable electron donor that drives the system towards reducing conditions, as was demonstrated at the Rifle Integrated Field Research Challenge in western Colorado (Williams et al., 2011; Dullies et al., 2010; Anderson et al., 2003). The engineered biostimulation of indigenous microorganisms like *Geobacter* (see Section 4.1) to catalyze the conversion of U^{VI} to a reduced immobile form of U, U^{IV}, was demonstrated convincingly at the field scale, although the longevity of such treatments has remained in question.

In the field experiments undertaken at the Rifle site, acetate was injected into a series of wells upgradient of a series of monitoring wells (Figure 8A). However, to simulate the acetate injection and resulting U reduction and immobilization as a result of microbial (primarily *Geobacter*) activity, it proved useful to begin with 1D column experiments (Li et al., 2009). With this approach, it was possible to show that the reactive transport modeling could capture both the sequence and distribution of redox processes (Figure 8B).

To capture the combined behavior of the acetate, U, and other electron acceptors/donors in the 2008 field experiment, it was necessary to use a fully 3D model for the site (Yabusaki et al., 2011). The injection of acetate drives the system to reducing conditions, with the result that the U^{VI} is immobilized as solid U^{IV}, and the ability to capture this behavior (along with associated redox processes) at the field scale is demonstrated convincingly with the simulations as shown in Figure 8C (Yabusaki et al., 2011).

Similarly, to understand the biogeochemical behavior of U within the groundwater and aquifer solids at the Oak Ridge Field Research Center, and as part of their Integrated Field Research Challenge, a conceptual model for simulating an emulsified vegetable

oil injection was developed and incorporated into the geochemistry code PHREEQC (Tang et al., 2013a,b). Numerous field experiments and subsequent interpretation of pyrosequencing and qPCR results in conjunction with geochemical data provided the basis for this hybrid microbial-geochemical conceptual model development(Gihring et al., 2011). Consistent with the field observations, the model demonstrated the biologically mediated reductive immobilization of U in groundwater with various electron donors and under diverse geochemical conditions (Wu et al., 2006a,b; Watson et al., 2013).

6 Hg: A Use Case To Study Watershed Biogeochemical Processes

Hg is a pollutant of global concern (Assessment, UNEP Global Mercury, 2019). Hg has a complex environmental cycle that has been significantly altered by anthropogenic activity. Elemental Hg (Hg^0) has a significant vapor pressure and long residence time in the atmosphere, facilitating long-range transport from source areas. Given that Hg mining dates back over 3,000 years, there may be no place on the Earth's surface that has not been affected by this altered cycle.

Inorganic Hg has well-documented deleterious health effects, and its transformation in the environment to the more toxic organomercurial compounds (primarily monomethylmercury, MeHg) poses increased risks to human and environmental health. The MeHg measured in environmental samples is the net result of the counteracting processes of Hg methylation and MeHg demethylation. Research into Hg environmental cycling has a long history, yet fundamental questions remain unanswered, particularly with respect to the watershed biogeochemical conditions that promote net MeHg generation. For example, although the gap is closing, research on lotic ecosystems (rivers and streams) is relatively underrepresented in comparison to lentic (lakes and ponds) ecosystems.

DOE-supported research on watershed-scale biogeochemistry has been conducted using an iterative pattern-to-process approach, in which the interactions and feedbacks among pattern and process were investigated across a range of spatiotemporal scales. These are interpreted to inform our understanding of watershed-scale function. This is being achieved through a combination of long-term observations, targeted event sampling, studies of seasonal and intraday patterns, and conducting field-informed experiments under controlled conditions in the laboratory. An important study site is EFPC (see Section 3.2), which has a well-documented history of Hg contamination that began at the headwaters and affected the creek and floodplain along its entire length (Brooks and Southworth, 2011; Loar et al., 2011).

6.1 Baseflow Sampling Identifies Additional Sources of Hg to the Creek

Long-term ($\sim$ 10 year) observations made at baseflow along the length of EFPC demonstrate consistent opposing patterns of Hg and MeHg concentration. Total and dissolved Hg (Hg_T and Hg_D, respectively) concentrations decrease from the headwaters downstream. Conversely, total and dissolved MeHg ($MeHg_T$ and $MeHg_D$) concentrations increase with distance downstream. Additionally, the MeHg concentrations show a seasonal dependence, with higher concentrations in spring and summer and lower concentrations in autumn and winter (Figure 9).

Discharge in EFPC increases with distance downstream, suggesting that one explanation for the decreasing Hg_T and Hg_D concentration is that the additional water is diluting

it in the channel. Nevertheless, dilution or particle settling cannot account for the concentration changes. In other words, the fact that the flux of Hg increases with distance downstream suggests that legacy sources of Hg in the watershed contribute additional Hg mass to EFPC (Peterson et al., 2018). These mass-balance-based estimates are supported by natural abundance Hg stable isotope signature studies (Demers et al., 2018; Donovan et al., 2014). By comparing Hg stable isotope signatures from different possible source areas and along the creek, hyporheic water was identified as the likely source of the added Hg, and the reduction of Hg^{II} to Hg^{0} by both microbially mediated and photochemical mechanisms was indicated.

Two controlling variables on Hg speciation and transport are NOM and dissolved organic matter (DOM), respectively and total suspended solids (TSS). Much of the Hg transported downstream is associated with suspended particles comprising a mixture of mineral particles, particulate organic detritus, and algae, predominantly diatoms. The nature of the association between Hg and particle surfaces has broader implications with respect to the reactivity and biogeochemical cycling of Hg in the creek ecosystem, including its release from particles and availability for methylation. Synchrotron-based x-ray fluorescence mapping of the suspended particles indicated that the mineral-bound Hg was closely associated with Fe and NOM (Gu et al., 2014). In conjunction with complementary Fourier-transform infrared spectroscopy (FTIR) analysis, these results suggested NOM-facilitated Hg bonding to Fe oxides, in which Hg was tightly bound to reduced S groups in the NOM, and the NOM was bound to Fe-oxides via its carboxyl and hydroxide functional groups. The diatom-associated Hg was found on the outer cell surface, suggesting passive sorption onto the cell surface rather than active uptake.

The filter-passing, or dissolved, Hg is strongly complexed by reduced S groups in DOM (Skyllberg et al., 2006). Using ultrahigh resolution Fourier transform ion cyclotron resonance mass spectrometry (FTICR-MS) coupled with electrospray ionization, investigators found that molecules containing multiple N and S atoms dominated the complexation of Hg (Chen et al., 2017). From both EFPC and Suwanee River, a 2:1 complex ($[C_5HNS_2-Hg-S_2NHC_5]+$) that dominated Hg complexation was identified in DOM isolates based on both molecular mass and Hg stable isotope distribution. Possible molecular structures of this complex were estimated using density functional theory calculations.

MeHg flux also increases with downstream distance, which is expected given that both concentration and discharge increase. As is the case for EFPC, MeHg is typically not the initial form of Hg entering the ecosystem; rather, it is formed in the environment from an inorganic Hg precursor via a microbially mediated reaction carried out by a diverse group of anaerobic bacteria possessing the *hgcAB* two-gene cluster (Gilmour et al., 2013; Parks et al., 2013; Podar et al., 2015).

Numerous studies have demonstrated that watershed wetland abundance is positively correlated with MeHg concentrations in the water bodies that drain those watersheds (Wentz et al., 2014). Nevertheless, the EFPC watershed has 3% wetland abundance, but EFPC has MeHg concentrations typical of watersheds with 30% wetland abundance. Like inorganic Hg, MeHg in the water column is either particle associated or complexed with NOM. An overarching goal of the research is to understand where and under what biogeochemical conditions Hg is methylated and MeHg demethylated.

6.2 Flood Sampling Reveals Terrestrial–Aquatic Connections and MeHg Sources

Targeted sampling of multiple storm-driven flood events revealed specific linkages between the terrestrial and aquatic environments. For instance, precipitation events delivered DOM and associated Hg to the creek, but not MeHg or particulate phases. Additionally, the recovery of dissolved solute concentrations to pre-flood levels closely followed the flood hydrograph, except for $MeHg_D$ which lagged significantly behind other solutes. Recovery of $MeHg_D$ concentrations closely followed the re-establishment of the diel cycle of dissolved O_2 concentration (Figure 10). Taken together, the results of targeted flood sampling implied that in-stream biological mechanisms are primarily responsible for MeHg generation in EFPC (Riscassi et al., 2016).

6.3 Seasonal and Intraday Patterns Highlight the Importance of Algal Biofilms

Natural cycles and anthropogenic activity affect stream ecology, water quality, and water quantity on timescales as short as months to hours. For example, the progression of the seasons leads to cyclic variation in creek discharge, water temperature, sunlight intensity, and duration. Well-established diel patterns of dissolved oxygen (DO) concentration and pH are driven by photosynthetic activity (Allan and Castillo, 2007). Wastewater treatment plants and hydroelectric dam operations are anthropogenic causes of short-time-scale water quality variations and river discharge.

Do Hg and MeHg concentrations have analogous cyclic variations to things like the daily photocycle, pH, and DO, and if so, how do they compare with other water-quality variations? Multiple sampling campaigns have been conducted to monitor changes in water chemistry over 30 to 48 hours to address this question. Previous research has documented the photochemical demethylation of MeHg and the role that various photosensitizers, including NOM, play in enhancing or inhibiting the reaction (Qian et al., 2014). Given these earlier results, lower MeHg concentrations were anticipated during the day, driven by photodemethylation. Instead, MeHg concentrations were positively correlated with the daily photocycle increasing during the day with overnight minima. While photodemethylation may have been occurring, the rate of MeHg production outpaced that of all demethylation reactions, resulting in net positive MeHg production (Brooks et al., 2021).

Long-term observations demonstrated seasonally dependent watershed sources of MeHg to EFPC. Targeted flood event sampling pointed to in-stream as opposed to out-of-stream sources of MeHg, and that the recovery of MeHg concentrations parallels the recovery of diel patterns in DO. Diel MeHg concentration variations are closely correlated with the daily photocycle. Together, these observations led us to hypothesize that periphyton biofilms are a source of MeHg in EFPC.

6.4 Field-Informed Laboratory Experiments Identify a Dominant Source of MeHg

Periphyton, or benthic algae, biofilms are complex assemblages comprising biotic (e.g., algae, fungi, bacteria, and archaea, insect larvae), abiotic (mineral grains, entrained sediment particles), and detrital (coarse and fine particulate organic matter) components often embedded in an extracellular gel-like matrix. These biofilms are in-stream, and their photosynthetic inhabitants produce O_2 in a pattern driven by the daily photocycle. Dur-

ing floods, the biofilms are buried and scoured, disrupting the daily DO cycle, gradually re-established as the biofilms return. However, bacterial MeHg production is only carried out by anaerobic bacteria. Specifically, the only known methylators are iron-reducing bacteria, SO_4^{-2}-reducing bacteria, fermentative microorganisms, and methanogenic archaea. For Hg methylation to occur in periphyton biofilms, these oxygenic systems must also harbor O_2-free zones where these anaerobic microorganisms can be active.

Chemical gradients within intact periphyton biofilms collected from EFPC were studied in the lab using microelectrode voltammetry. Using this technique, concentrations of DO, Fe^{II}, and S^{-II} were measured vertically from the periphyton-water interface down into the biofilm. Over a vertical distance of a few millimeters, conditions progressed from O_2-saturated to iron-reducing and SO_4^{-2}-reducing. The steep biogeochemical gradients within the biofilms were consistent with the biofilms harboring conditions conducive to MeHg production.

To further explore the role of periphyton biofilms in Hg cycling, biofilms were grown in the creek, returned to the lab, and amended with enriched stable isotopes of inorganic ^{201}Hg and $Me^{202}Hg$ (Olsen et al., 2016; Schwartz et al., 2019). The production of isotopically labeled $Me^{201}Hg$ and loss of $Me^{202}Hg$ was monitored over time as measures of Hg methylation and MeHg demethylation, respectively (Figure 11). Experiments were conducted in each of the four seasons. Although the biofilms were a net positive source of MeHg during most incubations, MeHg production was greater during spring and summer and for samples collected downstream versus upstream. Both results are consistent with the long-term field observations that show higher concentrations in those seasons and increased MeHg flux with downstream distance. Biofilms grown or incubated in the dark had substantially lower MeHg production, and in some cases, were net demethylating, which is consistent with the diel sampling in which MeHg concentrations increase during the day and decrease at night. Finally, biofilm structure was important to the measured activity and function of these communities; in biofilms with disrupted structure, methylation potentials decreased by 50%.

High-throughput amplicon sequencing has been applied to methylating periphyton communities to understand better the complex interactions that occur within them (Carrell et al., 2021). Bacterial and archaeal richness was lower in summer relative to biofilms in the autumn, while fungal richness showed the opposite pattern. Interestingly, Hg methylation potential correlated with numerous bacterial families that do not contain the Hg-methylation genes *hgcAB*, suggesting that overall microbiome structure and relationships within periphyton communities influence rates of Hg transformation.

Hg and MeHg in contact with periphyton are subject to other reactions in addition to methylation and demethylation, including sorption, desorption, and, in the case of Hg^{II}, reduction to Hg^0 and its reoxidation. These ancillary reactions were measured, and a novel model was created—the transient availability model (TAM)—to more accurately describe the periphyton methylation-demethylation results (Olsen et al., 2018). Consistent with lab incubations data of field-derived samples from EFPC, the TAM reproduced concentration versus time behavior that had previously been thought to be anomalous. Importantly, the TAM predicts faster Hg methylation rates than previous models, with broad implications for net MeHg generation in lotic ecosystems.

Using Hg biogeochemistry as a use case, we demonstrated that long-term observations in the EFPC, a DOE site (see Section 3.2, Oak Ridge Reservation Site), coupled with natural abundance stable isotope fractionation, identified sources and locations of Hg entering the creek. Additionally, it identified seasons of the year that supported higher

MeHg concentration. Targeted event sampling demonstrated that discrete and short-duration events connected the terrestrial and aquatic ecosystems in the watershed. In other words, these floods constitute hot moments with major implications for material and energy exchange. Event sampling also eliminated the floodplain as a source of MeHg to the creek and focused attention on in-stream sources. High temporal resolution sampling over daily periods produced the unexpected result of increasing MeHg concentration during the day. Controlled laboratory experiments confirmed that periphyton biofilms are a net positive source of MeHg and constitute hot spots of Hg, Fe, and S cycling. Further, biofilms with a higher degree of connectivity among its populations also have higher Hg methylation potential. This combination of approaches buttressed some ideas, but more importantly, highlighted previous misconceptions, identified HSHMs of governing processes, and opened new avenues of discovery to advance further our understanding of these systems that support diverse and vital ecosystem services for the global economy.

7 Evolution of Scientific Approaches and Strategies To Tackle Scale and Complexity

Significant progress has been made in process understanding at the hillslope and field scales, which is relevant in particular for watersheds such as the mountainous East River Site. Yet watershed-scale modeling has remained challenging because of the scale and wide underlying range of heterogeneity in watershed processes and parameters. Hyper-resolution watershed-scale models capable of exploiting high-performance computing are needed to resolve process complexity (level of details needed) and the spatial gradients that typically drive flow. However, these computationally expensive models pose a serious impediment to scientific progress, requiring abundant CPU hours. The variable resolution mesh or more sophisticated adaptive mesh refinement methods make it possible to focus on functionally dynamic regions compared to more conventional approaches. Efforts are underway to advance watershed-scale modeling using leadership-class computers, big data, and machine learning combined with learning-assisted physics-based simulation tools (e.g., `https://exasheds.org/`). However, the details of these efforts are well beyond the scope of this review. As an alternative, we have developed strategies to tackle scale and complexity over the years. Some examples of these strategies include multiscale, multiphysics, hybrid modeling, incorporating HSHMs, and functional zonation as part of scale-adaptive modeling.

7.1 Multiscale, Multiphysics and Hybrid Modeling

Historically there has been a mismatch between the spatial and temporal scales at which fundamental hydrologic and biogeochemical processes are most readily studied and understood (molecular to laboratory) and those of the ecosystems that they impact (field to watershed/basin). Because of nonlinear process interactions and complex heterogeneity in natural ecosystems, small-scale (e.g., laboratory) studies do not directly translate to field settings. Key reactive transport parameters, including permeability, dispersivity, and reaction-rate coefficients are all well known to be scale dependent and, in some cases, boundary-condition dependent. These challenges have motivated a variety of modeling approaches that are aimed at integrating information across scales and representing ecosystem processes at multiple levels of fidelity and complexity through DOE- and non-DOE supported research.

Multiple approaches have been developed to address this challenge, each with ad-

vantages and limitations. A summary of selected approaches used in DOE-supported research is provided here; for broader reviews, see Keyes et al. (2013) and Scheibe et al. (2015a).

Multiresolution methods use variable discretizations to capture effects of small-scale processes and properties on large-scale phenomena (e.g., Özgen-Xian et al., 2020). These methods include adaptive grid refinement (refining grids dynamically to put higher resolution where and when needed); multigrid methods (hierarchical sets of grids used to speed numerical convergence of a fine-grid solution), and nested or spatially varying grids that enhance resolution in specific subdomains (e.g., Figure 12).

Upscaling methods use assumptions about the nature of subgrid variability to derive effective parameters valid at the model resolution. These methods include numerical upscaling (direct solution of subgrid domains to derive approximate grid-scale parameters), various forms of homogenization and volume averaging, and perturbation solutions to stochastic partial differential equations.

Hybrid multiscale methods are similar to multiresolution methods. However, they use fundamentally different models in selected subdomains (for example, pore-scale simulations in portions of a domain where mixing-limited precipitation occurs; Scheibe et al., 2015b) and are sometimes referred to as "adaptive physics" models. These include hierarchical methods (e.g., the heterogeneous multiscale method; E et al., 2003) in which overlapping domains exchange information and concurrent methods (e.g., mortar methods; Balhoff et al., 2008), within which distinct subdomains pass information at domain boundaries.

7.2 HSHM: A Construct To Cope with Intense Biogeochemical Activity

The HSHM construct provides the basis for developing a robust predictive understanding of how contaminant behavior in subsurface heterogeneous media varies across spatiotemporal scales. Subsurface heterogeneities are sites of intense biogeochemical activity and are critical to watershed function. Recent studies have highlighted in greater detail the roles of the naturally reduced zones (or "redox heterogeneities") on biogeochemical function. For example, heterogeneity caused by clay lenses in high permeability soils provides opportunities to sorb contaminants in place (Janot et al., 2016; Campbell et al., 2012), while fracture networks can lead to rapid infiltration of contaminants to groundwater (e.g., Arora et al., 2019a; Berkowitz, 2002). Thus, high contaminant concentrations can be spatially diffused across large scales or concentrated at higher rates in specific areas, thereby forming contaminant hot spots. Similarly, these concentrations can be temporally diffused or more concentrated during specific times, thereby exhibiting contaminant hot moments. In addition, hydrological perturbations in transiently saturated zones drive changes in soil microbial communities, triggering a range of geochemical responses, thereby forming dynamic HSHMs. Figure 12 illustrates static hot spots (i.e., fixed in space) and dynamic hot spots (i.e., migrating in space).

Although the HSHM construct simplifies the characterization of complex heterogeneous systems and time scales at which biogeochemical processes occur—by subdividing the region and time into a finite number of relatively homogeneous units—it lacks a quantitative definition. Moreover, the HSHM construct is underutilized because of its dynamic nature. In response to that, Bernhardt et al. (2017) argued that the temporal dynamics of a putative hot spot are a fundamental trait that should be used in their description and, therefore, stressed the merger of HSHMs into a single descriptive term

"ecosystem control points." This definition indicates that knowledge of the rate distributions has more relevance than knowledge of maximum rates. Partly supported by DOE, Bernhardt et al. (2017) suggested four distinct categories of ecosystem control points: (a) permanent control points, experiencing high rates of biogeochemical activity relative to their proximity (e.g., floodplain), (b) activated control points, where higher biogeochemical activity is set off when certain substrates are delivered (e.g., low-lying topographic positions), (c) export control points that accumulate reactants until some hydraulic or diffusion threshold is not surpassed (e.g., geochemical exports through meanders), and (d) transport control points having extremely high transport capability without their direct intervention in exhibiting high biogeochemical activity (e.g., preferential flow paths). Table 2 presents some examples of HSHMs from DOE research in the backdrop of ecosystem control points.

7.2.1 Impact of HSHMs on Biogeochemistry of Legacy Contaminants and Nutrients

DOE investigations at former U ore processing sites within the Upper Colorado River Basin show the importance of HSHMs on legacy contamination (e.g., U) and nutrient cycling (e.g., Fe, S). Clayey lenses containing elevated organic C are common within coarse alluvium. These lenses host intense reducing activity (i.e., hot spots) and sustain halos of reducing conditions within the surrounding coarser aquifer sediments (Kumar et al., 2020a). Precipitation of iron monosulfides within these lenses and reductive attenuation of U^{VI} to U^{IV} cause S and U to become enriched to levels 25 and 200 fold higher, respectively, than surrounding sediments (Lefebvre et al., 2019; Janot et al., 2016; Noël et al., 2017b,a). As and non-redox active species such as Zn have also been shown to accumulate under these conditions through multiple chemical mechanisms involving association with reduced S species, as well as precipitation of double hydroxides (Kumar et al., 2020a; Engel et al., 2021). When clayey sulfidic lenses reside within the zone of annual water-table excursion, exposure to O_2 perfusion during summer drought conditions can cause SOM-complexed U^{IV} species to be oxidized to U^{VI}, providing a mechanism of release and contamination of groundwater. Desiccation of sediments during summer drought leads to precipitation of uranyl carbonates and silicates (Noël et al., 2019).

Although the relationship between hydrological change and microbial function is centrally important for predicting watershed function, only a few studies have explored the microbial ecology of dynamic HSHMs. Cardarelli et al. (2020) examined the microbial ecology of N-cycling archaea within transiently saturated and reduced zones at five contaminated DOE legacy floodplain sites (Shiprock in New Mexico, Rifle, Grand Junction, and Naturita in Colorado, and Riverton in Wyoming), which spans a 900 km N–S transect of the Upper Colorado River Basin. This study showed that ammonia-oxidizing "ecotypes" are strongly influenced by water table position, the location of reducing zones, or both. This study revealed that archaeal ammonia oxidation predominates within the terrestrial subsurface beyond a meter belowground. Recently, (Tolar et al., 2020) characterized microbial community diversity at the U-contaminated Riverton, Wyoming, legacy across transiently reduced zones. These results showed that microbial communities are surprisingly stable, despite robust flood-to-drought fluctuation and accompanying redox inversion. These findings were interpreted to indicate that microorganisms oscillate between "active" and "dormant" states, contingent upon prevailing environmental conditions, and their metabolic products play a more significant role in contaminant mobility than the organisms themselves. Taken together, these results indicate that microbial

community responses to drought and flood are complex and require more study.

7.3 Functional Zonation

Modeling eco-hydro-biogeochemical processes requires the characterization of the bedrock-to-canopy properties across watersheds. The tremendous heterogeneity of these properties is often a significant obstacle toward scaling modeling efforts from the hillslope and floodplain scales to a larger scale. Although various spatially extensive characterization techniques such as remote sensing and geophysics are available, it is still challenging to estimate each property distribution individually over the watershed scale, particularly soil and subsurface properties in the subsurface.

A functional zonation approach holds tremendous potential for tractably estimating individual property distributions over the watershed scale. In this approach, zones or spatial units within a landscape with unique distributions of multiple properties relative to neighboring regions can be identified using machine-learning-based spatial clustering approaches (e.g., Figure 12). The zonation approach essentially builds on a hydrofacies approach, which has been used in groundwater hydrology to define hydrological parameters in each facies (e.g., Fogg et al., 1998; Klingbeil et al., 1999). The reactive facies (Sassen et al., 2012; Wainwright et al., 2014) defined both hydrological and geochemical properties in each facies and stochastically mapped the reactive facies based on multiple geophysical data. Bea et al. (2013) documented the value of incorporating estimated reactive facies information within a reactive transport model to improve predictions of long-term U plume transport. These concepts have proved valuable in identifying zones and hot spots of biogeochemical activity (Wainwright et al., 2015; Flores Orozco et al., 2014, 2018).

More recently, the availability of enhanced remote-sensing (including hyperspectral) products and advanced machine-learning approaches has led to a paradigm shift in the zonation approach and demonstrated possibilities for characterizing the bedrock-to-canopy properties across watersheds. With this new paradigm shift, the zonation approach harnesses a suite of remote sensing datasets for identifying and distributing zones relevant to biogeochemistry and/or ecosystem functioning. In addition, the zonation approach takes advantage of the current scientific understanding of critical zone processes and insights into water and nutrient cycling and their exports within a watershed and its different compartments, particularly through the Critical Zone Observatory (CZO) network (Brantley et al., 2017).

Next, we briefly describe some prominent applications of the zonation approach at DOE sites. Hubbard et al. (2013) and Wainwright et al. (2015) used geophysical and remote sensing datasets to identify zones representing the heterogeneity of key properties and ecosystem functions—such as soil properties and C fluxes—in Arctic tundra. Devadoss et al. (2020) defined the ecosystem functioning zones (each of which has distinct time series signatures of soil moisture and plant dynamics) and investigated the relationship among soil, plant, and snow dynamics. Wainwright et al. (2016b) subsequently incorporated U reactive facies (e.g., Bea et al., 2013) into the zonation approach to identify biogeochemical hot spots (e.g., naturally reduced sediments) based on electrical geophysical methods at the Rifle site. Several additional modeling studies at the Rifle site represented naturally reduced sediments in their models to investigate the HSHMs of N, C, Fe, and DO and quantified their subsurface geochemical exports (e.g., Yabusaki et al., 2017; Dwivedi et al., 2018a; Arora et al., 2016b).

Recent investigations have been focused on examining how properties associated with

specific functional zones exert controls on water and N exports in response to snow dynamics and contribute to the aggregated watershed concentration–discharge signature in mountainous regions like the East River (Hubbard et al., 2018). A suite of remotely sensed bedrock-through-canopy watershed data layers and machine-learning approaches were utilized at the East River to identify watershed zonation. The zonation approach explored the sensitivity of different identified zones to foresummer drought (Wainwright et al., 2022). Zonation is also powerful for understanding the co-variability of above- and belowground processes, as well as identifying relevant field experimental sites throughout the domain. For example, research at the Hanford Site is using river channel morphology zonation (hydromorphic units, Ren et al. (2021)) as a framework for a transferable understanding of river–groundwater exchange fluxes and transit times.

8 Current Ecosystem Science and Legacy Contamination

Current ecosystem science comprehensively aims to couple and model ecological, hydrological, biogeochemical processes across the critical zone, ranging from the bedrock to the canopy. Water security challenges have motivated current ecosystem science, which has continued to emerge and expand well beyond traditional contaminant remediation-type studies. Recent severe weather events and hydro-climatic conditions have only added to these challenges, raising important concerns about geochemical exports of metals, C, N, and nutrients to the environment. In past assessments, the contribution to the riverine budgets of C and N were largely neglected, as part of the monitored natural attenuation strategy exclusively focused on stabilizing contaminants in place. More recently, an increased focus has been placed on constraining the exchanges and fates of different forms of C and N in river-floodplain settings, because of their important role in driving biogeochemical interactions with contaminants, and the potential of increased fluxes under changing precipitation regimes. Several studies have emphasized strong interlinkages between subsurface legacy contamination and hydrologically driven biogeochemical exports of metals, C, N, and nutrients in watersheds (e.g., Kumar et al., 2020b; Stucker et al., 2013; Zhang et al., 2018).

To illustrate this further, riparian zones and wetlands, where the contaminated groundwater interfaces with surface water, play a significant role in transforming contaminants because the presence of plant roots may facilitate the sequestration of trace metals. Large biogeochemical gradients exist in wetland ecosystems influenced by the primary production activities of plants that release large quantities of labile organic matter, and by the transport of O_2 in roots to maintain aerobic respiration. Plant roots also modulate mineralogy and promote contaminant immobilization through altering contaminant binding environment (e.g., Kaplan et al., 2016). Several studies have explored *in situ* immobilization of contaminants for remediation at several DOE sites (e.g., Szecsody et al., 1998; Dai et al., 2002; Zachara et al., 2013; Pawloski et al., 2009). Notably, the long-term sustainability of *in situ* reductive bioimmobilization of Cr^{VI} was examined under different biogeochemical regimes at Hanford 100 Area (e.g., Varadharajan et al., 2017; Beller et al., 2014; Faybishenko et al., 2008). Alternatively, the plants can offer an effective solution for the removal of hexavalent Cr by transforming it to less mobile, reduced Cr species as shown in the literature (Xu and Jaffé, 2006). Further, O_2 diffused from the wetland plant roots into their surrounding sediments can result in distinctive Fe plaques that precipitate on the surface of roots (Blute et al., 2004), which may consequently

facilitate active Fe cycling by stimulating Fe-reducing bacteria such as *Geobacter* spp. in anaerobic wetland sediments of the Savannah River Site (Chang et al., 2014). The enhanced Fe cycling can impact U attenuation by accumulating U near the plant roots in more oxidized states (U^{VI} or U^{V}), which are less susceptible to remobilization during episodic reoxidation events compared to U^{IV}, as observed at the Savannah River Site (Gilson et al., 2015; Kaplan et al., 2016).

Wetlands and river corridors experience episodic oxidation events associated with wetting and drying cycles Noël et al. (2017a); Tolar et al. (2020). Such cycling may facilitate the ongoing formation of fresh Fe oxyhydroxide, which can sorb or co-precipitate with U. The flow and transport of water links vegetation, soil, and contaminant transformations at the contaminated sites. The fraction of soil pore space that is water-filled vs. air-filled, i.e., the soil saturation, determines the rate at which water and O_2 can be transmitted to meet the transpiration and respiration demands of plant roots and aerobic soil microbes, thereby influencing soil redox potential (Yan et al., 2018). Aerobic microsites may form around the roots of wetland plants growing in saturated soils that are otherwise anoxic, leading to reaction hot spots. Redox reactions and cycling of redox-sensitive elements can alter the solubility and availability of key nutrients and metals, shifting microbial metabolism from largely oxidative reactions to methanogenesis, denitrification, and other less energetically efficient processes (Megonigal and Neubauer, 2019; Cardarelli et al., 2020). In turn, the history of water availability and rooting zone redox potential have direct and indirect effects on vegetation's distribution, structure, physiological state, and health.

9 Global Water Security Issues and Possible Solutions Through DOE-Supported Science

The existence of contaminants and the presence of high levels of nutrients in the environment is a major threat to water security. The problem of freshwater contamination is more pressing than ever, because most of the world's prominent rivers, supporting several million people, are under threat. For instance, India's Ganges River is considered one of the most polluted rivers globally: it contains many chemicals, including toxic Cr (Tripathi et al., 2016). A major drinking water source in China, the Yellow River, the second-longest in Asia and the sixth-longest river globally, has been suffering from severe pollution and is now on the verge of becoming unusable even for agricultural or industrial use (Brown and Halweil, 1998; Lu et al., 2018). The Citarum, the longest and largest river in West Java, Indonesia, faces extreme pollution from several contaminants, including Hg and As. The Hg concentrations in some parts of the river are as much as 100 times higher than levels considered acceptable by the EPA (maximum contaminant level is 2 ppb) (Paddison, 2016). As another example, every year the Mississippi River in the USA receives millions of pounds of toxic waste, poisonous chemicals (e.g., As), and excess nutrients (e.g., N), thereby turning the river's mouth into a dead zone (Dodds, 2006). The Colorado River and its tributaries, supporting over 36 million people in seven states in the western USA, have also experienced contamination from a variety of chemicals, including U and As (Gross, 2017). Groundwater contamination by As in Bangladesh represents one of the largest mass poisonings in history, with over a million people exposed to elevated As levels in their drinking water (Islam et al., 2010).

An accurate accounting of the fate and transport of these chemicals in the environment is key to ensuring water security. Many insights developed from several decades of research

work at DOE sites described in this paper can be used globally to examine the fate and transport of various contaminants and nutrient cycling. Capabilities developed as part of DOE research include hydrological and reactive transport modeling tools. These tools can comprehensively address water security problems and are transferable across DOE sites and worldwide. For example, several DOE codes such as PFLOTRAN and CRUNCH are currently being applied for various environmental applications globally (e.g., Knabe et al., 2021; Alt-Epping et al., 2015).

Finally, current ecosystem science is evolving through emerging and promising developments that include the use of artificial intelligence methods, such as machine learning to support zone identification, the association of system properties and functions with zonal types, HSHM detection, and the development of macroscale reduced-complexity models (Fang et al., 2020; Painter, 2018, 2021). Collaborations among hydrologists, geochemists, and microbiologists have led to advances in the use of increasingly abundant data from molecular biology studies ("omics") to inform reactive transport models that are beginning to mature (Meile and Scheibe, 2019). Multiscale heterogeneity and nonlinear process interactions in natural systems continue to challenge our predictive understanding, but these enhanced models and other recent advances offer promise for the future.

10 Summary, Conclusions, and Future Directions

Within the DOE's Office of Science, the BER and other related DOE programs (e.g., ASCR, EM, ER) have contributed significantly to environmental sciences' progress since the late 1980s. They have addressed several challenging subsurface problems, including treating radioactive waste (e.g., U, Pu) and heavy metals and metalloids (e.g., Cr, Hg, As). These efforts have provided transferable insights into process understanding, designed novel monitoring strategies to collect valuable field information, developed robust predictive capabilities, and devised scale-aware approaches to tackle underlying processes and the complexity resulting from the ecosystems' scales and magnitudes. To document these scientific advances that are generalizable and applicable to a range of water security problems worldwide, we have synthesized research activities conducted at representative DOE sites and testbeds, including the Savannah River Site in South Carolina, Oak Ridge Reservation in Tennessee, Hanford in Washington, Nevada National Security in Nevada, Riverton in Wyoming, and Rifle and East River in Colorado, over the last two decades. In particular, we have described the progress made in subsurface environmental sciences through DOE programs. To demonstrate the range of topics that have been studied in the environmental sciences through DOE-supported research, we show a word cloud highlighting key contributions (Figure 13), including keywords such as *subsurface*, *environment*, *contaminant*, *redox*, *reactive transport modeling*, and *watershed*.

Efforts through DOE-supported research have marked several breakthroughs, such as isolation of archaea from groundwater and expansion of the microbial "tree of life" using genomic methods in the subsurface microbiology; understanding the geochemical and biogeochemical behavior of S, Fe, Mn, U, Cr, Hg, C, and N in redox dynamic environments; and generating a robust predictive understanding of the relevant hydro-biogeochemistry and eco-hydro-biogeochemistry through novel field measurements and simulations. These findings have led the way in predicting the behavior and formation of HSHMs in the environment. Multiscale, multiphysics, and hybrid models have provided a framework for rigorous reactive flow and transport simulation capabilities. These modeling capabilities have the potential to telescope into watershed subsystems to simulate fine-scale detail, taking advantage of advanced meshing workflow, machine learning, and functional zona-

tion concepts.

We also discussed a paradigm shift in the ways that environmental science was done in the early 2010s. Until then, the investigations of small-scale (molecular to the millimeter) processes had been a primary focus. This approach was inadequate for addressing scaling behavior in the presence of a range of complex, coupled, nonlinear processes and a wide range of landscape heterogeneity. A holistic system science approach evolved to address these concerns, standing on the shoulders of active contaminant remediation-type studies. Since then, the DOE has supported the system science approach through sustained investments and bringing in multidisciplinary, multi-institutional teams together to unravel the intricacies and interconnectedness of system components that influence the behavior of both contaminated and natural systems across a range of spatial and temporal scales. This system science approach has investigated watershed science, including surface–subsurface hydrology; groundwater-surface water interactions; C, nutrient, and trace element transformations; ecosystem disturbances and resilience; Earth systems impacts; and Earth system models' development. Again, these relatively more recent science questions took advantage of capabilities developed over the past two decades for contaminant transport and transformation modeling. Modeling capabilities included using high-performance computers to simulate hydro-biogeochemistry, representing complex environmental biogeochemical cycles within diverse subsurface environments. We also detailed parallel development in monitoring strategies that started from the column scale and evolved through the field to watershed-scale investigation. These scientific advances and scale-aware modeling approaches have led to watershed and basin simulation capabilities that include processes from the bedrock to the canopy. In this context, we also described eco-hydro-biogeochemistry development across various representative DOE sites and testbeds.

To date, although great strides have been made in understanding the coupled biogeochemical cycling of Fe, S, and C, as well as their role in the transformation of nutrient and contaminant elements through bottom-up (i.e., reductionist) and top-down (complex system) approaches, knowledge gaps remain for addressing water security challenges. However, the science underlying water security challenges—such as water availability in drought-prone regions, excess nutrients, hypoxia, and extreme events—is complex and requires community-wide efforts to address such challenges. The crux of such efforts is to transfer the data and knowledge across sites, testbeds, and watershed systems globally. These efforts entail interagency coordination (e.g., collaborations across DOE, United States Geological Survey (USGS), National Science Foundation (NSF), national and international universities, and observational networks) and mission alignment. In essence, future water security requires collective action; it will take a collective effort to tackle it.

To maximize community efforts, the DOE has promoted open watershed system science, which involves identifying community needs, challenges, and opportunities in the areas of multiscale integration, measurement, computation, and cyberinfrastructure (collectively known as the Integrated Coordinated Open Networked (ICON) Science). As the data are highly valuable for advancing science, the DOE has advocated the FAIR (i.e., **f**indable, **a**ccessible, **i**nteroperable, **r**eusable) principle for data management. More details can be found in the open watershed science report (Scheibe and Stafford, 2020).

Finally, through collaborations and the advent of newer technologies, data in Earth system science will grow in magnitude, scale, complexity, and diversity. Our ability to collect and create data has already far exceeded our ability to assimilate them with predictive models (Reichstein et al., 2019; Luo et al., 2015; Gentine et al., 2018). This data

deluge will require improvements to interact with the growing observations and model outputs. Automated data-model analytics will be needed to enable the assimilation of diverse multiscale data into models for near-real-time prediction, the rapid identification of system-tipping-point precursors, and the development of models that inform the real-time optimization of autonomous sensing systems—from watershed to water basin to continental scales (Hubbard et al., 2020). Advanced machine learning approaches have the potential to provide actionable intelligence, which will enable efficient data management, smooth workflows, and interdisciplinary collaborations, all contributing to the scientific advancements needed to tackle water security problems in the future.

Acknowledgment

The work highlighted here was chosen because it was overwhelmingly supported by the DOE and would not have existed otherwise. However, the authors did not specifically require that each cited manuscript have a specific DOE funding source acknowledgment. The efforts of DD, CIS, BA, JB, SSH, PN, HMW, and KHW were supported by the Watershed Function Scientific Focus Area (SFA) funded by the US Department of Energy, Office of Science, Office of Biological and Environmental Research under Award Number DE-AC02-05CH11231. DD and CIS also acknowledge support from the ExaSheds Project at Lawrence Berkeley National Laboratory funded by the United States Department of Energy, Office of Science, Biological and Environmental Research under Contract No. DE-AC02-05CH11231. HMW also acknowledges support from the Department of Energy, Office of Environmental Management, ALTEMIS - Advanced Long-Term Environmental Monitoring Systems project. This research used resources of the National Energy Research Scientific Computing Center (NERSC), a United States Department of Energy Office of Science User Facility located at Lawrence Berkeley National Laboratory, operated under Contract No. DE-AC02-05CH11231. The efforts of MIB, DIK, KMK, and EJO were supported by the Wetlands Hydrobiogeochemistry Scientific Focus Area (SFA) at Argonne National Laboratory, which is supported by the Earth and Environmental System Science Program, Office of Biological and Environmental Research (BER), Office of Science, US Department of Energy (DOE), under contract DE-AC02- 06CH11357. Bargars's effort was supported by the SLAC Floodplain Hydro-Biogeochemistry SFA, funded by the US Department of Energy, Office of Biological and Environmental Research, Earth and Environmental Systems Sciences Division. SLAC National Accelerator Laboratory is supported by the US Department of Energy, Office of Science, Office of Basic Energy Sciences under Contract No. DE-AC02-76SF00515. The efforts of EP, SP, and SB were sponsored in part by the Office of Biological and Environmental Research within the Office of Science of the US Department of Energy (DOE), as part of the Hg Science Focus Area (Critical Interfaces SFA) and IDEAS-Watersheds projects at the Oak Ridge National Laboratory (ORNL). The DOE will provide public access to these results of federally sponsored research in accordance with the DOE Public Access Plan (`http://energy.gov/downloads/doe-public-access-plan`). ORNL is managed by UT-Battelle, LLC under Contract No. DE-AC05-00OR22725 with DOE. XC and TS were supported by the United States Department of Energy, Office of Science, Office of Biological and Environmental Research, Environmental System Science (ESS) Program through the River Corridor Scientific Focus Area project at Pacific Northwest National Laboratory. MZ's contribution was performed with funding from the Department of Energy, Office of Science, Biological and Environmental Research, Subsurface Biogeochemical Research program (SCW1053) and performed under the auspices of the

US Department of Energy by Lawrence Livermore National Laboratory under Contract DE-AC52-07NA27344. We thank Diana Swantek (LBNL) and Adam Malin (ORNL) for assistance with preparing figures 1, 3, and 8A. Finally, we thank the anonymous reviewer(s) for their insightful comment that helped improve the manuscript.

References

Abdelouas, A., Lutze, W., and Nuttall, H. Oxidative dissolution of uraninite precipitated on Navajo sandstone. *Journal of Contaminant Hydrology*, 36(3-4):353–375, 1999.

Al-Shayeb, B., Sachdeva, R., Chen, L.-X., Ward, F., Munk, P., Devoto, A., Castelle, C. J., Olm, M. R., Bouma-Gregson, K., Amano, Y., et al. Clades of huge phages from across earth's ecosystems. *Nature*, 578(7795):425–431, 2020.

Allan, J. D. and Castillo, M. M. *Stream ecology: Structure and function of running waters*. Springer Science & Business Media, 2007.

Allard, S. and Gallard, H. Abiotic formation of methyl iodide on synthetic birnessite: A mechanistic study. *Science of the Total Environment*, 463:169–175, 2013.

Alley, W. M., Healy, R. W., LaBaugh, J. W., and Reilly, T. E. Flow and storage in groundwater systems. *Science*, 296(5575):1985–1990, 2002.

Alt-Epping, P., Tournassat, C., Rasouli, P., Steefel, C., Mayer, K., Jenni, A., Mäder, U., Sengor, S., and Fernández, R. Benchmark reactive transport simulations of a column experiment in compacted bentonite with multispecies diffusion and explicit treatment of electrostatic effects. *Computational Geosciences*, 19(3):535–550, 2015.

Anantharaman, K., Brown, C. T., Hug, L. A., Sharon, I., Castelle, C. J., Probst, A. J., Thomas, B. C., Singh, A., Wilkins, M. J., Karaoz, U., et al. Thousands of microbial genomes shed light on interconnected biogeochemical processes in an aquifer system. *Nature Communications*, 7(1):1–11, 2016.

Anderson, R. T., Vrionis, H. A., Ortiz-Bernad, I., Resch, C. T., Long, P. E., Dayvault, R., Karp, K., Marutzky, S., Metzler, D. R., Peacock, A., et al. Stimulating the *in situ* activity of *Geobacter* species to remove uranium from the groundwater of a uranium-contaminated aquifer. *Applied and Environmental Microbiology*, 69(10): 5884–5891, 2003.

Appelo, C. and Rolle, M. PHT3D: A reactive multicomponent transport model for saturated porous media. *Ground Water*, 48(5):627–632, 2010.

Arora, B., Dwivedi, D., Hubbard, S. S., Steefel, C. I., and Williams, K. H. Identifying geochemical hot moments and their controls on a contaminated river floodplain system using wavelet and entropy approaches. *Environmental Modelling & Software*, 85:27–41, 2016a.

Arora, B., Spycher, N. F., Steefel, C. I., Molins, S., Bill, M., Conrad, M. E., Dong, W., Faybishenko, B., Tokunaga, T. K., Wan, J., et al. Influence of hydrological, biogeochemical and temperature transients on subsurface carbon fluxes in a flood plain environment. *Biogeochemistry*, 127(2-3):367–396, 2016b.

Arora, B., Davis, J. A., Spycher, N. F., Dong, W., and Wainwright, H. M. Comparison of electrostatic and non-electrostatic models for U^{VI} sorption on aquifer sediments. *Groundwater*, 56(1):73–86, 2018.

Arora, B., Dwivedi, D., Faybishenko, B., Jana, R. B., and Wainwright, H. M. Understanding and predicting vadose zone processes. *Reviews in Mineralogy and Geochemistry*, 85 (1):303–328, 2019a.

Arora, B., Ireson, A., Bouteiller, C. L., Hector, B., Ali, G., Stegen, J., Wymore, A., Sullivan, P. L., and Groh, J. Toward an international critical zone network-of-networks for the next generation through shared science, tools, data, and philosophy, 2019b.

Arora, B., Wainwright, H. M., Dwivedi, D., Vaughn, L. J., Curtis, J. B., Torn, M. S., Dafflon, B., and Hubbard, S. S. Evaluating temporal controls on greenhouse gas (GHG) fluxes in an Arctic tundra environment: An entropy-based approach. *Science of the Total Environment*, 649:284–299, 2019c.

Arora, B., Burrus, M., Newcomer, M., Steefel, C. I., Carroll, R. W., Dwivedi, D., Dong, W., Williams, K. H., and Hubbard, S. S. Differential CQ Analysis: A New Approach to Inferring Lateral Transport and Hydrologic Transients within Multiple Reaches of a Mountainous Headwater Catchment. *Front. Water 2: 24. doi: 10.3389/frwa*, 2020.

Asner, G. P., Martin, R. E., Anderson, C. B., and Knapp, D. E. Quantifying forest canopy traits: Imaging spectroscopy versus field survey. *Remote Sensing of Environment*, 158: 15–27, 2015.

Assessment, UNEP Global Mercury. UN Environment Programme. *Chemicals and Health Branch: Geneva, Switzerland*, 2019.

Balhoff, M. T., Thomas, S. G., and Wheeler, M. F. Mortar coupling and upscaling of pore-scale models. *Computational Geosciences*, 12(1):15–27, 2008.

Ball, L. B., Davis, T., Minsley, B. J., Gillespie, J. M., and Landon, M. K. Probabilistic categorical groundwater salinity mapping from airborne electromagnetic data adjacent to California's Lost Hills and Belridge oil fields. *Water Resources Research*, 56(6): e2019WR026273, 2020.

Barfod, A. A., Møller, I., Christiansen, A. V., Høyer, A.-S., Hoffimann, J., Straubhaar, J., and Caers, J. Hydrostratigraphic modeling using multiple-point statistics and airborne transient electromagnetic methods. *Hydrology and Earth System Sciences*, 22(6):3351–3373, 2018.

Bargar, J. R., Reitmeyer, R., Lenhart, J. J., and Davis, J. A. Characterization of U^{VI}-carbonato ternary complexes on hematite: EXAFS and electrophoretic mobility measurements. *Geochimica et Cosmochimica Acta*, 64(16):2737–2749, 2000.

Bargar, J. R., Fuller, C. C., Marcus, M. A., Brearley, A. J., De la Rosa, M. P., Webb, S. M., and Caldwell, W. A. Structural characterization of terrestrial microbial Mn oxides from Pinal Creek, AZ. *Geochimica et Cosmochimica Acta*, 73(4):889–910, 2009.

Bargar, J. R., Williams, K. H., Campbell, K. M., Long, P. E., Stubbs, J. E., Suvorova, E. I., Lezama-Pacheco, J. S., Alessi, D. S., Stylo, M., Webb, S. M., et al. Uranium redox transition pathways in acetate-amended sediments. *Proceedings of the National Academy of Sciences*, 110(12):4506–4511, 2013.

Batson, V. L., Bertsch, P., and Herbert, B. Transport of anthropogenic uranium from sediments to surface waters during episodic storm events. Technical report, Wiley Online Library, 1996.

Bea, S. A., Wainwright, H., Spycher, N., Faybishenko, B., Hubbard, S. S., and Denham, M. E. Identifying key controls on the behavior of an acidic-U^{VI} plume in the Savannah River Site using reactive transport modeling. *Journal of Contaminant Hydrology*, 151: 34–54, 2013.

Begg, J. D., Zavarin, M., and Kersting, A. B. Desorption of plutonium from montmorillonite: An experimental and modeling study. *Geochimica et Cosmochimica Acta*, 197: 278–293, 2017.

Begg, J. D., Edelman, C., Zavarin, M., and Kersting, A. B. Sorption kinetics of plutonium(V)/(VI) to three montmorillonite clays. *Applied Geochemistry*, 96:131–137, 2018.

Beller, H. R. Anaerobic, nitrate-dependent oxidation of U^{IV} oxide minerals by the chemolithoautotrophic bacterium thiobacillus denitrificans. *Applied and Environmental Microbiology*, 71(4):2170–2174, 2005.

Beller, H. R., Yang, L., Varadharajan, C., Han, R., Lim, H. C., Karaoz, U., Molins, S., Marcus, M. A., Brodie, E. L., Steefel, C. I., et al. Divergent aquifer biogeochemical systems converge on similar and unexpected Cr^{VI} reduction products. *Environmental Science & Technology*, 48(18):10699–10706, 2014.

Bender, J., Duff, M., Phillips, P., and Hill, M. Bioremediation and bioreduction of dissolved U^{VI} by microbial mat consortium supported on silica gel particles. *Environmental Science & Technology*, 34(15):3235–3241, 2000.

Berkowitz, B. Characterizing flow and transport in fractured geological media: A review. *Advances in Water Resources*, 25(8-12):861–884, 2002.

Bernhard, G., Geipel, G., Reich, T., Brendler, V., Amayri, S., and Nitsche, H. Uranyl(VI) carbonate complex formation: Validation of the $Ca_2UO_2(CO_3)_{3aq.}$ species. *Radiochimica Acta*, 89(8):511–518, 2001.

Bernhardt, E. S., Blaszczak, J. R., Ficken, C. D., Fork, M. L., Kaiser, K. E., and Seybold, E. C. Control points in ecosystems: moving beyond the hot spot hot moment concept. *Ecosystems*, 20(4):665–682, 2017.

Bi, Y., Stylo, M., Bernier-Latmani, R., and Hayes, K. F. Rapid mobilization of noncrystalline U^{IV} coupled with FeS oxidation. *Environmental Science & Technology*, 50(3): 1403–1411, 2016.

Binley, A., Hubbard, S. S., Huisman, J. A., Revil, A., Robinson, D. A., Singha, K., and Slater, L. D. The emergence of hydrogeophysics for improved understanding of subsurface processes over multiple scales. *Water Resources Research*, 51(6):3837–3866, 2015.

Blute, N. K., Brabander, D. J., Hemond, H. F., Sutton, S. R., Newville, M. G., and Rivers, M. L. Arsenic sequestration by ferric iron plaque on cattail roots. *Environmental Science & Technology*, 38(22):6074–6077, 2004.

Bond, D. L. and Fendorf, S. Kinetics and structural constraints of chromate reduction by green rusts. *Environmental Science & Technology*, 37(12):2750–2757, 2003.

Bone, S. E., Cahill, M. R., Jones, M. E., Fendorf, S., Davis, J., Williams, K. H., and Bargar, J. R. Oxidative uranium release from anoxic sediments under diffusion-limited conditions. *Environmental Science & Technology*, 51(19):11039–11047, 2017a.

Bone, S. E., Dynes, J. J., Cliff, J., and Bargar, J. R. U^{IV} adsorption by natural organic matter in anoxic sediments. *Proceedings of the National Academy of Sciences*, 114(4): 711–716, 2017b.

Bone, S. E., Cliff, J., Weaver, K., Takacs, C. J., Roycroft, S., Fendorf, S., and Bargar, J. R. Complexation by organic matter controls uranium mobility in anoxic sediments. *Environmental Science & Technology*, 54(3):1493–1502, 2020.

Boyanov, M., Latta, D. E., Mishra, B., Scherer, M. M., E.J., O., and K., K. The effect of iron oxides and montmorillonite clays on the trans-formations of uranium under reducing conditions. In *In: 3rd International Workshop on Advanced Techniques in Actinide Spectroscopy. Richland, WA*, 2016.

Boyanov, M., Latta, D. E., Mishra, B., Scherer, M. M., E.J., O., and K., K. Stabilization of a mixed-valence U^{V}-U^{VI} phase in systems with reduced SWy-2 and NAu-1 clays. In *Goldschmidt, Paris, France. 15 Aug*, 2017a.

Boyanov, M. I., O'Loughlin, E. J., Roden, E. E., Fein, J. B., and Kemner, K. M. Adsorption of Fe^{II} and U^{VI} to carboxyl-functionalized microspheres: The influence of speciation on uranyl reduction studied by titration and XAFS. *Geochimica et Cosmochimica Acta*, 71(8):1898–1912, 2007.

Boyanov, M. I., Fletcher, K. E., Kwon, M. J., Rui, X., O'Loughlin, E. J., Löfflerr, F. E., and Kemner, K. M. Solution and microbial controls on the formation of reduced U^{IV} species. *Environmental Science & Technology*, 45(19):8336–8344, 2011.

Boyanov, M. I., Latta, D. E., Scherer, M. M., O'Loughlin, E. J., and Kemner, K. M. Surface area effects on the reduction of U^{VI} in the presence of synthetic montmorillonite. *Chemical Geology*, 464:110–117, 2017b.

Boyanov, M., Kelly, S., Kemner, K., Bunker, B., Fein, J., and Fowle, D. Adsorption of cadmium to *Bacillus subtilis* bacterial cell walls: A pH-dependent X-ray absorption fine structure spectroscopy study. *Geochimica et Cosmochimica Acta*, 67(18):3299–3311, 2003.

Boye, K., Noël, V., Tfaily, M. M., Bone, S. E., Williams, K. H., Bargar, J. R., and Fendorf, S. Thermodynamically controlled preservation of organic carbon in floodplains. *Nature Geoscience*, 10(6):415–419, 2017.

Brantley, S. L., McDowell, W. H., Dietrich, W. E., White, T. S., Kumar, P., Anderson, S. P., Chorover, J., Lohse, K. A., Bales, R. C., Richter, D. D., et al. Designing a network of critical zone observatories to explore the living skin of the terrestrial Earth. *Earth Surface Dynamics*, 5(4):841–860, 2017.

Brender, J. D., Weyer, P. J., Romitti, P. A., Mohanty, B. P., Shinde, M. U., Vuong, A. M., Sharkey, J. R., Dwivedi, D., Horel, S. A., Kantamneni, J., et al. Prenatal nitrate intake from drinking water and selected birth defects in offspring of participants in the national birth defects prevention study. *Environmental Health Perspectives*, 121(9): 1083–1089, 2013.

Brooks, S. C. and Southworth, G. R. History of mercury use and environmental contamination at the Oak Ridge Y-12 Plant. *Environmental Pollution*, 159(1):219–228, 2011.

Brooks, S. C., Fredrickson, J. K., Carroll, S. L., Kennedy, D. W., Zachara, J. M., Plymale, A. E., Kelly, S. D., Kemner, K. M., and Fendorf, S. Inhibition of bacterial U^{VI} reduction by calcium. *Environmental Science & Technology*, 37(9):1850–1858, 2003.

Brooks, S. C., Riscassi, A. L., and Miller, C. L. Diel mercury concentration variations in a mercury-impacted stream. *in prep.*, 2021.

Brown, C. T., Hug, L. A., Thomas, B. C., Sharon, I., Castelle, C. J., Singh, A., Wilkins, M. J., Wrighton, K. C., Williams, K. H., and Banfield, J. F. Unusual biology across a group comprising more than 15% of domain bacteria. *Nature*, 523(7559):208–211, 2015.

Brown, L. R. and Halweil, B. China's water shortage could shake world food security. *World Watch*, 11(4):10–21, 1998.

Campbell, K. M., Kukkadapu, R. K., Qafoku, N., Peacock, A. D., Lesher, E., Williams, K. H., Bargar, J. R., Wilkins, M. J., Figueroa, L., Ranville, J., et al. Geochemical, mineralogical and microbiological characteristics of sediment from a naturally reduced zone in a uranium-contaminated aquifer. *Applied Geochemistry*, 27(8):1499–1511, 2012.

Cardarelli, E. L., Bargar, J. R., and Francis, C. A. Diverse *Thaumarchaeota* dominate subsurface ammonia-oxidizing communities in semi-arid floodplains in the western united states. *Microbial Ecology*, 80(4):778–792, 2020.

Carnevali, P. B. M., Lavy, A., Thomas, A. D., Crits-Christoph, A., Diamond, S., Méheust, R., Olm, M. R., Sharrar, A., Lei, S., Dong, W., et al. Meanders as a scaling motif for understanding of floodplain soil microbiome and biogeochemical potential at the watershed scale. *Microbiome*, 9(1):1–23, 2021.

Carrell, A. A., Schwartz, G. E., Cregger, M., Gionfriddo, C. M., Elias, D. A., Wilpiszeski, R. L., Klingeman, D. M., Wymore, A. M., Muller, K. A., and Brooks, S. Nutrient exposure alters microbial composition, structure, and mercury methylating activity in periphyton in a contaminated watershed. *Frontiers in Microbiology*, 12:543, 2021.

Castelle, C. J., Hug, L. A., Wrighton, K. C., Thomas, B. C., Williams, K. H., Wu, D., Tringe, S. G., Singer, S. W., Eisen, J. A., and Banfield, J. F. Extraordinary phylogenetic diversity and metabolic versatility in aquifer sediment. *Nature Communications*, 4(1): 1–10, 2013.

Cerrato, J. M., Ashner, M. N., Alessi, D. S., Lezama-Pacheco, J. S., Bernier-Latmani, R., Bargar, J. R., and Giammar, D. E. Relative reactivity of biogenic and chemogenic uraninite and biogenic noncrystalline U^{IV}. *Environmental Science & Technology*, 47 (17):9756–9763, 2013.

Chadwick, K. D., Brodrick, P., Grant, K., Henderson, A., Bill, M., Breckheimer, I., Williams, C. F. R., Goulden, T., Falco, N., McCormick, M., Musinsky, J., Pierce, S., Hastings Porro, M., Scott, A., Brodie, E., Hancher, M., Steltzer, H., Wainwright, H., Williams, K., Maher, K., Blonder, B., Chen, J., Dafflon, B., Lawrence, C., Sorensen, P., Damerow, J., Lamb, J., Khurram, A., Polussa, A., Wu Singh, H., Varadharajan, C., and Whitney, B. NEON AOP foliar trait maps, maps of model uncertainty estimates, and conifer map, East River, CO 2018. 6 2020a. doi: 10.15485/1618133. URL `https://www.osti.gov/biblio/1618133`.

Chadwick, K. D., Grant, K., Henderson, A., Breckheimer, I., Williams, C. F. R., Falco, N., Chen, J., Henry, H., Khurram, A., Lamb, J., McCormick, M., McOmber, H., Pierce, S., Polussa, A., Hastings Porro, M., Scott, A., Wu Singh, H., Whitney, B., Brodie, E., Carroll, R., Dewey, C., Kueppers, L., Maavara, T., Steltzer, H., Williams, K., Maher, K., and Powell, T. Locations, metadata, and species cover from field sampling survey associated with NEON AOP survey, East River, CO 2018. 1 2020b. doi: 10.15485/1618130.

Chadwick, K. D., Grant, K., Henderson, A., Scott, A., McCormick, M., Pierce, S., Hastings Porro, M., and Maher, K. Leaf mass per area and leaf water content measurements from field survey in association with NEON AOP survey, East River, CO 2018. 6 2020c. doi: 10.15485/1618132.

Chang, H.-s., Buettner, S. W., Seaman, J. C., Jaffé, P. R., Koster van Groos, P. G., Li, D., Peacock, A. D., Scheckel, K. G., and Kaplan, D. I. Uranium immobilization in an iron-rich rhizosphere of a native wetland plant from the Savannah River Site under reducing conditions. *Environmental Science & Technology*, 48(16):9270–9278, 2014.

Chen, H., Johnston, R. C., Mann, B. F., Chu, R. K., Tolic, N., Parks, J. M., and Gu, B. Identification of mercury and dissolved organic matter complexes using ultrahigh resolution mass spectrometry. *Environmental Science & Technology Letters*, 4(2):59–65, 2017.

Chen, J., Hubbard, S., Rubin, Y., Murray, C., Roden, E., and Majer, E. Geochemical characterization using geophysical data and Markov Chain Monte Carlo methods: A case study at the South Oyster bacterial transport site in Virginia. *Water Resources Research*, 40(12), 2004.

Chen, X., Lee, R. M., Dwivedi, D., Son, K., Fang, Y., Zhang, X., Graham, E., Stegen, J., Fisher, J. B., Moulton, D., et al. Integrating field observations and process-based modeling to predict watershed water quality under environmental perturbations. *Journal of Hydrology*, page 125762, 2020.

Christensen, N. S. and Lettenmaier, D. P. A multimodel ensemble approach to assessment of climate change impacts on the hydrology and water resources of the Colorado River Basin. *Hydrology and Earth System Sciences*, 11(4):1417–1434, 2007.

Colombo, R., Meroni, M., Marchesi, A., Busetto, L., Rossini, M., Giardino, C., and Panigada, C. Estimation of leaf and canopy water content in poplar plantations by means of hyperspectral indices and inverse modeling. *Remote Sensing of Environment*, 112(4):1820–1834, 2008.

Coon, E. T., Moulton, J. D., and Painter, S. L. Managing complexity in simulations of land surface and near-surface processes. *Environmental Modelling & Software*, 78: 134–149, 2016.

Coon, E. T., Moulton, J. D., Kikinzon, E., Berndt, M., Manzini, G., Garimella, R., Lipnikov, K., and Painter, S. L. Coupling surface flow and subsurface flow in complex soil structures using mimetic finite differences. *Advances in Water Resources*, 144: 103701, 2020.

Cumberland, S. A., Douglas, G., Grice, K., and Moreau, J. W. Uranium mobility in organic matter-rich sediments: A review of geological and geochemical processes. *Earth-Science Reviews*, 159:160–185, 2016.

Curtis, G. P., Fox, P., Kohler, M., and Davis, J. A. Comparison of *in situ* uranium K_D values with a laboratory determined surface complexation model. *Applied Geochemistry*, 19(10):1643–1653, 2004.

Curtis, G. P., Davis, J. A., and Naftz, D. L. Simulation of reactive transport of uranium(VI) in groundwater with variable chemical conditions. *Water Resources Research*, 42(4), 2006.

Dafflon, B., Irving, J., and Barrash, W. Inversion of multiple intersecting high-resolution crosshole GPR profiles for hydrological characterization at the Boise Hydrogeophysical Research Site. *Journal of Applied Geophysics*, 73(4):305–314, 2011.

Dafflon, B., Malenda, H., and Dwivedi, D. Groundwater level elevation and temperature across meander c at the lower montane in the east river watershed, colorado. Technical report, Environmental System Science Data Infrastructure for a Virtual Ecosystem, 2020.

Dai, M., Kelley, J. M., and Buesseler, K. O. Sources and migration of plutonium in groundwater at the savannah river site. *Environmental Science & Technology*, 36(17): 3690–3699, 2002.

Dam, W. L., Campbell, S., Johnson, R. H., Looney, B. B., Denham, M. E., Eddy-Dilek, C. A., and Babits, S. J. Refining the site conceptual model at a former uranium mill site in Riverton, Wyoming, USA. *Environmental Earth Sciences*, 74(10):7255–7265, 2015.

Dangelmayr, M. A., Reimus, P. W., Wasserman, N. L., Punsal, J. J., Johnson, R. H., Clay, J. T., and Stone, J. J. Laboratory column experiments and transport modeling to evaluate retardation of uranium in an aquifer downgradient of a uranium *in-situ* recovery site. *Applied Geochemistry*, 80:1–13, 2017.

Davis, J., Coston, J., Kent, D., and Fuller, C. Application of the surface complexation concept to complex mineral assemblages. *Environmental Science & Technology*, 32(19): 2820–2828, 1998.

Davis, J. A., Meece, D. E., Kohler, M., and Curtis, G. P. Approaches to surface complexation modeling of uranium(VI) adsorption on aquifer sediments. *Geochimica et Cosmochimica Acta*, 68(18):3621–3641, 2004.

Deblonde, G. J.-P., Kersting, A. B., and Zavarin, M. Open questions on the environmental chemistry of radionuclides. *Communications Chemistry*, 3(1):1–5, 2020.

DeFlaun, M. F., Fuller, M. E., Zhang, P., Johnson, W. P., Mailloux, B. J., Holben, W. E., Kovacik, W. P., Balkwill, D. L., and Onstott, T. C. Comparison of methods for monitoring bacterial transport in the subsurface. *Journal of Microbiological Methods*, 47(2):219–231, 2001.

Demers, J. D., Blum, J. D., Brooks, S. C., Donovan, P. M., Riscassi, A. L., Miller, C. L., Zheng, W., and Gu, B. Hg isotopes reveal in-stream processing and legacy inputs in East Fork Poplar Creek, Oak Ridge, Tennessee, USA. *Environmental Science: Processes & Impacts*, 20(4):686–707, 2018.

Dempsey, D., Simmons, S., Archer, R., and Rowland, J. Delineation of catchment zones of geothermal systems in large-scale rifted settings. *Journal of Geophysical Research: Solid Earth*, 117(B10), 2012.

Devadoss, J., Falco, N., Dafflon, B., Wu, Y., Franklin, M., Hermes, A., Hinckley, E.-L. S., and Wainwright, H. Remote sensing-informed zonation for understanding snow, plant and soil moisture dynamics within a mountain ecosystem. *Remote Sensing*, 12(17): 2733, 2020.

Dewey, C., Sokaras, D., Kroll, T., Bargar, J. R., and Fendorf, S. Calcium-uranyl-carbonato species kinetically limit U^{VI} reduction by Fe^{II} and lead to U^{V}-bearing ferrihydrite. *Environmental Science & Technology*, 54(10):6021–6030, 2020.

Diamond, S., Andeer, P. F., Li, Z., Crits-Christoph, A., Burstein, D., Anantharaman, K., Lane, K. R., Thomas, B. C., Pan, C., Northen, T. R., et al. Mediterranean grassland soil C–N compound turnover is dependent on rainfall and depth, and is mediated by genomically divergent microorganisms. *Nature Microbiology*, 4(8):1356–1367, 2019.

Dodds, W. K. Nutrients and the "dead zone": The link between nutrient ratios and dissolved oxygen in the northern Gulf of Mexico. *Frontiers in Ecology and the Environment*, 4(4):211–217, 2006.

DOE. *The 1996 Baseline Environmental Management Report (Volume I and II)*. DOE/EM-0319, Office of Environmental Management, Washington, D.C., 1996.

DOE. *Linking Legacies: Connecting the Cold War Nuclear Weapons Processes to Their Environmental Consequences)*. DOE/EM-0319, US DOE Office of Environmental Management, Washington, DC., 1997.

DOE-Complexity. Complex Systems Science for Subsurface Fate and Transport. `https://doesbr.org/complexityreport/SubsurfaceComplexitywithCover_03-05-10HR200dpi.pdf`, 2009. Accessed: 2021-03-15.

DOE-LM. Final site observational work plan for the UMTRA Project Site at Riverton, Wyoming. Document U0013801. Grand Junction, CO. `https://www.lm.doe.gov/Riverton/RVT00000133.pdf`, 1998. Accessed: 2021-03-15.

DOE, Nevada Operations Office. *United States Nuclear Tests: July 1945 Through September 1992*. Department of Energy, Nevada Operations Office, 2000.

Dong, H., Onstott, T. C., DeFlaun, M. F., Fuller, M. E., Scheibe, T. D., Streger, S. H., Rothmel, R. K., and Mailloux, B. J. Relative dominance of physical versus chemical effects on the transport of adhesion-deficient bacteria in intact cores from South Oyster, Virginia. *Environmental Science & Technology*, 36(5):891–900, 2002a.

Dong, H., Onstott, T. C., Ko, C.-H., Hollingsworth, A. D., Brown, D. G., and Mailloux, B. J. Theoretical prediction of collision efficiency between adhesion-deficient bacteria and sediment grain surface. *Colloids and Surfaces B: Biointerfaces*, 24(3-4):229–245, 2002b.

Dong, Y., Sanford, R. A., Boyanov, M. I., Flynn, T. M., O'Loughlin, E. J., Kemner, K. M., George, S., Fouke, K. E., Li, S., Huang, D., et al. Controls on iron reduction and biomineralization over broad environmental conditions as suggested by the *Firmicutes Orenia metallireducens* strain Z6. *Environmental Science & Technology*, 54(16):10128–10140, 2020.

Donovan, P. M., Blum, J. D., Demers, J. D., Gu, B., Brooks, S. C., and Peryam, J. Identification of multiple mercury sources to stream sediments near Oak Ridge, TN, USA. *Environmental Science & Technology*, 48(7):3666–3674, 2014.

Droz, B., Dumas, N., Duckworth, O. W., and Peña, J. A comparison of the sorption reactivity of bacteriogenic and mycogenic Mn oxide nanoparticles. *Environmental Science & Technology*, 49(7):4200–4208, 2015.

Duckworth, O. W., Bargar, J. R., Jarzecki, A. A., Oyerinde, O., Spiro, T. G., and Sposito, G. The exceptionally stable cobalt(III)–desferrioxamine B complex. *Marine Chemistry*, 113(1-2):114–122, 2009.

Duckworth, O. W., Akafia, M. M., Andrews, M. Y., and Bargar, J. R. Siderophore-promoted dissolution of chromium from hydroxide minerals. *Environmental Science: Processes & Impacts*, 16(6):1348–1359, 2014.

Dullies, F., Lutze, W., Gong, W., and Nuttall, H. E. Biological reduction of uranium—from the laboratory to the field. *Science of the Total Environment*, 408(24): 6260–6271, 2010.

Duncan, J. M., Groffman, P. M., and Band, L. E. Towards closing the watershed nitrogen budget: Spatial and temporal scaling of denitrification. *Journal of Geophysical Research: Biogeosciences*, 118(3):1105–1119, 2013.

Durrant, C. B., Begg, J. D., Kersting, A. B., and Zavarin, M. Cesium sorption reversibility and kinetics on illite, montmorillonite, and kaolinite. *Science of the Total Environment*, 610:511–520, 2018.

Dwivedi, D., Steefel, C., Siirila-Woodburn, E., Kallemov, B., Moulton, J. D., Kikinzon, C. E., Hammond, G., Foster, L., and Maxwell, R. Testing code interoperability and productivity on modeling integrated surface subsurface water flow and biogeochemical cycling in the hyporheic zone – IDEAS use case 1. Technical report, Annual joint investigators meeting of the Department of Energy's Office of Biological and Environmental Research (BER) at: Potomac, Maryland, 2016a.

Dwivedi, D., Riley, W., Torn, M., Spycher, N., Maggi, F., and Tang, J. Mineral properties, microbes, transport, and plant-input profiles control vertical distribution and age of soil carbon stocks. *Soil Biology and Biochemistry*, 107:244–259, 2017a.

Dwivedi, D., Mohanty, B. P., and Lesikar, B. J. Estimating *Escherichia coli* loads in streams based on various physical, chemical, and biological factors. *Water Resources Research*, 49(5):2896–2906, 2013.

Dwivedi, D., Mohanty, B. P., and Lesikar, B. J. Impact of the linked surface water-soil water-groundwater system on transport of *E. coli* in the subsurface. *Water, Air, & Soil Pollution*, 227(9):1–16, 2016b.

Dwivedi, D., Steefel, I. C., Arora, B., and Bisht, G. Impact of intra-meander hyporheic flow on nitrogen cycling. *Procedia Earth and Planetary Science*, 17:404–407, 2017b.

Dwivedi, D., Arora, B., Steefel, C. I., Dafflon, B., and Versteeg, R. Hot spots and hot moments of nitrogen in a riparian corridor. *Water Resources Research*, 54(1):205–222, 2018a.

Dwivedi, D., Steefel, C. I., Arora, B., Newcomer, M., Moulton, J. D., Dafflon, B., Faybishenko, B., Fox, P., Nico, P., Spycher, N., et al. Geochemical exports to river from the intrameander hyporheic zone under transient hydrologic conditions: East River Mountainous Watershed, Colorado. *Water Resources Research*, 54(10):8456–8477, 2018b.

Dwivedi, D., Tang, J., Bouskill, N., Georgiou, K., Chacon, S. S., and Riley, W. J. Abiotic and biotic controls on soil organo–mineral interactions: Developing model structures to analyze why soil organic matter persists. *Reviews in Mineralogy and Geochemistry*, 85(1):329–348, 2019.

Dwivedi, D., Mital, U., Faybishenko, B., Dafflon, B., Varadharajan, C., Agarwal, D., Williams, K. H., Steefel, C. I., and Hubbard, S. S. Imputation of contiguous gaps and extremes of subhourly groundwater time series using random forests. *Journal of Machine Learning for Modeling and Computing*, 3(2), 2022.

Dzombak, D. A. and Morel, F. M. *Surface Complexation Modeling: Hydrous ferric oxide*. John Wiley & Sons, 1990.

E, W., Bjorn, E., and Zhongyi, H. Heterogeneous multiscale method: A general methodology for multiscale modeling. *Physical Review B*, 67(9):092101, 2003.

Ellis, P. A., Mackay, R., and Rivett, M. O. Quantifying urban river–aquifer fluid exchange processes: A multi-scale problem. *Journal of Contaminant Hydrology*, 91(1-2):58–80, 2007.

Engel, M., Boye, K., Noël, V., Babey, T., Bargar, J. R., and Fendorf, S. Simulated aquifer heterogeneity leads to enhanced attenuation and multiple retention processes of zinc. *Environmental Science & Technology*, 2021.

Estes, E., Andeer, P., Nordlund, D., Wankel, S., and Hansel, C. Biogenic manganese oxides as reservoirs of organic carbon and proteins in terrestrial and marine environments. *Geobiology*, 15(1):158–172, 2017.

Falco, N., Wainwright, H., Dafflon, B., Ulrich, C., Uhlemann, S., Arora, B., Siirila-Woodburn, E., Minsley, B., Carroll, R., Williams, K., et al. Watershed functioning zonation: Advanced watershed characterization across scales. In *AGU Fall Meeting Abstracts*, volume 2018, pages H51O–1512, 2018.

Famiglietti, J. S. The global groundwater crisis. *Nature Climate Change*, 4(11):945–948, 2014.

Fan, D., Anitori, R. P., Tebo, B. M., Tratnyek, P. G., Lezama Pacheco, J. S., Kukkadapu, R. K., Kovarik, L., Engelhard, M. H., and Bowden, M. E. Oxidative remobilization of technetium sequestered by sulfide-transformed nano zerovalent iron. *Environmental Science & Technology*, 48(13):7409–7417, 2014.

Fang, Y., Song, X., Ren, H., Perkins, W. A., Shuai, P., Richmond, M. C., Hou, Z., Bao, J., Chen, X., and Scheibe, T. D. High-performance simulation of dynamic hydrologic exchange and implications for surrogate flow and reactive transport modeling in a large river corridor. *Frontiers in Water*, 2(PNNL-SA-153319), 2020.

Faybishenko, B., Hazen, T. C., Long, P. E., Brodie, E. L., Conrad, M. E., Hubbard, S. S., Christensen, J. N., Joyner, D., Borglin, S. E., Chakraborty, R., et al. *In situ* long-term reductive bioimmobilization of Cr^{VI} in groundwater using hydrogen release compound. *Environmental Science & Technology*, 42(22):8478–8485, 2008.

Faybishenko, B., Versteeg, R., Pastorello, G., Dwivedi, D., Varadharajan, C., and Agarwal, D. Challenging problems of quality assurance and quality control (QA/QC) of meteorological time series data. *Stochastic Environmental Research and Risk Assessment*, pages 1436–3259, 2021.

Feilhauer, H., Asner, G. P., and Martin, R. E. Multi-method ensemble selection of spectral bands related to leaf biochemistry. *Remote Sensing of Environment*, 164:57–65, 2015.

Felmy, A. R. and Rustad, J. R. Molecular statics calculations of proton binding to goethite surfaces: Thermodynamic modeling of the surface charging and protonation of goethite in aqueous solution. *Geochimica et Cosmochimica Acta*, 62(1):25–31, 1998.

Felmy, A. R., Moore, D. A., Rosso, K. M., Qafoku, O., Rai, D., Buck, E. C., and Ilton, E. S. Heterogeneous reduction of PuO_2 with Fe^{II}: Importance of the Fe^{III} reaction product. *Environmental Science & Technology*, 45(9):3952–3958, 2011.

Fendorf, S. E. and Li, G. Kinetics of chromate reduction by ferrous iron. *Environmental Science & Technology*, 30(5):1614–1617, 1996.

Finneran, K. T., Housewright, M. E., and Lovley, D. R. Multiple influences of nitrate on uranium solubility during bioremediation of uranium-contaminated subsurface sediments. *Environmental Microbiology*, 4(9):510–516, 2002.

Finsterle, S., Sonnenthal, E. L., and Spycher, N. Advances in subsurface modeling using the TOUGH suite of simulators. *Computers & Geosciences*, 65:2–12, 2014.

Fletcher, K. E., Boyanov, M. I., Thomas, S. H., Wu, Q., Kemner, K. M., and Löffler, F. E. U(VI) reduction to mononuclear U^{IV} by *Desulfitobacterium* species. *Environmental Science & Technology*, 44(12):4705–4709, 2010.

Flores Orozco, A., Williams, K. H., Long, P. E., Hubbard, S. S., and Kemna, A. Using complex resistivity imaging to infer biogeochemical processes associated with bioremediation of an uranium-contaminated aquifer. *Journal of Geophysical Research: Biogeosciences*, 116(G3), 2011.

Flores Orozco, A., Bücker, M., and Williams, K. Characterization of natural attenuation in a uranium-contaminated site by means of induced polarization imaging. In *EGU General Assembly Conference Abstracts*, page 8942, 2014.

Flores Orozco, A., Gallistl, J., Bücker, M., and Williams, K. H. Decay curve analysis for data error quantification in time-domain induced polarization imaging. *Geophysics*, 83 (2):E75–E86, 2018.

Flynn, T. M., O'Loughlin, E. J., Mishra, B., DiChristina, T. J., and Kemner, K. M. Sulfur-mediated electron shuttling during bacterial iron reduction. *Science*, 344(6187): 1039–1042, 2014.

Fogg, G. E., Noyes, C. D., and Carle, S. F. Geologically based model of heterogeneous hydraulic conductivity in an alluvial setting. *Hydrogeology Journal*, 6(1):131–143, 1998.

Fox, P. M., Davis, J. A., and Zachara, J. M. The effect of calcium on aqueous uranium(VI) speciation and adsorption to ferrihydrite and quartz. *Geochimica et Cosmochimica Acta*, 70(6):1379–1387, 2006.

Fox, P. M., Davis, J. A., Hay, M. B., Conrad, M. E., Campbell, K. M., Williams, K. H., and Long, P. E. Rate-limited U^{VI} desorption during a small-scale tracer test in a heterogeneous uranium-contaminated aquifer. *Water Resources Research*, 48(5), 2012.

Frazier, S. W., Kretzschmar, R., and Kraemer, S. M. Bacterial siderophores promote dissolution of UO_2 under reducing conditions. *Environmental Science & Technology*, 39(15):5709–5715, 2005.

Fredrickson, J. K., Zachara, J. M., Kennedy, D. W., Dong, H., Onstott, T. C., Hinman, N. W., and Li, S.-m. Biogenic iron mineralization accompanying the dissimilatory reduction of hydrous ferric oxide by a groundwater bacterium. *Geochimica et Cosmochimica Acta*, 62(19-20):3239–3257, 1998.

Fredrickson, J. K., Zachara, J. M., Kennedy, D. W., Duff, M. C., Gorby, Y. A., Shu-mei, W. L., and Krupka, K. M. Reduction of U^{VI} in goethite (α-FeOOH) suspensions by a dissimilatory metal-reducing bacterium. *Geochimica et Cosmochimica Acta*, 64(18): 3085–3098, 2000.

Fredrickson, J. K., Zachara, J. M., Kennedy, D. W., Kukkadapu, R. K., McKinley, J. P., Heald, S. M., Liu, C., and Plymale, A. E. Reduction of TcO_4^- by sediment-associated biogenic Fe^{III}. *Geochimica et Cosmochimica Acta*, 68(15):3171–3187, 2004.

Fritz, B. G. and Arntzen, E. V. Effect of rapidly changing river stage on uranium flux through the hyporheic zone. *Groundwater*, 45(6):753–760, 2007.

Fuller, C. C. and Bargar, J. R. Processes of zinc attenuation by biogenic manganese oxides forming in the hyporheic zone of pinal creek, arizona. *Environmental Science & Technology*, 48(4):2165–2172, 2014.

Fuller, M. E., Streger, S. H., Rothmel, R. K., Mailloux, B. J., Hall, J. A., Onstott, T. C., Fredrickson, J. K., Balkwill, D. L., and DeFlaun, M. F. Development of a vital fluorescent staining method for monitoring bacterial transport in subsurface environments. *Applied and Environmental Microbiology*, 66(10):4486–4496, 2000.

Garimella, R. V., Perkins, W. A., Buksas, M. W., Berndt, M., Lipnikov, K., Coon, E., Moulton, J. D., and Painter, S. L. Mesh infrastructure for coupled multiprocess geophysical simulations. *Procedia Engineering*, 82:34–45, 2014.

Gentine, P., Pritchard, M., Rasp, S., Reinaudi, G., and Yacalis, G. Could machine learning break the convection parameterization deadlock? *Geophysical Research Letters*, 45 (11):5742–5751, 2018.

Geszvain, K., Butterfield, C., Davis, R. E., Madison, A. S., Lee, S.-W., Parker, D. L., Soldatova, A., Spiro, T. G., Luther III, G. W., and Tebo, B. M. The molecular biogeochemistry of manganese(II) oxidation. *Biochemical Society Transactions*, 40(6): 1244–1248, 2012.

Ghiorse, W. and Wobber, F. Special issue on deep subsurface microbiology-introduction, 1989.

Gihring, T. M., Zhang, G., Brandt, C. C., Brooks, S. C., Campbell, J. H., Carroll, S., Criddle, C. S., Green, S. J., Jardine, P., Kostka, J. E., et al. A limited microbial consortium is responsible for extended bioreduction of uranium in a contaminated aquifer. *Applied and Environmental Microbiology*, 77(17):5955–5965, 2011.

Gillin, C. P., Bailey, S. W., McGuire, K. J., and Gannon, J. P. Mapping of hydropedologic spatial patterns in a steep headwater catchment. *Soil Science Society of America Journal*, 79(2):440–453, 2015.

Gilmour, C. C., Podar, M., Bullock, A. L., Graham, A. M., Brown, S. D., Somenahally, A. C., Johs, A., Hurt Jr, R. A., Bailey, K. L., and Elias, D. A. Mercury methylation by novel microorganisms from new environments. *Environmental Science & Technology*, 47(20):11810–11820, 2013.

Gilson, E. R., Huang, S., Koster van Groos, P. G., Scheckel, K. G., Qafoku, O., Peacock, A. D., Kaplan, D. I., and Jaffé, P. R. Uranium redistribution due to water table fluctuations in sandy wetland mesocosms. *Environmental Science & Technology*, 49 (20):12214–12222, 2015.

Ginder-Vogel, M., Criddle, C. S., and Fendorf, S. Thermodynamic constraints on the oxidation of biogenic UO_2 by Fe^{III}(hydr) oxides. *Environmental Science & Technology*, 40(11):3544–3550, 2006.

Gomez-Velez, J. D. and Harvey, J. W. A hydrogeomorphic river network model predicts where and why hyporheic exchange is important in large basins. *Geophysical Research Letters*, 41(18):6403–6412, 2014.

Gorby, Y. A. and Lovley, D. R. Enzymic uranium precipitation. *Environmental Science & Technology*, 26(1):205–207, 1992.

Gorby, Y. A., Yanina, S., McLean, J. S., Rosso, K. M., Moyles, D., Dohnalkova, A., Beveridge, T. J., Chang, I. S., Kim, B. H., Kim, K. S., et al. Electrically conductive bacterial nanowires produced by *Shewanella Oneidensis* strain MR-1 and other microorganisms. *Proceedings of the National Academy of Sciences*, 103(30):11358–11363, 2006.

Greskowiak, J., Prommer, H., Liu, C., Post, V., Ma, R., Zheng, C., and Zachara, J. M. Comparison of parameter sensitivities between a laboratory and field-scale model of uranium transport in a dual domain, distributed rate reactive system. *Water Resources Research*, 46(9), 2010.

Gross, T. The world's threatened rivers - in pictures. `https://www.npr.org/2017/04/13/523717152/how-can-the-colorado-river-continue-to-support-36-million-people-in-7-states`, 2017. Accessed: 2021-03-15.

Gu, B., Schmitt, J., Chen, Z., Liang, L., and McCarthy, J. F. Adsorption and desorption of natural organic matter on iron oxide: Mechanisms and models. *Environmental Science & Technology*, 28(1):38–46, 1994.

Gu, B., Schmitt, J., Chen, Z., Liang, L., and McCarthy, J. F. Adsorption and desorption of different organic matter fractions on iron oxide. *Geochimica et Cosmochimica Acta*, 59(2):219–229, 1995.

Gu, B., Yan, H., Zhou, P., Watson, D. B., Park, M., and Istok, J. Natural humics impact uranium bioreduction and oxidation. *Environmental Science & Technology*, 39(14): 5268–5275, 2005.

Gu, B., Mishra, B., Miller, C., Wang, W., Lai, B., Brooks, S. C., Kemner, K. M., and Liang, L. X-ray fluorescence mapping of mercury on suspended mineral particles and diatoms in a contaminated freshwater system. *Biogeosciences*, 11(18):5259–5267, 2014.

Hammond, G., Lichtner, P., Lu, C., and Mills, R. T. PFLOTRAN: Reactive flow & transport code for use on laptops to leadership-class supercomputers. *Groundwater Reactive Transport Models*, pages 141–159, 2012.

Hammond, G., Lichtner, P., and Lu, C. Subsurface multiphase flow and multicomponent reactive transport modeling using high-performance computing. In *Journal of Physics: Conference Series*, volume 78(1), page 012025. IOP Publishing, 2007.

Hammond, G. E. and Lichtner, P. C. Field-scale model for the natural attenuation of uranium at the Hanford 300 Area using high-performance computing. *Water Resources Research*, 46(9), 2010.

Hammond, G. E., Lichtner, P. C., and Mills, R. Evaluating the performance of parallel subsurface simulators: An illustrative example with PFLOTRAN. *Water Resources Research*, 50(1):208–228, 2014.

Hansel, C. M., Zeiner, C. A., Santelli, C. M., and Webb, S. M. Mn(II) oxidation by an ascomycete fungus is linked to superoxide production during asexual reproduction. *Proceedings of the National Academy of Sciences*, 109(31):12621–12625, 2012.

Hansel, C. M., Lentini, C. J., Tang, Y., Johnston, D. T., Wankel, S. D., and Jardine, P. M. Dominance of sulfur-fueled iron oxide reduction in low-sulfate freshwater sediments. *The ISME Journal*, 9(11):2400–2412, 2015.

Hao, Y., Sun, Y., and Nitao, J. Overview of NUFT: A versatile numerical model for simulating flow and reactive transport in porous media. *Groundwater Reactive Transport Models*, pages 212–239, 2012.

Hausladen, D. M. and Fendorf, S. Hexavalent chromium generation within naturally structured soils and sediments. *Environmental Science & Technology*, 51(4):2058–2067, 2017.

Hazen, T. C. and Tabak, H. H. Developments in bioremediation of soils and sediments polluted with metals and radionuclides: 2. Field research on bioremediation of metals and radionuclides. *Reviews in Environmental Science and Bio/Technology*, 4(3):157–183, 2005.

He, C., Keren, R., Whittaker, M. L., Farag, I. F., Doudna, J. A., Cate, J. H., and Banfield, J. F. Genome-resolved metagenomics reveals site-specific diversity of episymbiotic CPR bacteria and DPANN archaea in groundwater ecosystems. *Nature Microbiology*, pages 1–12, 2021.

Heathwaite, A. Multiple stressors on water availability at global to catchment scales: Understanding human impact on nutrient cycles to protect water quality and water availability in the long term. *Freshwater Biology*, 55:241–257, 2010.

Howarth, R. W., Stewart, J., Ivanov, M. V., et al. *Sulphur cycling on the continents: Wetlands, terrestrial ecosystems and associated water bodies.* John Wiley & Sons, Ltd, 1992.

Hsi, C.-k. D. and Langmuir, D. Adsorption of uranyl onto ferric oxyhydroxides: Application of the surface complexation site-binding model. *Geochimica et Cosmochimica Acta*, 49(9):1931–1941, 1985.

Hubbard, S. S. and Rubin, Y. Introduction to hydrogeophysics. In *Hydrogeophysics*, pages 3–21. Springer, 2005.

Hubbard, S. S., Chen, J., Peterson, J., Majer, E. L., Williams, K. H., Swift, D. J., Mailloux, B., and Rubin, Y. Hydrogeological characterization of the South Oyster Bacterial Transport Site using geophysical data. *Water Resources Research*, 37(10): 2431–2456, 2001.

Hubbard, S. S., Gangodagamage, C., Dafflon, B., Wainwright, H., Peterson, J., Gusmeroli, A., Ulrich, C., Wu, Y., Wilson, C., Rowland, J., et al. Quantifying and relating land-surface and subsurface variability in permafrost environments using LiDAR and surface geophysical datasets. *Hydrogeology Journal*, 21(1):149–169, 2013.

Hubbard, S. S., Williams, K. H., Agarwal, D., Banfield, J., Beller, H., Bouskill, N., Brodie, E., Carroll, R., Dafflon, B., Dwivedi, D., et al. The East River, Colorado, Watershed: A mountainous community testbed for improving predictive understanding of multiscale hydrological–biogeochemical dynamics. *Vadose Zone Journal*, 17(1):1–25, 2018.

Hubbard, S. S., Varadharajan, C., Wu, Y., Wainwright, H., and Dwivedi, D. Emerging technologies and radical collaboration to advance predictive understanding of watershed hydrobiogeochemistry. *Hydrological Processes*, 34(15):3175–3182, 2020.

Hug, L. A., Castelle, C. J., Wrighton, K. C., Thomas, B. C., Sharon, I., Frischkorn, K. R., Williams, K. H., Tringe, S. G., and Banfield, J. F. Community genomic analyses constrain the distribution of metabolic traits across the Chloroflexi phylum and indicate roles in sediment carbon cycling. *Microbiome*, 1(1):1–17, 2013.

Hug, L. A., Thomas, B. C., Brown, C. T., Frischkorn, K. R., Williams, K. H., Tringe, S. G., and Banfield, J. F. Aquifer environment selects for microbial species cohorts in sediment and groundwater. *The ISME Journal*, 9(8):1846–1856, 2015.

Hug, L. A., Baker, B. J., Anantharaman, K., Brown, C. T., Probst, A. J., Castelle, C. J., Butterfield, C. N., Hernsdorf, A. W., Amano, Y., Ise, K., et al. A new view of the tree of life. *Nature Microbiology*, 1(5):1–6, 2016.

Ilton, E. S., Haiduc, A., Cahill, C. L., and Felmy, A. R. Mica surfaces stabilize pentavalent uranium. *Inorganic Chemistry*, 44(9):2986–2988, 2005.

Islam, M., Islam, F., and IWA, W. W. Arsenic contamination in groundwater in Bangladesh: An environmental and social disaster. *IWA Water Wiki*, 2010.

Istok, J., Senko, J., Krumholz, L. R., Watson, D., Bogle, M. A., Peacock, A., Chang, Y.-J., and White, D. C. *In situ* bioreduction of technetium and uranium in a nitrate-contaminated aquifer. *Environmental Science & Technology*, 38(2):468–475, 2004.

Ithurbide, A., Peulon, S., Miserque, F., Beaucaire, C., and Chaussé, A. Interaction between uranium(VI) and siderite ($FeCO_3$) surfaces in carbonate solutions. *Radiochimica Acta*, 97(3):177–180, 2009.

Jacques, D. and Simunek, J. User manual of the multicompenent variably-saturated flow and transport model HP1. Technical report, SCK-CEN, 2005.

Jacques, D., Šimůnek, J., Mallants, D., and Van Genuchten, M. T. Operator-splitting errors in coupled reactive transport codes for transient variably saturated flow and contaminant transport in layered soil profiles. *Journal of Contaminant Hydrology*, 88 (3-4):197–218, 2006.

Jacques, D., Smith, C., Šimůnek, J., and Smiles, D. Inverse optimization of hydraulic, solute transport, and cation exchange parameters using HP1 and UCODE to simulate cation exchange. *Journal of Contaminant Hydrology*, 142:109–125, 2012.

Jacques, D., Šimůnek, J., Mallants, D., van Genuchten, M. T., and Kodešová, R. The HPx reactive transport models: Summary of recent developments and applications. In *Proc. of the 4th International Conference, HYDRUS Software Applications to Subsurface Flow and Contaminant Transport Problems, Invited paper, 21–22 Mar. 2013*, pages

7–16. Dep. of Soil Science and Geology, Czech Univ. of Life Sciences Prague, Czech, 2013.

Jan, A., Coon, E. T., and Painter, S. L. Toward more mechanistic representations of biogeochemical processes in river networks: Implementation and demonstration of a multiscale model. *Environmental Modelling & Software*, 145:105166, 2021.

Janot, N., Lezama Pacheco, J. S., Pham, D. Q., O'Brien, T. M., Hausladen, D., Noël, V., Lallier, F., Maher, K., Fendorf, S., Williams, K. H., et al. Physico-chemical heterogeneity of organic-rich sediments in the Rifle aquifer, CO: Impact on uranium biogeochemistry. *Environmental Science & Technology*, 50(1):46–53, 2016.

Jardine, P., Fendorf, S., Mayes, M., Larsen, I., Brooks, S., and Bailey, W. Fate and transport of hexavalent chromium in undisturbed heterogeneous soil. *Environmental Science & Technology*, 33(17):2939–2944, 1999.

Jemison, N. E., Bizjack, M. T., Johnson, T. M., and Druhan, J. L. Influence of physical and chemical hydrology on bioremediation of a U-contaminated aquifer informed by reactive transport modeling incorporating 238U/235U ratios. *Geochimica et Cosmochimica Acta*, 269:303–328, 2020.

Jencso, K. G., McGlynn, B. L., Gooseff, M. N., Wondzell, S. M., Bencala, K. E., and Marshall, L. A. Hydrologic connectivity between landscapes and streams: Transferring reach-and plot-scale understanding to the catchment scale. *Water Resources Research*, 45(4), 2009.

Johnson, C. R., Antonopoulos, D. A., Boyanov, M. I., Flynn, T. M., Koval, J. C., Kemner, K. M., and O'Loughlin, E. J. Reduction of Sb^V by coupled biotic-abiotic processes under sulfidogenic conditions. *Heliyon*, 7(2):e06275, 2021.

Johnson, P., Zhang, P., Fuller, M. E., Scheibe, T. D., Mailloux, B. J., Onstott, T. C., DeFlaun, M. F., Hubbard, S., Radtke, J., Kovacik, W., et al. Ferrographic tracking of bacterial transport in the field at the Narrow Channel Focus Area, Oyster, VA. *Environmental Science & Technology*, 35(1):182–191, 2001.

Johnson, T., Versteeg, R., Thomle, J., Hammond, G., Chen, X., and Zachara, J. Four-dimensional electrical conductivity monitoring of stage-driven river water intrusion: Accounting for water table effects using a transient mesh boundary and conditional inversion constraints. *Water Resources Research*, 51(8):6177–6196, 2015.

Johnson, T. C., Versteeg, R. J., Ward, A., Day-Lewis, F. D., and Revil, A. Improved hydrogeophysical characterization and monitoring through parallel modeling and inversion of time-domain resistivity andinduced-polarization data. *Geophysics*, 75(4): WA27–WA41, 2010.

Johnson, T. C., Versteeg, R. J., Rockhold, M., Slater, L. D., Ntarlagiannis, D., Greenwood, W. J., and Zachara, J. Characterization of a contaminated wellfield using 3D electrical resistivity tomography implemented with geostatistical, discontinuous boundary, and known conductivity constraints. *Geophysics*, 77(6):EN85–EN96, 2012.

Jones, M. E., Nico, P. S., Ying, S., Regier, T., Thieme, J., and Keiluweit, M. Manganese-driven carbon oxidation at oxic–anoxic interfaces. *Environmental Science & Technology*, 52(21):12349–12357, 2018.

Jones, M. E., LaCroix, R. E., Zeigler, J., Ying, S. C., Nico, P. S., and Keiluweit, M. Enzymes, manganese, or iron? Drivers of oxidative organic matter decomposition in soils. *Environmental Science & Technology*, 54(21):14114–14123, 2020.

Jung, Y., Pau, G. S. H., Finsterle, S., and Pollyea, R. M. TOUGH3: A new efficient version of the TOUGH suite of multiphase flow and transport simulators. *Computers & Geosciences*, 108:2–7, 2017.

Jung, Y., Pau, G. S. H., Finsterle, S., and Doughty, C. TOUGH3 user's guide. *University of California, Berkeley*, 2018.

Kantor, R. S., Wrighton, K. C., Handley, K. M., Sharon, I., Hug, L. A., Castelle, C. J., Thomas, B. C., and Banfield, J. F. Small genomes and sparse metabolisms of sediment-associated bacteria from four candidate phyla. *MBio*, 4(5), 2013.

Kaplan, D. I., Kukkadapu, R., Seaman, J. C., Arey, B. W., Dohnalkova, A. C., Buettner, S., Li, D., Varga, T., Scheckel, K. G., and Jaffé, P. R. Iron mineralogy and uranium-binding environment in the rhizosphere of a wetland soil. *Science of the Total Environment*, 569:53–64, 2016.

Keiluweit, M., Nico, P., Harmon, M. E., Mao, J., Pett-Ridge, J., and Kleber, M. Long-term litter decomposition controlled by manganese redox cycling. *Proceedings of the National Academy of Sciences*, 112(38):E5253–E5260, 2015.

Keiluweit, M., Nico, P. S., Kleber, M., and Fendorf, S. Are oxygen limitations under recognized regulators of organic carbon turnover in upland soils? *Biogeochemistry*, 127 (2):157–171, 2016.

Kelly, S., Kemner, K., Fein, J., Fowle, D., Boyanov, M., Bunker, B., and Yee, N. X-ray absorption fine structure determination of pH-dependent U-bacterial cell wall interactions. *Geochimica et Cosmochimica Acta*, 66(22):3855–3871, 2002.

Kelly, S. D., Kemner, K. M., Carley, J., Criddle, C., Jardine, P. M., Marsh, T. L., Phillips, D., Watson, D., and Wu, W.-M. Speciation of uranium in sediments before and after *in situ* biostimulation. *Environmental Science & Technology*, 42(5):1558–1564, 2008.

Kemner, K. M., Kelly, S. D., Lai, B., Maser, J., O'Loughlin, E. J., Sholto-Douglas, D., Cai, Z., Schneegurt, M. A., Kulpa, C. F., and Nealson, K. H. Elemental and redox analysis of single bacterial cells by X-ray microbeam analysis. *Science*, 306(5696): 686–687, 2004.

Keppler, F., Eiden, R., Niedan, V., Pracht, J., and Schöler, H. Halocarbons produced by natural oxidation processes during degradation of organic matter. *Nature*, 403(6767): 298–301, 2000.

Kerisit, S., Felmy, A. R., and Ilton, E. S. Atomistic simulations of uranium incorporation into iron (hydr)-oxides. *Environmental Science & Technology*, 45(7):2770–2776, 2011.

Kersting, A., Efurd, D., Finnegan, D., Rokop, D., Smith, D., and Thompson, J. Migration of plutonium in ground water at the Nevada Test Site. *Nature*, 397(6714):56–59, 1999.

Keyes, D. E., McInnes, L. C., Woodward, C., Gropp, W., Myra, E., Pernice, M., Bell, J., Brown, J., Clo, A., Connors, J., et al. Multiphysics simulations: Challenges and opportunities. *The International Journal of High Performance Computing Applications*, 27(1):4–83, 2013.

Klingbeil, R., Kleineidam, S., Asprion, U., Aigner, T., and Teutsch, G. Relating lithofacies to hydrofacies: Outcrop-based hydrogeological characterisation of Quaternary gravel deposits. *Sedimentary Geology*, 129(3-4):299–310, 1999.

Knabe, D., Guadagnini, A., Riva, M., and Engelhardt, I. Uncertainty analysis and identification of key parameters controlling bacteria transport within a riverbank filtration scenario. *Water Resources Research*, 57(4):e2020WR027911, 2021.

Kolditz, O., Bauer, S., Bilke, L., Böttcher, N., Delfs, J.-O., Fischer, T., Görke, U. J., Kalbacher, T., Kosakowski, G., McDermott, C., et al. OpenGeoSys: An open-source initiative for numerical simulation of thermo-hydro-mechanical/chemical (THM/C) processes in porous media. *Environmental Earth Sciences*, 67(2):589–599, 2012.

Kollet, S. J. and Maxwell, R. M. Demonstrating fractal scaling of baseflow residence time distributions using a fully-coupled groundwater and land surface model. *Geophysical Research Letters*, 35(7), 2008.

Kollet, S. J., Maxwell, R. M., Woodward, C. S., Smith, S., Vanderborght, J., Vereecken, H., and Simmer, C. Proof of concept of regional scale hydrologic simulations at hydrologic resolution utilizing massively parallel computer resources. *Water Resources Research*, 46(4), 2010.

Kuffour, B. N., Engdahl, N. B., Woodward, C. S., Condon, L. E., Kollet, S., and Maxwell, R. M. Simulating coupled surface–subsurface flows with ParFlow v3. 5.0: Capabilities, applications, and ongoing development of an open-source, massively parallel, integrated hydrologic model. *Geoscientific Model Development*, 13(3):1373–1397, 2020.

Kukkadapu, R. K., Zachara, J. M., Smith, S. C., Fredrickson, J. K., and Liu, C. Dissimilatory bacterial reduction of Al-substituted goethite in subsurface sediments. *Geochimica et Cosmochimica Acta*, 65(17):2913–2924, 2001.

Kumar, N., Noël, V., Planer-Friedrich, B., Besold, J., Lezama-Pacheco, J., Bargar, J. R., Brown Jr, G. E., Fendorf, S., and Boye, K. Redox heterogeneities promote thioarsenate formation and release into groundwater from low arsenic sediments. *Environmental Science & Technology*, 54(6):3237–3244, 2020a.

Kumar, R., Heße, F., Rao, P., Musolff, A., Jawitz, J., Sarrazin, F., Samaniego, L., Fleckenstein, J., Rakovec, O., Thober, S., et al. Strong hydroclimatic controls on vulnerability to subsurface nitrate contamination across europe. *Nature Communications*, 11(1):1–10, 2020b.

Kurosaki, H., Kaplan, D. I., and Clark, S. B. Impact of environmental curium on plutonium migration and isotopic signatures. *Environmental Science & Technology*, 48(23): 13985–13991, 2014.

Kwon, K. D., Refson, K., and Sposito, G. On the role of Mn(IV) vacancies in the photoreductive dissolution of hexagonal birnessite. *Geochimica et Cosmochimica Acta*, 73(14):4142–4150, 2009.

Kwon, K. D., Refson, K., and Sposito, G. Understanding the trends in transition metal sorption by vacancy sites in birnessite. *Geochimica et Cosmochimica Acta*, 101:222–232, 2013.

Kwon, M. J., Boyanov, M. I., Antonopoulos, D. A., Brulc, J. M., Johnston, E. R., Skinner, K. A., Kemner, K. M., and O'Loughlin, E. J. Effects of dissimilatory sulfate reduction on Fe^{III}(hydr)oxide reduction and microbial community development. *Geochimica et Cosmochimica Acta*, 129:177–190, 2014a.

Kwon, M. J., Yang, J.-S., Shim, M. J., Boyanov, M. I., Kemner, K. M., and O'Loughlin, E. J. Acid extraction overestimates the total Fe^{II} in the presence of iron (hydr) oxide and sulfide minerals. *Environmental Science & Technology Letters*, 1(7):310–314, 2014b.

Labrenz, M., Druschel, G. K., Thomsen-Ebert, T., Gilbert, B., Welch, S. A., Kemner, K. M., Logan, G. A., and Summons, R. E. Gelsomina De Stasio, Philip L. Bond, Barry Lai, Shelly D. Kelly, and Jillian F. Banfield, Sphalerite (ZnS) deposits forming in natural biofilms of sulfate-reducing bacteria. *Science*, 290:1744–47, 2000.

Latta, D. E., Boyanov, M. I., Kemner, K. M., O'Loughlin, E. J., and Scherer, M. M. Abiotic reduction of uranium by Fe^{II} in soil. *Applied Geochemistry*, 27(8):1512–1524, 2012a.

Latta, D. E., Gorski, C. A., Boyanov, M. I., O'Loughlin, E. J., Kemner, K. M., and Scherer, M. M. Influence of magnetite stoichiometry on U^{VI} reduction. *Environmental Science & Technology*, 46(2):778–786, 2012b.

Latta, D. E., Mishra, B., Cook, R. E., Kemner, K. M., and Boyanov, M. I. Stable U^{IV} complexes form at high-affinity mineral surface sites. *Environmental Science & Technology*, 48(3):1683–1691, 2014.

Latta, D. E., Kemner, K. M., Mishra, B., and Boyanov, M. I. Effects of calcium and phosphate on uranium(IV) oxidation: Comparison between nanoparticulate uraninite and amorphous U^{IV}–phosphate. *Geochimica et Cosmochimica Acta*, 174:122–142, 2016.

Learman, D., Wankel, S., Webb, S., Martinez, N., Madden, A., and Hansel, C. M. Coupled biotic–abiotic Mn(II) oxidation pathway mediates the formation and structural evolution of biogenic Mn oxides. *Geochimica et Cosmochimica Acta*, 75(20):6048–6063, 2011.

Lefebvre, P., Noël, V., Lau, K. V., Jemison, N. E., Weaver, K. L., Williams, K. H., Bargar, J. R., and Maher, K. Isotopic fingerprint of uranium accumulation and redox cycling in floodplains of the Upper Colorado River Basin. *Environmental Science & Technology*, 53(7):3399–3409, 2019.

Lezama-Pacheco, J. S., Cerrato, J. M., Veeramani, H., Alessi, D. S., Suvorova, E., Bernier-Latmani, R., Giammar, D. E., Long, P. E., Williams, K. H., and Bargar, J. R. Long-term *in situ* oxidation of biogenic uraninite in an alluvial aquifer: Impact of dissolved oxygen and calcium. *Environmental Science & Technology*, 49(12):7340–7347, 2015.

Li, L., Steefel, C. I., Williams, K. H., Wilkins, M. J., and Hubbard, S. S. Mineral transformation and biomass accumulation associated with uranium bioremediation at Rifle, Colorado. *Environmental Science & Technology*, 43(14):5429–5435, 2009.

Li, L., Steefel, C. I., Kowalsky, M. B., Englert, A., and Hubbard, S. S. Effects of physical and geochemical heterogeneities on mineral transformation and biomass accumulation during biostimulation experiments at Rifle, Colorado. *Journal of Contaminant Hydrology*, 112(1-4):45–63, 2010.

Li, L., Maher, K., Navarre-Sitchler, A., Druhan, J., Meile, C., Lawrence, C., Moore, J., Perdrial, J., Sullivan, P., Thompson, A., et al. Expanding the role of reactive transport models in critical zone processes. *Earth-Science Reviews*, 165:280–301, 2017.

Lichtner, P. C., Hammond, G. E., Lu, C., Karra, S., Bisht, G., Andre, B., Mills, R., and Kumar, J. PFLOTRAN user manual: A massively parallel reactive flow and transport model for describing surface and subsurface processes. Technical report, Los Alamos National Lab.(LANL), Los Alamos, NM (United States); Sandia, 2015.

Ling, F. T., Post, J. E., Heaney, P. J., Santelli, C. M., Ilton, E. S., Burgos, W. D., and Rose, A. W. A multi-method characterization of natural terrestrial birnessites. *American Mineralogist: Journal of Earth and Planetary Materials*, 105(6):833–847, 2020.

Liu, Y., Xu, F., and Liu, C. Coupled hydro-biogeochemical processes controlling Cr reductive immobilization in Columbia River hyporheic zone. *Environmental Science & Technology*, 51(3):1508–1517, 2017.

Loar, J. M., Stewart, A. J., and Smith, J. G. Twenty-five years of ecological recovery of East Fork Poplar Creek: Review of environmental problems and remedial actions. *Environmental Management*, 47(6):1010–1020, 2011.

Long, P. E., Banfield, J., Chandler, D. P., Davis, J. A., Hettich, B., VerBerkmoes, N., Jaffe, P. R., Kerkhof, L. J., Kukkadapu, R. K., Lipton, M., et al. Microbiological, geochemical and hydrologic processes controlling uranium mobility: An integrated field scale subsurface research challenge site at Rifle, Colorado, February 2011 to January 2012. Technical report, Lawrence Berkeley National Lab.(LBNL), Berkeley, CA (United States), 2012.

Lovley, D. R. Dissimilatory metal reduction. *Annual Review of Microbiology*, 47(1): 263–290, 1993.

Lovley, D. R. Fe(III) and Mn(IV) reduction. *Environmental Microbe-Metal Interactions*, pages 1–30, 2000.

Lovley, D. R. Cleaning up with genomics: Applying molecular biology to bioremediation. *Nature Reviews Microbiology*, 1(1):35–44, 2003.

Lovley, D. R. and Phillips, E. J. Bioremediation of uranium contamination with enzymatic uranium reduction. *Environmental Science & Technology*, 26(11):2228–2234, 1992.

Lovley, D. R., Stolz, J. F., Nord, G. L., and Phillips, E. J. Anaerobic production of magnetite by a dissimilatory iron-reducing microorganism. *Nature*, 330(6145):252–254, 1987.

Lu, J., Tian, Z., Yu, J., Yang, M., and Zhang, Y. Distribution and abundance of antibiotic resistance genes in sand settling reservoirs and drinking water treatment plants across the Yellow River, China. *Water*, 10(3):246, 2018.

Luef, B., Frischkorn, K. R., Wrighton, K. C., Holman, H.-Y. N., Birarda, G., Thomas, B. C., Singh, A., Williams, K. H., Siegerist, C. E., Tringe, S. G., et al. Diverse uncultivated ultra-small bacterial cells in groundwater. *Nature Communications*, 6(1): 1–8, 2015.

Luo, W. and Gu, B. Dissolution and mobilization of uranium in a reduced sediment by natural humic substances under anaerobic conditions. *Environmental Science & Technology*, 43(1):152–156, 2009.

Luo, Y., Keenan, T. F., and Smith, M. Predictability of the terrestrial carbon cycle. *Global Change Biology*, 21(5):1737–1751, 2015.

Madritch, M. D., Kingdon, C. C., Singh, A., Mock, K. E., Lindroth, R. L., and Townsend, P. A. Imaging spectroscopy links aspen genotype with below-ground processes at landscape scales. *Philosophical Transactions of the Royal Society B: Biological Sciences*, 369(1643):20130194, 2014.

Maggi, F., Gu, C., Riley, W., Hornberger, G., Venterea, R., Xu, T., Spycher, N., Steefel, C., Miller, N., and Oldenburg, C. A mechanistic treatment of the dominant soil nitrogen cycling processes: Model development, testing, and application. *Journal of Geophysical Research: Biogeosciences*, 113(G2), 2008.

Maher, K., Bargar, J. R., and Brown Jr, G. E. Environmental speciation of actinides. *Inorganic Chemistry*, 52(7):3510–3532, 2013.

Mailloux, B. J., Fuller, M. E., Onstott, T. C., Hall, J., Dong, H., DeFlaun, M. F., Streger, S. H., Rothmel, R. K., Green, M., Swift, D. J., et al. The role of physical, chemical, and microbial heterogeneity on the field-scale transport and attachment of bacteria. *Water Resources Research*, 39(6), 2003.

Massey, M. S., Lezama-Pacheco, J. S., Michel, F. M., and Fendorf, S. Uranium incorporation into aluminum-substituted ferrihydrite during iron(II)-induced transformation. *Environmental Science: Processes & Impacts*, 16(9):2137–2144, 2014.

Mayer, K. U., Frind, E. O., and Blowes, D. W. Multicomponent reactive transport modeling in variably saturated porous media using a generalized formulation for kinetically controlled reactions. *Water Resources Research*, 38(9):13–1, 2002.

Mayes, M., Jardine, P., Larsen, I., Brooks, S., and Fendorf, S. Multispecies transport of metal–EDTA complexes and chromate through undisturbed columns of weathered fractured saprolite. *Journal of Contaminant Hydrology*, 45(3-4):243–265, 2000.

McCarthy, J. F., Czerwinski, K. R., Sanford, W. E., Jardine, P. M., and Marsh, J. D. Mobilization of transuranic radionuclides from disposal trenches by natural organic matter. *Journal of Contaminant Hydrology*, 30(1-2):49–77, 1998.

McClain, C. N., Fendorf, S., Webb, S. M., and Maher, K. Quantifying Cr^{VI} production and export from serpentine soil of the California Coast Range. *Environmental Science & Technology*, 51(1):141–149, 2017.

Megonigal, J. P. and Neubauer, S. C. Biogeochemistry of tidal freshwater wetlands. In *Coastal Wetlands*, pages 641–683. Elsevier, 2019.

Megonigal, J. P., Hines, M., and Visscher, P. Anaerobic metabolism: Linkages to trace gases and aerobic processes. *Biogeochemistry*, 2004.

Meile, C. and Scheibe, T. D. Reactive transport modeling of microbial dynamics. *Elements: An International Magazine of Mineralogy, Geochemistry, and Petrology*, 15(2): 111–116, 2019.

Mital, U., Dwivedi, D., Brown, J. B., Faybishenko, B., Painter, S. L., and Steefel, C. I. Sequential Imputation of Missing Spatio-Temporal Precipitation Data Using Random Forests. *Front. Water 2: 20. doi: 10.3389/frwa*, 2020.

Moon, H. S., Komlos, J., and Jaffé, P. R. Uranium reoxidation in previously bioreduced sediment by dissolved oxygen and nitrate. *Environmental Science & Technology*, 41 (13):4587–4592, 2007.

Moon, H., Komlos, J., and Jaffe, P. R. Biogenic U^{IV} oxidation by dissolved oxygen and nitrate in sediment after prolonged $U^{VI}/Fe^{III}/{SO_4}^{2-}$ reduction. *Journal of Contaminant Hydrology*, 105(1-2):18–27, 2009.

Morin, G., Mangeret, A., Othmane, G., Stetten, L., Seder-Colomina, M., Brest, J., Ona-Nguema, G., Bassot, S., Courbet, C., Guillevic, J., et al. Mononuclear U^{IV} complexes and ningyoite as major uranium species in lake sediments. *Geochem. Perspect. Lett*, 2: 95–105, 2016.

Mulholland, P. J., Helton, A. M., Poole, G. C., Hall, R. O., Hamilton, S. K., Peterson, B. J., Tank, J. L., Ashkenas, L. R., Cooper, L. W., Dahm, C. N., et al. Stream denitrification across biomes and its response to anthropogenic nitrate loading. *Nature*, 452(7184):202–205, 2008.

NABIR. Introducing NABIR. `https://www2.lbl.gov/NABIRarchive/generalinfo/intro.html`, 2006. Accessed: 2021-03-15.

Nagel, T., Shao, H., Singh, A., Watanabe, N., Roßkopf, C., Linder, M., Wörner, A., and Kolditz, O. Non-equilibrium thermochemical heat storage in porous media: Part 1–Conceptual model. *Energy*, 60:254–270, 2013.

National Research Council. *Research needs in subsurface science*. National Academies Press, 2000.

National Research Council. *Basic Research Opportunities in Earth Science*. The National Academies Press, Washington, DC, 2001. ISBN 978-0-309-07133-8. doi: 10.17226/9981. URL `https://www.nap.edu/catalog/9981/basic-research-opportunities-in-earth-science`.

Nealson, K. H. and Saffarini, D. Iron and manganese in anaerobic respiration: Environmental significance, physiology, and regulation. *Annual Review of Microbiology*, 48: 311–344, 1994.

Neeway, J. J., Kaplan, D. I., Bagwell, C. E., Rockhold, M. L., Szecsody, J. E., Truex, M. J., and Qafoku, N. P. A review of the behavior of radioiodine in the subsurface at two DOE sites. *Science of the Total Environment*, 691:466–475, 2019.

Nevin, K. P. and Lovley, D. R. Potential for nonenzymatic reduction of Fe^{III} via electron shuttling in subsurface sediments. *Environmental Science & Technology*, 34(12):2472–2478, 2000.

Nevin, K. P. and Lovley, D. R. Mechanisms for accessing insoluble Fe^{III} oxide during dissimilatory Fe^{III} reduction by *Geothrix fermentans*. *Applied and Environmental Microbiology*, 68(5):2294–2299, 2002.

Newcomer, M., Bouskill, N. J., Wainwright, H., Maavara, T., Arora, B., Siirila-Woodburn, E. R., Dwivedi, D., Williams, K., Steefel, C., and Hubbard, S. S. Hysteresis Patterns of Watershed Nitrogen Retention and Loss over the past 50 years in United States Hydrological Basins. *Global Biogeochemical Cycles*, 2021.

Newsome, L., Morris, K., Shaw, S., Trivedi, D., and Lloyd, J. R. The stability of microbially reduced U^{IV}; impact of residual electron donor and sediment ageing. *Chemical Geology*, 409:125–135, 2015.

N'Guessan, A. L., Moon, H. S., Peacock, A. D., Tan, H., Sinha, M., Long, P. E., and Jaffé, P. R. Postbiostimulation microbial community structure changes that control the reoxidation of uranium. *FEMS Microbiology Ecology*, 74(1):184–195, 2010.

Nico, P. S., Anastasio, C., and Zasoski, R. J. Rapid photo-oxidation of Mn(II) mediated by humic substances. *Geochimica et Cosmochimica Acta*, 66(23):4047–4056, 2002.

Nico, P. S., Kumfer, B. M., Kennedy, I. M., and Anastasio, C. Redox dynamics of mixed metal (Mn, Cr, and Fe) ultrafine particles. *Aerosol Science and Technology*, 43(1): 60–70, 2009a.

Nico, P. S., Stewart, B. D., and Fendorf, S. Incorporation of oxidized uranium into Fe (hydr) oxides during Fe^{II} catalyzed remineralization. *Environmental Science & Technology*, 43(19):7391–7396, 2009b.

Noël, V., Boye, K., Kukkadapu, R. K., Bone, S., Pacheco, J. S. L., Cardarelli, E., Janot, N., Fendorf, S., Williams, K. H., and Bargar, J. R. Understanding controls on redox processes in floodplain sediments of the Upper Colorado River Basin. *Science of the Total Environment*, 603:663–675, 2017a.

Noël, V., Boye, K., Lezama Pacheco, J. S., Bone, S. E., Janot, N., Cardarelli, E., Williams, K. H., and Bargar, J. R. Redox controls over the stability of U^{IV} in floodplains of the Upper Colorado River Basin. *Environmental Science & Technology*, 51(19):10954–10964, 2017b.

Noël, V., Boye, K., Kukkadapu, R. K., Li, Q., and Bargar, J. R. Uranium storage mechanisms in wet-dry redox cycled sediments. *Water Research*, 152:251–263, 2019.

O'Loughlin, E. J., Kelly, S. D., Cook, R. E., Csencsits, R., and Kemner, K. M. Reduction of uranium(VI) by mixed iron(II)/iron(III) hydroxide (green rust): Formation of UO_2 nanoparticles. *Environmental Science & Technology*, 37(4):721–727, 2003a.

O'Loughlin, E. J., Kemner, K. M., and Burris, D. R. Effects of Ag^{I}, Au^{III}, and Cu^{II} on the reductive dechlorination of carbon tetrachloride by green rust. *Environmental Science & Technology*, 37(13):2905–2912, 2003b.

Olsen, T. A., Brandt, C. C., and Brooks, S. C. Periphyton biofilms influence net methylmercury production in an industrially contaminated system. *Environmental Science & Technology*, 50(20):10843–10850, 2016.

Olsen, T. A., Muller, K. A., Painter, S. L., and Brooks, S. C. Kinetics of methylmercury production revisited. *Environmental Science & Technology*, 52(4):2063–2070, 2018.

O'Reilly, A. M., Chang, N.-B., and Wanielista, M. P. Cyclic biogeochemical processes and nitrogen fate beneath a subtropical stormwater infiltration basin. *Journal of Contaminant Hydrology*, 133:53–75, 2012.

Özgen-Xian, I., Kesserwani, G., Caviedes-Voullième, D., Molins, S., Xu, Z., Dwivedi, D., Moulton, J. D., and Steefel, C. I. Wavelet-based local mesh refinement for rainfall–runoff simulations. *Journal of Hydroinformatics*, 22(5):1059–1077, 2020.

O'Loughlin, E. J. Effects of electron transfer mediators on the bioreduction of lepidocrocite (γ-FeOOH) by *Shewanella putrefaciens* CN32. *Environmental Science & Technology*, 42(18):6876–6882, 2008.

O'Loughlin, E. J., Kelly, S. D., and Kemner, K. M. XAFS investigation of the interactions of U^{VI} with secondary mineralization products from the bioreduction of Fe^{III} oxides. *Environmental Science & Technology*, 44(5):1656–1661, 2010.

O'Loughlin, E. J., Boyanov, M. I., Antonopoulos, D. A., and Kemner, K. M. Redox processes affecting the speciation of technetium, uranium, neptunium, and plutonium in aquatic and terrestrial environments. In *Aquatic Redox Chemistry*, pages 477–517. ACS Publications, 2011.

O'Loughlin, E. J., Boyanov, M. I., Flynn, T. M., Gorski, C. A., Hofmann, S. M., McCormick, M. L., Scherer, M. M., and Kemner, K. M. Effects of bound phosphate on the bioreduction of lepidocrocite (γ-FeOOH) and maghemite (γ-Fe_2O_3) and formation of secondary minerals. *Environmental Science & Technology*, 47(16):9157–9166, 2013.

O'Loughlin, E. J., Gorski, C. A., Flynn, T. M., and Scherer, M. M. Electron donor utilization and secondary mineral formation during the bioreduction of lepidocrocite by *Shewanella putrefaciens* CN32. *Minerals*, 9(7):434, 2019.

O'Loughlin, E. J., Boyanov, M. I., Kemner, K. M., and Thalhammer, K. O. Reduction of Hg(II) by Fe^{II}-Bearing Smectite Clay Minerals. *Minerals*, 10(12):1079, 2020.

O'Loughlin, E. J., Boyanov, M. I., Gorski, C. A., Scherer, M. M., and Kemner, K. M. Effects of Fe^{III} oxide mineralogy and phosphate on Fe^{II} secondary mineral formation during microbial iron reduction. *Minerals*, 11(2):149, 2021.

Paddison, L. The world's threatened rivers - in pictures. `https://www.theguardian.com/sustainable-business/gallery/2016/sep/22/worlds-threatened-rivers-pollution-industry-agriculture-in-pictures`, 2016. Accessed: 2021-03-15.

Painter, S. L. Multiscale framework for modeling multicomponent reactive transport in stream corridors. *Water Resources Research*, 54(10):7216–7230, 2018.

Painter, S. L. On the representation of hyporheic exchange in models for reactive transport in stream and river corridors. *Frontiers in Water*, 2:69, 2021.

Painter, S. L., Coon, E. T., Atchley, A. L., Berndt, M., Garimella, R., Moulton, J. D., Svyatskiy, D., and Wilson, C. J. Integrated surface/subsurface permafrost thermal hydrology: Model formulation and proof-of-concept simulations. *Water Resources Research*, 52(8):6062–6077, 2016a.

Painter, T. H., Berisford, D. F., Boardman, J. W., Bormann, K. J., Deems, J. S., Gehrke, F., Hedrick, A., Joyce, M., Laidlaw, R., Marks, D., et al. The Airborne Snow Observatory: Fusion of scanning lidar, imaging spectrometer, and physically-based modeling for mapping snow water equivalent and snow albedo. *Remote Sensing of Environment*, 184:139–152, 2016b.

Pan, C., Jiao, Y., Kersting, A. B., and Zavarin, M. Plutonium redox transformation in the presence of iron, organic matter, and hydroxyl radicals: Kinetics and mechanistic insights. *Environmental Science & Technology*, 55(3):1800–1810, 2021.

Paniconi, C. and Putti, M. Physically based modeling in catchment hydrology at 50: Survey and outlook. *Water Resources Research*, 51(9):7090–7129, 2015.

Parks, J. M., Johs, A., Podar, M., Bridou, R., Hurt, R. A., Smith, S. D., Tomanicek, S. J., Qian, Y., Brown, S. D., Brandt, C. C., et al. The genetic basis for bacterial mercury methylation. *Science*, 339(6125):1332–1335, 2013.

Patton, N. R., Lohse, K. A., Godsey, S. E., Crosby, B. T., and Seyfried, M. S. Predicting soil thickness on soil mantled hillslopes. *Nature Communications*, 9(1):1–10, 2018.

Pawloski, G., Wurtz, J., and Drellack, S. The underground test area project of the nevada test site: building confidence in groundwater flow and transport models at pahute mesa through focused characterization studies. Technical report, Lawrence Livermore National Lab.(LLNL), Livermore, CA (United States), 2009.

Peña, J., Bargar, J. R., and Sposito, G. Copper sorption by the edge surfaces of synthetic birnessite nanoparticles. *Chemical Geology*, 396:196–207, 2015.

Peretyazhko, T., Zachara, J. M., Heald, S. M., Jeon, B.-H., Kukkadapu, R. K., Liu, C., Moore, D., and Resch, C. T. Heterogeneous reduction of Tc^{VII} by Fe^{II} at the solid–water interface. *Geochimica et Cosmochimica Acta*, 72(6):1521–1539, 2008.

Peterson, M. J., Mayes, M. A., Brooks, S. C., Mathews, T. J., Johs, A., Rodriguez, L. G., DeRolph, C. R., Pierce, E. M., Watson, D. B., Muller, K. A., et al. Mercury Remediation Technology Development for Lower East Fork Poplar Creek—FY 2017 Progress Report. Technical report, Oak Ridge National Lab.(ORNL), Oak Ridge, TN (United States), 2018.

Phelps, T., Fliermans, C., Garland, T., Pfiffner, S., and White, D. Methods for recovery of deep terrestrial subsurface sediments for microbiological studies. *Journal of Microbiological Methods*, 9(4):267–279, 1989.

Plathe, K. L., Lee, S.-W., Tebo, B. M., Bargar, J. R., and Bernier-Latmani, R. Impact of microbial Mn oxidation on the remobilization of bioreduced U^{IV}. *Environmental Science & Technology*, 47(8):3606–3613, 2013.

Podar, M., Gilmour, C. C., Brandt, C. C., Soren, A., Brown, S. D., Crable, B. R., Palumbo, A. V., Somenahally, A. C., and Elias, D. A. Global prevalence and distribution of genes and microorganisms involved in mercury methylation. *Science Advances*, 1(9):e1500675, 2015.

Powell, B. A., Fjeld, R. A., Kaplan, D. I., Coates, J. T., and Serkiz, S. M. Adsorption and reduction by synthetic hematite and goethite. *Environmental Science&Technology*, 39(7), 2005.

Powell, B. A., Dai, Z., Zavarin, M., Zhao, P., and Kersting, A. B. Stabilization of plutonium nano-colloids by epitaxial distortion on mineral surfaces. *Environmental Science & Technology*, 45(7):2698–2703, 2011.

Powell, R. M., Puls, R. W., Hightower, S. K., and Sabatini, D. A. Coupled iron corrosion and chromate reduction: Mechanisms for subsurface remediation. *Environmental Science & Technology*, 29(8):1913–1922, 1995.

Prancevic, J. P. and Kirchner, J. W. Topographic controls on the extension and retraction of flowing streams. *Geophysical Research Letters*, 46(4):2084–2092, 2019.

Prein, A. F., Holland, G. J., Rasmussen, R. M., Clark, M. P., and Tye, M. R. Running dry: The US Southwest's drift into a drier climate state. *Geophysical Research Letters*, 43(3):1272–1279, 2016.

Prikryl, J. D., Jain, A., Turner, D. R., and Pabalan, R. T. Uranium(VI) sorption behavior on silicate mineral mixtures. *Journal of Contaminant Hydrology*, 47(2-4):241–253, 2001.

Pruess, K. TOUGH user's guide, 1987.

Pruess, K. The TOUGH codes—A family of simulation tools for multiphase flow and transport processes in permeable media. *Vadose Zone Journal*, 3(3):738–746, 2004.

Qian, Y., Yin, X., Lin, H., Rao, B., Brooks, S. C., Liang, L., and Gu, B. Why dissolved organic matter enhances photodegradation of methylmercury. *Environmental Science & Technology Letters*, 1(10):426–431, 2014.

Ragnarsdottir, K., Charlet, L., et al. Uranium behaviour in natural environments. *Environmental mineralogy: Microbial interactions, anthropogenic influences, contaminated land and waste management*, pages 245–289, 2000.

Rathore, S. S., Jan, A., Coon, E. T., and Painter, S. L. On the reliability of parameter inferences in a multiscale model for transport in stream corridors. *Water Resources Research*, 57(5):e2020WR028908, 2021.

Reguera, G., McCarthy, K. D., Mehta, T., Nicoll, J. S., Tuominen, M. T., and Lovley, D. R. Extracellular electron transfer via microbial nanowires. *Nature*, 435(7045):1098–1101, 2005.

Reichstein, M., Camps-Valls, G., Stevens, B., Jung, M., Denzler, J., Carvalhais, N., et al. Deep learning and process understanding for data-driven Earth system science. *Nature*, 566(7743):195–204, 2019.

Ren, H., Song, X., Fang, Y., Hou, Z. J., and Scheibe, T. D. Machine learning analysis of hydrologic exchange flows and transit time distributions in a large regulated river. *Frontiers in Artificial Intelligence*, 4:39, 2021.

Riley, W., Maggi, F., Kleber, M., Torn, M., Tang, J., Dwivedi, D., and Guerry, N. Long residence times of rapidly decomposable soil organic matter: Application of a multi-phase, multi-component, and vertically resolved model (BAMS1) to soil carbon dynamics. *Geoscientific Model Development*, 7(4):1335–1355, 2014.

Riscassi, A., Miller, C., and Brooks, S. Seasonal and flow-driven dynamics of particulate and dissolved mercury and methylmercury in a stream impacted by an industrial mercury source. *Environmental Toxicology and Chemistry*, 35(6):1386–1400, 2016.

Rodell, M., Velicogna, I., and Famiglietti, J. S. Satellite-based estimates of groundwater depletion in India. *Nature*, 460(7258):999–1002, 2009.

Roden, E. E. and Wetzel, R. G. Organic carbon oxidation and suppression of methane production by microbial Fe^{III} oxide reduction in vegetated and unvegetated freshwater wetland sediments. *Limnology and Oceanography*, 41(8):1733–1748, 1996.

Roden, E. E., Kappler, A., Bauer, I., Jiang, J., Paul, A., Stoesser, R., Konishi, H., and Xu, H. Extracellular electron transfer through microbial reduction of solid-phase humic substances. *Nature Geoscience*, 3(6):417–421, 2010.

Rogers, D. B., Newcomer, M., Raberg, J., Dwivedi, D., Steefel, C., Bouskill, N., Nico, P., Faybishenko, B., Fox, P., Conrad, M., et al. Modeling the impact of riparian hollows on river corridor nitrogen exports. *Frontiers in Water*, 3:7, 2021.

Royer, R. A., Burgos, W. D., Fisher, A. S., Jeon, B.-H., Unz, R. F., and Dempsey, B. A. Enhancement of hematite bioreduction by natural organic matter. *Environmental Science & Technology*, 36(13):2897–2904, 2002.

Sani, R. K., Peyton, B. M., Dohnalkova, A., and Amonette, J. E. Reoxidation of reduced uranium with iron(III)(hydr) oxides under sulfate-reducing conditions. *Environmental Science & Technology*, 39(7):2059–2066, 2005.

Santelli, C. M., Webb, S. M., Dohnalkova, A. C., and Hansel, C. M. Diversity of Mn oxides produced by Mn(II)-oxidizing fungi. *Geochimica et Cosmochimica Acta*, 75(10): 2762–2776, 2011.

Santschi, P. H., Roberts, K. A., and Guo, L. Organic nature of colloidal actinides transported in surface water environments. *Environmental Science & Technology*, 36(17): 3711–3719, 2002.

Sassen, D. S., Hubbard, S. S., Bea, S. A., Chen, J., Spycher, N., and Denham, M. E. Reactive facies: An approach for parameterizing field-scale reactive transport models using geophysical methods. *Water Resources Research*, 48(10), 2012.

Scheibe, T. D. and Chien, Y.-J. An evaluation of conditioning data for solute transport prediction. *Groundwater*, 41(2):128–141, 2003.

Scheibe, T. D. and Stafford, R. A. Integrated hydro-terrestrial modeling: Development of a national capability, 2020.

Scheibe, T. D., Chien, Y.-J., and Radtke, J. S. Use of quantitative models to design microbial transport experiments in a sandy aquifer. *Groundwater*, 39(2):210–222, 2001.

Scheibe, T. D., , Fang, Y., Murray, C. J., Roden, E. E., Chen, J., Chien, Y.-J., Brooks, S. C., and Hubbard, S. S. Transport and biogeochemical reaction of metals in a physically and chemically heterogeneous aquifer. *Geosphere*, 2(4):220–235, 2006.

Scheibe, T. D., Hubbard, S. S., Onstott, T. C., and Deflaun, M. F. Lessons learned from bacterial transport experiments at the South Oyster Site. *Ground Water*, 49 (PNNL-SA-76534), 2011.

Scheibe, T. D., Murphy, E. M., Chen, X., Rice, A. K., Carroll, K. C., Palmer, B. J., Tartakovsky, A. M., Battiato, I., and Wood, B. D. An analysis platform for multiscale hydrogeologic modeling with emphasis on hybrid multiscale methods. *Groundwater*, 53(1):38–56, 2015a.

Scheibe, T. D., Schuchardt, K., Agarwal, K., Chase, J., Yang, X., Palmer, B. J., Tartakovsky, A. M., Elsethagen, T., and Redden, G. Hybrid multiscale simulation of a mixing-controlled reaction. *Advances in Water Resources*, 83:228–239, 2015b.

Schmidt, M. W., Torn, M. S., Abiven, S., Dittmar, T., Guggenberger, G., Janssens, I. A., Kleber, M., Kögel-Knabner, I., Lehmann, J., Manning, D. A., et al. Persistence of soil organic matter as an ecosystem property. *Nature*, 478(7367):49–56, 2011.

Schwartz, G. E., Olsen, T. A., Muller, K. A., and Brooks, S. C. Ecosystem controls on methylmercury production by periphyton biofilms in a contaminated stream: Implications for predictive modeling. *Environmental Toxicology and Chemistry*, 38(11): 2426–2435, 2019.

Senko, J. M., Istok, J. D., Suflita, J. M., and Krumholz, L. R. *In-situ* evidence for uranium immobilization and remobilization. *Environmental Science & Technology*, 36 (7):1491–1496, 2002.

Senko, J. M., Mohamed, Y., Dewers, T. A., and Krumholz, L. R. Role for Fe^{III}) minerals in nitrate-dependent microbial U^{IV} oxidation. *Environmental Science & Technology*, 39(8):2529–2536, 2005a.

Senko, J. M., Suflita, J. M., and Krumholz, L. R. Geochemical controls on microbial nitrate-dependent U^{IV} oxidation. *Geomicrobiology Journal*, 22(7-8):371–378, 2005b.

Senko, J. M., Kelly, S. D., Dohnalkova, A. C., McDonough, J. T., Kemner, K. M., and Burgos, W. D. The effect of U^{VI} bioreduction kinetics on subsequent reoxidation of biogenic U^{IV}. *Geochimica et Cosmochimica Acta*, 71(19):4644–4654, 2007.

Sharon, I., Kertesz, M., Hug, L. A., Pushkarev, D., Blauwkamp, T. A., Castelle, C. J., Amirebrahimi, M., Thomas, B. C., Burstein, D., Tringe, S. G., et al. Accurate, multi-kb reads resolve complex populations and detect rare microorganisms. *Genome Research*, 25(4):534–543, 2015.

Sharp, J. O., Lezama-Pacheco, J. S., Schofield, E. J., Junier, P., Ulrich, K.-U., Chinni, S., Veeramani, H., Margot-Roquier, C., Webb, S. M., Tebo, B. M., et al. Uranium speciation and stability after reductive immobilization in aquifer sediments. *Geochimica et Cosmochimica Acta*, 75(21):6497–6510, 2011.

Shi, L., Richardson, D. J., Wang, Z., Kerisit, S. N., Rosso, K. M., Zachara, J. M., and Fredrickson, J. K. The roles of outer membrane cytochromes of *shewanella* and *geobacter* in extracellular electron transfer. *Environmental Microbiology Reports*, 1(4): 220–227, 2009.

Shuai, P., Chen, X., Song, X., Hammond, G. E., Zachara, J., Royer, P., Ren, H., Perkins, W. A., Richmond, M. C., and Huang, M. Dam operations and subsurface hydrogeology control dynamics of hydrologic exchange flows in a regulated river reach. *Water Resources Research*, 55(4):2593–2612, 2019.

Simanova, A. A., Kwon, K. D., Bone, S. E., Bargar, J. R., Refson, K., Sposito, G., and Peña, J. Probing the sorption reactivity of the edge surfaces in birnessite nanoparticles using nickel(II). *Geochimica et Cosmochimica Acta*, 164:191–204, 2015.

Šimůnek, J., Van Genuchten, M. T., and Šejna, M. The HYDRUS software package for simulating two-and three-dimensional movement of water, heat, and multiple solutes in variably-saturated media. *Technical Manual, Version*, 1:241, 2006.

Šimůnek, J., van Genuchten, M. T., and Šejna, M. Development and applications of the HYDRUS and STANMOD software packages and related codes. *Vadose Zone Journal*, 7(2):587–600, 2008.

Šimůnek, J. and van Genuchten, M. T. Modeling nonequilibrium flow and transport processes using HYDRUS. *Vadose Zone Journal*, 7(2):782–797, 2008.

Singer, D. M., Chatman, S. M., Ilton, E. S., Rosso, K. M., Banfield, J. F., and Waychunas, G. A. U(VI) sorption and reduction kinetics on the magnetite (111) surface. *Environmental Science & Technology*, 46(7):3821–3830, 2012.

Sivaswamy, V., Boyanov, M. I., Peyton, B. M., Viamajala, S., Gerlach, R., Apel, W. A., Sani, R. K., Dohnalkova, A., Kemner, K. M., and Borch, T. Multiple mechanisms of uranium immobilization by *Cellulomonas* sp. strain ES6. *Biotechnology and Bioengineering*, 108(2):264–276, 2011.

Skyllberg, U., Bloom, P. R., Qian, J., Lin, C.-M., and Bleam, W. F. Complexation of mercury(II) in soil organic matter: EXAFS evidence for linear two-coordination with reduced sulfur groups. *Environmental Science & Technology*, 40(13):4174–4180, 2006.

Smith, D., Finnegan, D., and Bowen, S. An inventory of long-lived radionuclides residual from underground nuclear testing at the Nevada test site, 1951–1992. *Journal of Environmental Radioactivity*, 67(1):35–51, 2003.

Song, X., Chen, X., Stegen, J., Hammond, G., Song, H.-S., Dai, H., Graham, E., and Zachara, J. M. Drought conditions maximize the impact of high-frequency flow variations on thermal regimes and biogeochemical function in the hyporheic zone. *Water Resources Research*, 54(10):7361–7382, 2018.

Sonnenthal, E., Spycher, N., Xu, T., and Zheng, L. TOUGHREACT V4. 12-OMP and TReactMech V1. 0 Geochemical and Reactive-Transport User Guide. 2021.

Spiro, T. G., Bargar, J. R., Sposito, G., and Tebo, B. M. Bacteriogenic manganese oxides. *Accounts of Chemical Research*, 43(1):2–9, 2010.

Spycher, N. F., Issarangkun, M., Stewart, B. D., Şengör, S. S., Belding, E., Ginn, T. R., Peyton, B. M., and Sani, R. K. Biogenic uraninite precipitation and its reoxidation by Fe^{III}(hydr) oxides: A reaction modeling approach. *Geochimica et Cosmochimica Acta*, 75(16):4426–4440, 2011.

Steefel, C. I. Reactive transport at the crossroads. *Reviews in Mineralogy and Geochemistry*, 85(1):1–26, 2019.

Steefel, C. I., Carroll, S., Zhao, P., and Roberts, S. Cesium migration in Hanford sediment: A multisite cation exchange model based on laboratory transport experiments. *Journal of Contaminant Hydrology*, 67(1-4):219–246, 2003.

Steefel, C. I., DePaolo, D. J., and Lichtner, P. C. Reactive transport modeling: An essential tool and a new research approach for the Earth sciences. *Earth and Planetary Science Letters*, 240(3-4):539–558, 2005.

Steefel, C., Appelo, C., Arora, B., Jacques, D., Kalbacher, T., Kolditz, O., Lagneau, V., Lichtner, P., Mayer, K. U., Meeussen, J., et al. Reactive transport codes for subsurface environmental simulation. *Computational Geosciences*, 19(3):445–478, 2015.

Stegen, J. C. and Goldman, A. E. WHONDRS: A community resource for studying dynamic river corridors, 2018.

Stetten, L., Mangeret, A., Brest, J., Seder-Colomina, M., Le Pape, P., Ikogou, M., Zeyen, N., Thouvenot, A., Julien, A., Alcalde, G., et al. Geochemical control on the reduction of U^{VI} to mononuclear U^{IV} species in lacustrine sediments. *Geochimica et Cosmochimica Acta*, 222:171–186, 2018.

Stewart, B. D., Girardot, C., Spycher, N., Sani, R. K., and Peyton, B. M. Influence of chelating agents on biogenic uraninite reoxidation by Fe^{III}(hydr) oxides. *Environmental Science & Technology*, 47(1):364–371, 2013.

Stoliker, D. L., Campbell, K. M., Fox, P. M., Singer, D. M., Kaviani, N., Carey, M., Peck, N. E., Bargar, J. R., Kent, D. B., and Davis, J. A. Evaluating chemical extraction techniques for the determination of uranium oxidation state in reduced aquifer sediments. *Environmental Science & Technology*, 47(16):9225–9232, 2013.

Stucker, V. K., Williams, K. H., Robbins, M. J., and Ranville, J. F. Arsenic geochemistry in a biostimulated aquifer: An aqueous speciation study. *Environmental Toxicology and Chemistry*, 32(6):1216–1223, 2013.

Stucker, V. K., Silverman, D. R., Williams, K. H., Sharp, J. O., and Ranville, J. F. Thioarsenic species associated with increased arsenic release during biostimulated subsurface sulfate reduction. *Environmental Science & Technology*, 48(22):13367–13375, 2014.

Stylo, M., Alessi, D. S., Shao, P. P., Lezama-Pacheco, J. S., Bargar, J. R., and Bernier-Latmani, R. Biogeochemical controls on the product of microbial U^{VI} reduction. *Environmental Science & Technology*, 47(21):12351–12358, 2013.

Suzuki, Y., Kelly, S. D., Kemner, K. M., and Banfield, J. F. Nanometre-size products of uranium bioreduction. *Nature*, 419(6903):134–134, 2002.

Szecsody, J. E., Krupka, K. M., Williams, M. D., Cantrell, K. J., Resch, C. T., and Fruchter, J. S. Uranium mobility during *in situ* redox manipulation of the 100 Areas of the Hanford Site. Technical report, Pacific Northwest National Lab.(PNNL), Richland, WA (United States), 1998.

Taillefert, M., Beckler, J. S., Carey, E., Burns, J. L., Fennessey, C. M., and DiChristina, T. J. *Shewanella putrefaciens* produces an Fe^{III}-solubilizing organic ligand during anaerobic respiration on insoluble Fe^{III} oxides. *Journal of Inorganic Biochemistry*, 101(11-12):1760–1767, 2007.

Tan, H., Zhang, G., Heaney, P. J., Webb, S. M., and Burgos, W. D. Characterization of manganese oxide precipitates from appalachian coal mine drainage treatment systems. *Applied Geochemistry*, 25(3):389–399, 2010.

Tang, G., Watson, D. B., Wu, W.-M., Schadt, C. W., Parker, J. C., and Brooks, S. C. U^{VI} bioreduction with emulsified vegetable oil as the electron donor–model application to a field test. *Environmental Science & Technology*, 47(7):3218–3225, 2013a.

Tang, G., Wu, W.-M., Watson, D. B., Parker, J. C., Schadt, C. W., Shi, X., and Brooks, S. C. U^{VI} bioreduction with emulsified vegetable oil as the electron donor–microcosm tests and model development. *Environmental Science & Technology*, 47(7):3209–3217, 2013b.

Tang, Y., Webb, S. M., Estes, E. R., and Hansel, C. M. Chromium(III) oxidation by biogenic manganese oxides with varying structural ripening. *Environmental Science: Processes & Impacts*, 16(9):2127–2136, 2014.

Tokunaga, T. K., Wan, J., Kim, Y., Sutton, S. R., Newville, M., Lanzirotti, A., and Rao, W. Real-time x-ray absorption spectroscopy of uranium, iron, and manganese in contaminated sediments during bioreduction. *Environmental Science & Technology*, 42 (8):2839–2844, 2008.

Tolar, B. B., Boye, K., Bobb, C., Maher, K., Bargar, J. R., and Francis, C. A. Stability of floodplain subsurface microbial communities through seasonal hydrological and geochemical cycles. *Frontiers in Earth Science*, 8, 2020.

Tripathi, A., Tripathi, D. K., Chauhan, D., and Kumar, N. Chromium(VI)-induced phytotoxicity in river catchment agriculture: Evidence from physiological, biochemical and anatomical alterations in *Cucumis sativus* (L.) used as model species. *Chemistry and Ecology*, 32(1):12–33, 2016.

Ulrich, K.-U., Ilton, E. S., Veeramani, H., Sharp, J. O., Bernier-Latmani, R., Schofield, E. J., Bargar, J. R., and Giammar, D. E. Comparative dissolution kinetics of biogenic and chemogenic uraninite under oxidizing conditions in the presence of carbonate. *Geochimica et Cosmochimica Acta*, 73(20):6065–6083, 2009.

van Genuchten, C. M. and Peña, J. Sorption selectivity of birnessite particle edges: a d-pdf analysis of Cd(II) and Pb(II) sorption by δ-MnO_2 and ferrihydrite. *Environmental Science: Processes & Impacts*, 18(8):1030–1041, 2016.

Varadharajan, C., Beller, H. R., Bill, M., Brodie, E. L., Conrad, M. E., Han, R., Irwin, C., Larsen, J. T., Lim, H.-C., Molins, S., et al. Reoxidation of chromium(III) products formed under different biogeochemical regimes. *Environmental Science & Technology*, 51(9):4918–4927, 2017.

Varol, M. and Şen, B. Assessment of nutrient and heavy metal contamination in surface water and sediments of the upper Tigris River, Turkey. *Catena*, 92:1–10, 2012.

Vaughn, L. J., Conrad, M. E., Bill, M., and Torn, M. S. Isotopic insights into methane production, oxidation, and emissions in Arctic polygon tundra. *Global Change Biology*, 22(10):3487–3502, 2016.

Veeramani, H., Alessi, D. S., Suvorova, E. I., Lezama-Pacheco, J. S., Stubbs, J. E., Sharp, J. O., Dippon, U., Kappler, A., Bargar, J. R., and Bernier-Latmani, R. Products of abiotic U^{VI} reduction by biogenic magnetite and vivianite. *Geochimica et Cosmochimica Acta*, 75(9):2512–2528, 2011.

Vörösmarty, C. J., McIntyre, P. B., Gessner, M. O., Dudgeon, D., Prusevich, A., Green, P., Glidden, S., Bunn, S. E., Sullivan, C. A., Liermann, C. R., et al. Global threats to human water security and river biodiversity. *Nature*, 467(7315):555–561, 2010.

Wainwright, H., Faybishenko, B., Molins, S., Davis, J., Arora, B., Pau, G., Johnson, J., Flach, G., Denham, M., Eddy-Dilek, C., et al. Effective long-term monitoring strategies by integrating reactive transport models with *in situ* geochemical measurements 16212. In *WM2016 Conf*, pages 1–15, 2016a.

Wainwright, H. M., Dafflon, B., Smith, L. J., Hahn, M. S., Curtis, J. B., Wu, Y., Ulrich, C., Peterson, J. E., Torn, M. S., and Hubbard, S. S. Identifying multiscale zonation and assessing the relative importance of polygon geomorphology on carbon fluxes in an Arctic tundra ecosystem. *Journal of Geophysical Research: Biogeosciences*, 120(4): 788–808, 2015.

Wainwright, H. M., Flores Orozco, A., Bücker, M., Dafflon, B., Chen, J., Hubbard, S. S., and Williams, K. H. Hierarchical Bayesian method for mapping biogeochemical hot spots using induced polarization imaging. *Water Resources Research*, 52(1):533–551, 2016b.

Wainwright, H. M., Steefel, C., Trutner, S. D., Henderson, A. N., Nikolopoulos, E. I., Wilmer, C. F., Chadwick, K. D., Falco, N., Schaettle, K. B., Brown, J. B., et al. Satellite-derived foresummer drought sensitivity of plant productivity in Rocky Mountain headwater catchments: Spatial heterogeneity and geological-geomorphological control. *Environmental Research Letters*, 15(8):084018, 2020.

Wainwright, H. M., Uhlemann, S., Franklin, M., Falco, N., Bouskill, N. J., Newcomer, M. E., Dafflon, B., Siirila-Woodburn, E. R., Minsley, B. J., Williams, K. H., et al. Watershed zonation through hillslope clustering for tractably quantifying above-and below-ground watershed heterogeneity and functions. *Hydrology and Earth System Sciences*, 26(2):429–444, 2022.

Wainwright, H., Sassen, D., Chen, J., and Hubbard, S. Bayesian hierarchical approach for estimation of reactive facies over plume-scales using geophysical datasets. *Water Resources Research*, 2014.

Wall, J. D. and Krumholz, L. R. Uranium reduction. *Annu. Rev. Microbiol.*, 60:149–166, 2006.

Wan, J., Tokunaga, T. K., Brodie, E., Wang, Z., Zheng, Z., Herman, D., Hazen, T. C., Firestone, M. K., and Sutton, S. R. Reoxidation of bioreduced uranium under reducing conditions. *Environmental Science & Technology*, 39(16):6162–6169, 2005.

Wang, S., Jaffe, P. R., Li, G., Wang, S., and Rabitz, H. A. Simulating bioremediation of uranium-contaminated aquifers; uncertainty assessment of model parameters. *Journal of Contaminant Hydrology*, 64(3-4):283–307, 2003.

Wang, Z., Lee, S.-W., Catalano, J. G., Lezama-Pacheco, J. S., Bargar, J. R., Tebo, B. M., and Giammar, D. E. Adsorption of uranium(VI) to manganese oxides: X-ray absorption spectroscopy and surface complexation modeling. *Environmental Science & Technology*, 47(2):850–858, 2013a.

Wang, Z., Lee, S.-W., Kapoor, P., Tebo, B. M., and Giammar, D. E. Uraninite oxidation and dissolution induced by manganese oxide: A redox reaction between two insoluble minerals. *Geochimica et Cosmochimica Acta*, 100:24–40, 2013b.

Wang, Z., Tebo, B. M., and Giammar, D. E. Effects of Mn^{II} on UO_2 dissolution under anoxic and oxic conditions. *Environmental Science & Technology*, 48(10):5546–5554, 2014a.

Wang, Z., Xiong, W., Tebo, B. M., and Giammar, D. E. Oxidative UO_2 dissolution induced by soluble Mn(III). *Environmental Science & Technology*, 48(1):289–298, 2014b.

Wang, Z., Ulrich, K.-U., Pan, C., and Giammar, D. E. Measurement and modeling of U^{IV} adsorption to metal oxide minerals. *Environmental Science & Technology Letters*, 2(8):227–232, 2015.

Watson, D. B., Wu, W.-M., Mehlhorn, T., Tang, G., Earles, J., Lowe, K., Gihring, T. M., Zhang, G., Phillips, J., Boyanov, M. I., et al. *In situ* bioremediation of uranium with emulsified vegetable oil as the electron donor. *Environmental Science & Technology*, 47(12):6440–6448, 2013.

Wentz, D. A., Brigham, M. E., Chasar, L. C., Lutz, M. A., and Krabbenhoft, D. P. Mercury in the nation's streams-Levels, trends, and implications. Technical report, US Geological Survey, 2014.

White, M. D. and Oostrom, M. STOMP subsurface transport over multiple phases version 3.0 User's guide. Technical report, Pacific Northwest National Lab., Richland, WA (US), 2003.

White, M. D. and Oostrom, M. STOMP subsurface transport over multiple phases version 2.0 theory guide. Technical report, Pacific Northwest National Lab.(PNNL), Richland, WA (United States), 2000.

White, M. D., Bacon, D. H., McGrail, B. P., Watson, D. J., White, S. K., and Zhang, Z. STOMP subsurface transport over multiple phases: STOMP-CO_2 and STOMP-CO_2e guide: version 1.0. Technical report, Pacific Northwest National Lab.(PNNL), Richland, WA (United States), 2012.

Wiatrowski, H. A., Das, S., Kukkadapu, R., Ilton, E. S., Barkay, T., and Yee, N. Reduction of Hg^{I} to Hg^{0} by magnetite. *Environmental Science & Technology*, 43(14): 5307–5313, 2009.

Wilkins, M. J., VerBerkmoes, N. C., Williams, K. H., Callister, S. J., Mouser, P. J., Elifantz, H., Thomas, B. C., Nicora, C. D., Shah, M. B., Abraham, P., et al. Proteogenomic monitoring of *Geobacter* physiology during stimulated uranium bioremediation. *Applied and Environmental Microbiology*, 75(20):6591–6599, 2009.

Williams, K. H., Long, P. E., Davis, J. A., Wilkins, M. J., N'Guessan, A. L., Steefel, C. I., Yang, L., Newcomer, D., Spane, F. A., Kerkhof, L. J., et al. Acetate availability and its influence on sustainable bioremediation of uranium-contaminated groundwater. *Geomicrobiology Journal*, 28(5-6):519–539, 2011.

Williams, K. H., Bargar, J. R., Lloyd, J. R., and Lovley, D. R. Bioremediation of uranium-contaminated groundwater: A systems approach to subsurface biogeochemistry. *Current Opinion in Biotechnology*, 24(3):489–497, 2013.

Wrighton, K. C., Thomas, B. C., Sharon, I., Miller, C. S., Castelle, C. J., VerBerkmoes, N. C., Wilkins, M. J., Hettich, R. L., Lipton, M. S., Williams, K. H., et al. Fermentation, hydrogen, and sulfur metabolism in multiple uncultivated bacterial phyla. *Science*, 337(6102):1661–1665, 2012.

Wu, R., Chen, X., Hammond, G., Bisht, G., Song, X., Huang, M., Niu, G.-Y., and Ferre, T. Coupling surface flow with high-performance subsurface reactive flow and transport code PFLOTRAN. *Environmental Modelling & Software*, 137:104959, 2021.

Wu, W.-M., Carley, J., Fienen, M., Mehlhorn, T., Lowe, K., Nyman, J., Luo, J., Gentile, M. E., Rajan, R., Wagner, D., et al. Pilot-scale *in situ* bioremediation of uranium in a highly contaminated aquifer. 1. Conditioning of a treatment zone. *Environmental Science & Technology*, 40(12):3978–3985, 2006a.

Wu, W.-M., Carley, J., Gentry, T., Ginder-Vogel, M. A., Fienen, M., Mehlhorn, T., Yan, H., Caroll, S., Pace, M. N., Nyman, J., et al. Pilot-scale *in situ* bioremedation of uranium in a highly contaminated aquifer. 2. reduction of U^{VI} and geochemical control of U^{VI} bioavailability. *Environmental Science & Technology*, 40(12):3986–3995, 2006b.

Wu, W.-M., Carley, J., Green, S. J., Luo, J., Kelly, S. D., Nostrand, J. V., Lowe, K., Mehlhorn, T., Carroll, S., Boonchayanant, B., et al. Effects of nitrate on the stability of uranium in a bioreduced region of the subsurface. *Environmental Science & Technology*, 44(13):5104–5111, 2010.

Xu, C., Santschi, P., Roberts, K., Zhong, J., Hatcher, P., Hung, C., Francis, A., Dodge, C., and Honeyman, B. Colloidal cutin-like siderophoric molecules mobilize plutonium from contaminated soils of the Rocky Flats Environmental Technology Site (RFETS), USA. *Environmental Science and Technology*, 42(22):8211–8217, 2008.

Xu, S. and Jaffé, P. R. Effects of plants on the removal of hexavalent chromium in wetland sediments. *Journal of Environmental Quality*, 35(1):334–341, 2006.

Yabusaki, S. B., Steefel, C. I., and Wood, B. Multidimensional, multicomponent, subsurface reactive transport in nonuniform velocity fields: Code verification using an advective reactive streamtube approach. *Journal of Contaminant Hydrology*, 30(3-4): 299–331, 1998.

Yabusaki, S. B., Fang, Y., Long, P. E., Resch, C. T., Peacock, A. D., Komlos, J., Jaffe, P. R., Morrison, S. J., Dayvault, R. D., White, D. C., et al. Uranium removal from groundwater via *in situ* biostimulation: Field-scale modeling of transport and biological processes. *Journal of Contaminant Hydrology*, 93(1-4):216–235, 2007.

Yabusaki, S. B., Fang, Y., Williams, K. H., Murray, C. J., Ward, A. L., Dayvault, R. D., Waichler, S. R., Newcomer, D. R., Spane, F. A., and Long, P. E. Variably saturated flow and multicomponent biogeochemical reactive transport modeling of a uranium bioremediation field experiment. *Journal of Contaminant Hydrology*, 126(3-4):271–290, 2011.

Yabusaki, S. B., Wilkins, M. J., Fang, Y., Williams, K. H., Arora, B., Bargar, J., Beller, H. R., Bouskill, N. J., Brodie, E. L., Christensen, J. N., et al. Water table dynamics and biogeochemical cycling in a shallow, variably-saturated floodplain. *Environmental Science & Technology*, 51(6):3307–3317, 2017.

Yan, J., Wang, L., Hu, Y., Tsang, Y. F., Zhang, Y., Wu, J., Fu, X., and Sun, Y. Plant litter composition selects different soil microbial structures and in turn drives different litter decomposition pattern and soil carbon sequestration capability. *Geoderma*, 319: 194–203, 2018.

Zachara, J., Cowan, C., Schmidt, R., and Ainsworth, C. Chromate adsorption by kaolinite. *Clays and Clay Minerals*, 36(4):317–326, 1988.

Zachara, J., Fredrickson, J., Li, S., Kennedy, D., Smith, S., and Gassman, P. Bacterial reduction of crystalline Fe^{3+} oxides in single phase suspensions and subsurface materials. *The American Mineralogist*, 83(B):11–12:1426–1443, 1995.

Zachara, J. M., Girvin, D. C., Schmidt, R. L., and Resch, C. T. Chromate adsorption on amorphous iron oxyhydroxide in the presence of major groundwater ions. *Environmental Science & Technology*, 21(6):589–594, 1987.

Zachara, J. M., Fredrickson, J. K., Li, S.-M., Kennedy, D. W., Smith, S. C., and Gassman, P. L. Bacterial reduction of crystalline Fe(super 3+) oxides in single phase suspensions and subsurface materials. *American mineralogist*, 83(11-12_Part_2):1426–1443, 1998.

Zachara, J. M., Smith, S. C., Liu, C., McKinley, J. P., Serne, R. J., and Gassman, P. L. Sorption of Cs^+ to micaceous subsurface sediments from the Hanford site, USA. *Geochimica et Cosmochimica Acta*, 66(2):193–211, 2002.

Zachara, J. M., Long, P. E., Bargar, J., Davis, J. A., Fox, P., Fredrickson, J. K., Freshley, M. D., Konopka, A. E., Liu, C., McKinley, J. P., et al. Persistence of uranium groundwater plumes: Contrasting mechanisms at two DOE sites in the groundwater–river interaction zone. *Journal of Contaminant Hydrology*, 147:45–72, 2013.

Zachara, J. M., Chen, X., Song, X., Shuai, P., Murray, C., and Resch, C. T. Kilometer-scale hydrologic exchange flows in a gravel bed river corridor and their implications to solute migration. *Water Resources Research*, 56(2):e2019WR025258, 2020.

Zaunbrecher, L. K., Cygan, R. T., and Elliott, W. C. Molecular models of cesium and rubidium adsorption on weathered micaceous minerals. *The Journal of Physical Chemistry A*, 119(22):5691–5700, 2015.

Zhang, J., Ma, T., Yan, Y., Xie, X., Abass, O. K., Liu, C., Zhao, Z., and Wang, Z. Effects of Fe-S-As coupled redox processes on arsenic mobilization in shallow aquifers of Datong Basin, northern China. *Environmental Pollution*, 237:28–38, 2018.

Zhao, P., Zavarin, M., Leif, R. N., Powell, B. A., Singleton, M. J., Lindvall, R. E., and Kersting, A. B. Mobilization of actinides by dissolved organic compounds at the Nevada Test Site. *Applied Geochemistry*, 26(3):308–318, 2011.

Zhao, P., Zavarin, M., Dai, Z., and Kersting, A. B. Stability of plutonium oxide nanoparticles in the presence of montmorillonite and implications for colloid facilitated transport. *Applied Geochemistry*, 122:104725, 2020.

Zheng, Z., Tokunaga, T. K., and Wan, J. Influence of calcium carbonate on U(VI) sorption to soils. *Environmental Science & Technology*, 37(24):5603–5608, 2003.

Zhuang, K., Izallalen, M., Mouser, P., Richter, H., Risso, C., Mahadevan, R., and Lovley, D. R. Genome-scale dynamic modeling of the competition between *Rhodoferax* and *Geobacter* in anoxic subsurface environments. *The ISME journal*, 5(2):305–316, 2011.

Zyvoloski, G. A., Robinson, B. A., Dash, Z. V., and Trease, L. L. Summary of the models and methods for the FEHM application-a finite-element heat-and mass-transfer code. Technical report, Los Alamos National Lab., NM (US), 1997a.

Zyvoloski, G. A., Robinson, B. A., Dash, Z. V., and Trease, L. L. User's manual for the FEHM application-A finite-element heat-and mass-transfer code. Technical report, Los Alamos National Lab., 1997b.

List of Tables

List of Figures

7. Example demonstrating inadequacy of K_d (linear sorption) models to describe U transport. (A) K_d values for Naturita sediment as a function of partial pressure of CO_2, pH, and solid/liquid ratio (From Davis et al., 2004). (B) Simulated values of field scale dissolved U, alkalinity, and spatially variable K_d at the Naturita site (From Curtis et al., 2006).

8. Acetate injection-induced reduction and immobilization of U^{VI} at the Rifle site. (A) Well layout for the 2008 field experiment at the Rifle site (from Yabusaki et al., 2011). (B) Comparison of simulated (red solid line) and observed dissolved U^{VI} in groundwater as monitored during 2008 acetate injection experiment (from Yabusaki et al., 2011). (C) Comparison of column experimental data (symbols) and 1D reactive transport modeling (from Li et al., 2009).

9. Filter passing total Hg (A) and MeHg (B) along EFPC sampled under baseflow conditions as a function of season. Creek flow is from left to right. Smoothed curves are added to help visualize the data.

10. Flood hydrograph from EFPC illustrating (A) creek discharge and specific conductance as a proxy measure of dissolved ions, and (B) dissolved MeHg and DO dynamics before, during, and after the storm event. The specific conductance mirrors the flood hydrograph diluting during higher flow and returning to pre-flood levels approximately one and a half days after the start of the flood. In contrast, DO and $MeHg_D$ do not return to pre-flood conditions until ten days after the flood start (from Riscassi et al., 2016).

11. Hg methylation (production of $Me^{201}Hg$) and MeHg demethylation (loss of $Me^{202}Hg$) by periphyton biofilms over time. Samples were grown in winter and incubated at ambient stream temperature. These biofilms are a net positive source of MeHg to the creek (from Olsen et al., 2016).

12. Several scale-aware constructs have emerged over the years to tackle scale and complexity of ecosystem processes. Examples illustrate multiresolution mesh, HSHMs, and functional zonation. Zoomed-in view of the mesh figure courtesy of Ilhan Özgen-Xian (LBNL).

13. Word cloud shows a spectrum of science topics covered through DOE research over the past two decades. Font sizes show topical importance.

Table 1: *Geologic and Climatologic Variability Across the DOE Sites (National Research Council, 2000; Zachara et al., 2013; Dam et al., 2015; Dwivedi et al., 2018b)*

DOE Site	Research Focus	Climate	Geology and Hydrogeology	Surface Water Body	Approximate Depth to Groundwater
Savannah River Site	Wetland hydro-biogeochemistry	Humid, subtropical; average annual rainfall 122 cm	Atlantic Coastal Plain with clay soils; the strata are deeply dissected by creeks, and most groundwater eventually seeps into and is diluted by creeks.	Savannah River and its tributaries	0 m to 46 m
Oak Ridge Reservation	Stream corridor hydro-biogeochemistry	Humid, typical of the southern Appalachian region; average annual rainfall 138 cm	Valley and ridge province bordering the Cumberland Plateau; primary porosity is low, but fracture porosity present; high clay content; shallow water table.	Clinch River	1 m to 37 m
Hanford Site	River corridor eco-hydro-biogeochemistry	Arid, cool, mild winters and warm summers; average rainfall 16 cm	Alluvial plain of bedded sediments with sands and gravels; Groundwater flows toward the Columbia River.	Columbia River	10 m to 90 m
Nevada National Security Site	Hydro-biogeochemistry of actinides	Arid, mild winters and warm summers; average rainfall 13-32 cm	Alluvium, volcanic, and carbonate geology that is part of the Death Valley regional flow system.	Ephemeral streams, transient ponding, springs	210 m to 610 m
Riverton Site	Floodplain hydro-biogochemistry	Arid to semi-arid, steppe; average annual rainfall 25 cm	Gravel bed alluvial floodplain overlain by redox-active fine sediments; Wind River Formation.	Little Wind River	0 m to 2.5 m
Rifle Site	Contaminants, C and N cycling	Semiarid; average annual rainfall 35 cm	Wasatch Formation overlain by Quaternary floodplain deposit.	Colorado River	1 m to 5 m
East River	Watershed function	Arid to semiarid; annual rainfall 30 cm and 70-90 cm as snow	A diverse suite of Paleozoic and Mesozoic sedimentary rocks intruded by Tertiary igneous laccoliths and ore-rich stocks; Cretaceous Mancos Shale bedrock overlain by glacial moraine deposits.	East River and several tributaries representative of a headwater system	0 m to 100 m

Table 2: *Examples of HSHMs in the Context of Ecosystem Control Points*

Examples	Study	Type of ecosystem control point
Storm events constituted hot moments of Hg and MeHg in EFPC and U discharge in Tims Branch, resulting in orders-of-magnitude higher concentrations than observed during baseflow conditions	Riscassi et al. (2016) Batson et al. (1996)	Activated control points
Seasonal river stage fluctuations of more than 2 m resulted in U hot moments at the Hanford site by promoting water intrusion and increasing residence times	Zachara et al. (2020)	Activated control points
Naturally reduced zones or zones enriched with Fe and S minerals in sediments adjacent to the riverbanks at the Rifle floodplain site constituted hot spots of C, N, S, and U	Arora et al. (2016a) Dwivedi et al. (2018a) Wainwright et al. (2016b) Noël et al. (2017b) Boye et al. (2017) Janot et al. (2016) Campbell et al. (2012)	Permanent control points
Seasonal meltwater-driven water-table rise at the Rifle floodplain site creates short-lived carbonate solutes (calcium ions) for 2-week, but intense oxidizing hot moments, during which the majority of annual U oxidation occurs	Lezama-Pacheco et al. (2015)	Activated control points
Microtopographic features such as low-centered polygons act as CH_4 hot spots in arctic tundra environments and have a significant impact on ecosystem-scale C fluxes	Arora et al. (2019c) Vaughn et al. (2016)	Activated control points
Meander acts as a sink for organic and inorganic C as well as Fe during the extended baseflow and high-water conditions	Dwivedi et al. (2018b)	Export control points
Microtopographic features such as gullies at the East River floodplain exert significant impacts on redox processes in the hyporheic zone and thereby controlling subsurface geochemical exports of Fe and C	Dwivedi et al. (2018b) Rogers et al. (2021)	Transport control points

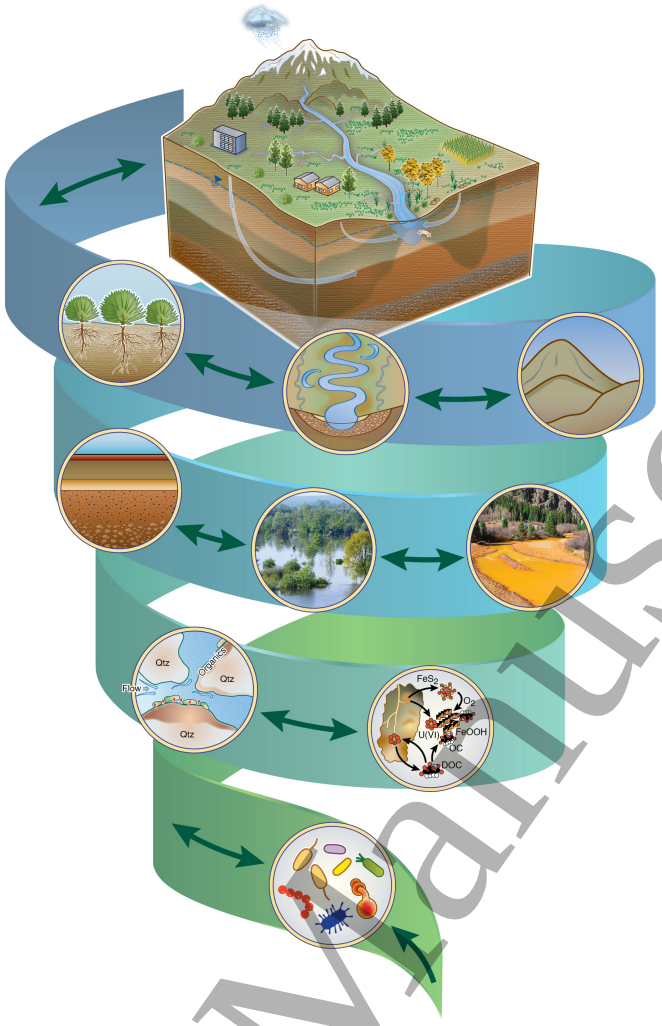

Figure 1: *The spiral shows the progression of DOE-supported science that evolved in both scale and complexity. Significant scientific progress has been achieved from fundamental subsurface microbiology to geochemistry and biogeochemistry to hydro-biogeochemistry and now to eco-hydro-biogeochemistry over the past two decades.*

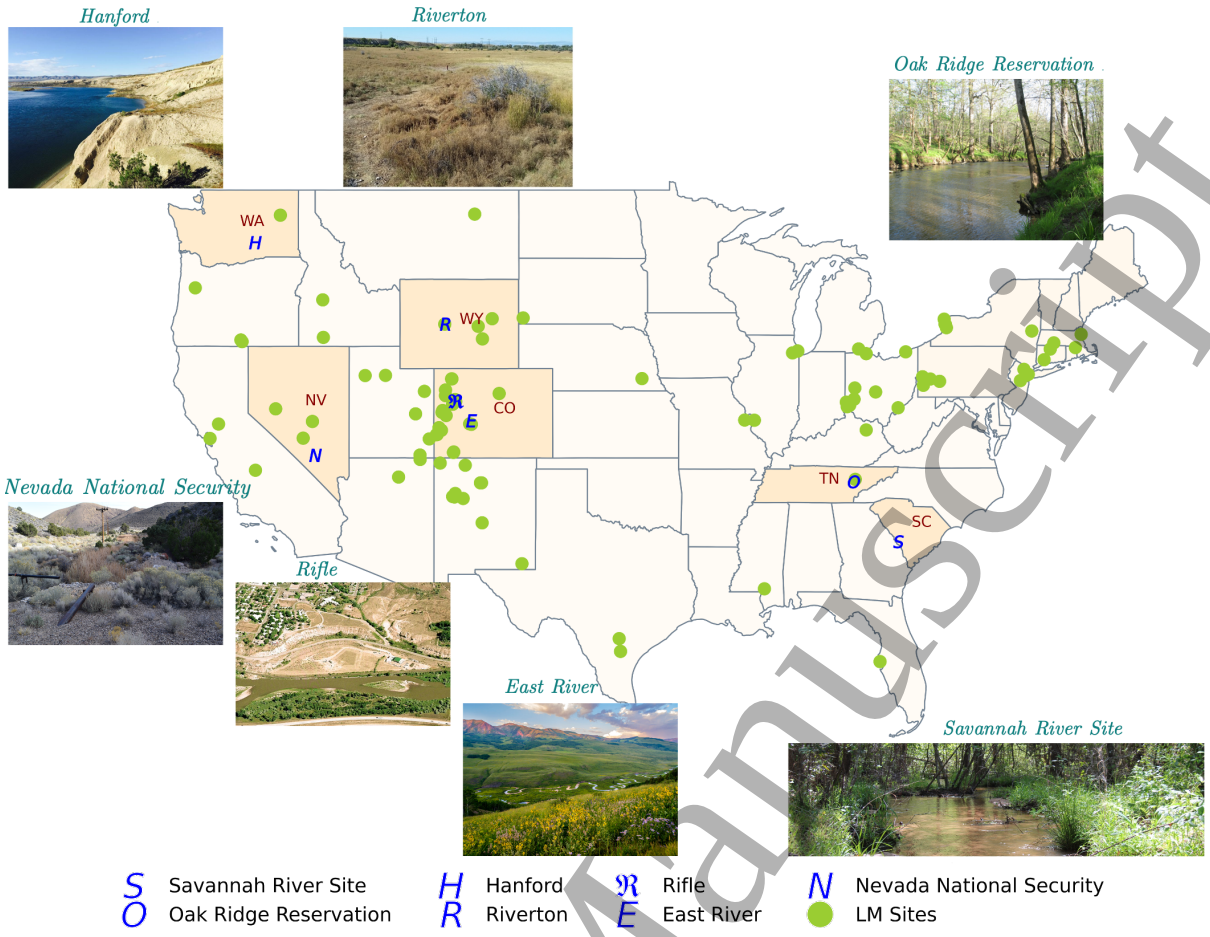

Figure 2: *The DOE's EM and ER programs have been responsible for the restoration of as many as 107 sites across the country. The sites also exist outside the contiguous states in the USA (not shown here). Here we show only DOE-LM sites to demonstrate the extent of DOE cleanup activities spreading across the nation. In this review, we chose seven representative DOE sites and testbeds, including Savannah River Site in South Carolina, Oak Ridge Reservation in Tennessee, Hanford in Washington, Nevada National Security in Nevada, Riverton in Wyoming, and Rifle and East River in Colorado. Note that the Riverton and Rifle are DOE-LM sites, whereas the Savannah River Site, Oak Ridge Reservation, Hanford, and Nevada National Security are DOE-EM sites. The East River is not associated with any DOE historical contamination site. We have synthesized these seven sites as representative DOE sites and testbeds in this review.*

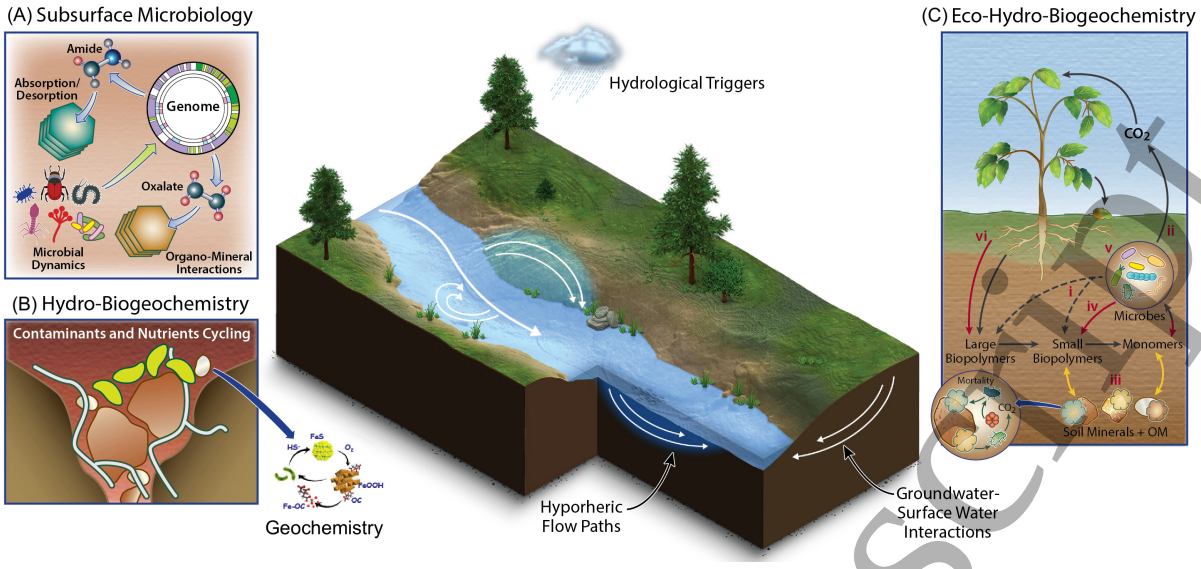

Figure 3: *Schematic depiction of processes within (A) subsurface microbiology (B) geochemistry, biogeochemistry, and hydro-biogeochemistry, and (C) eco-hydro-biogeochemistry. These processes are intimately coupled, and their aggregated responses drive ecosystem function. These processes occur from the genome to watershed scales, and perturbations such as hydrologic triggers lead to the formation of HSHMs through groundwater–surface water interactions, particularly hyporheic flow paths.*

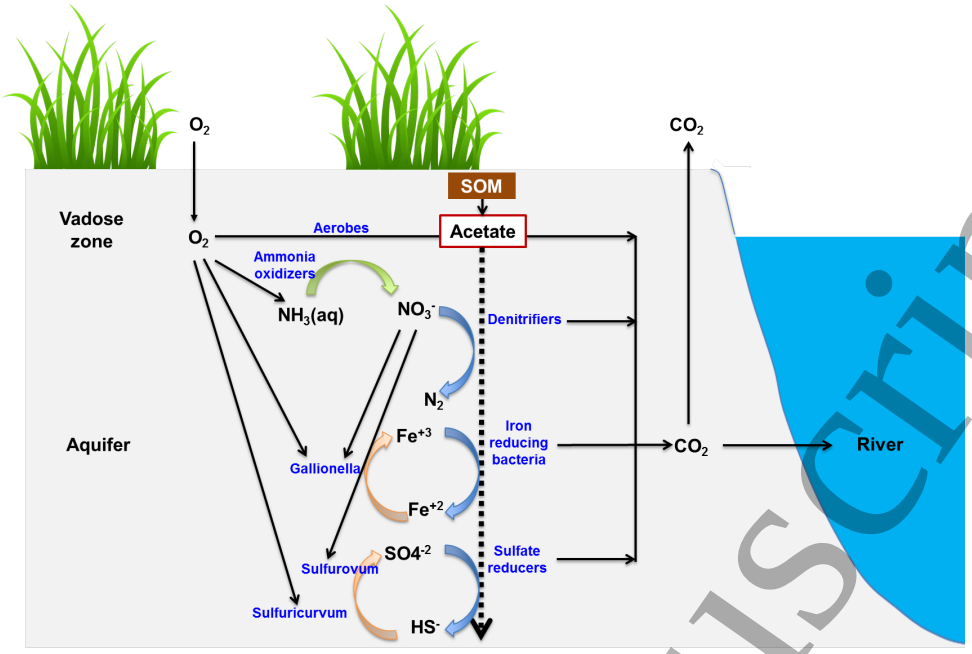

Figure 4: *Example of a biogeochemical reaction network used to simulate processes in the Rifle flood plain (from Arora et al., 2016b).*

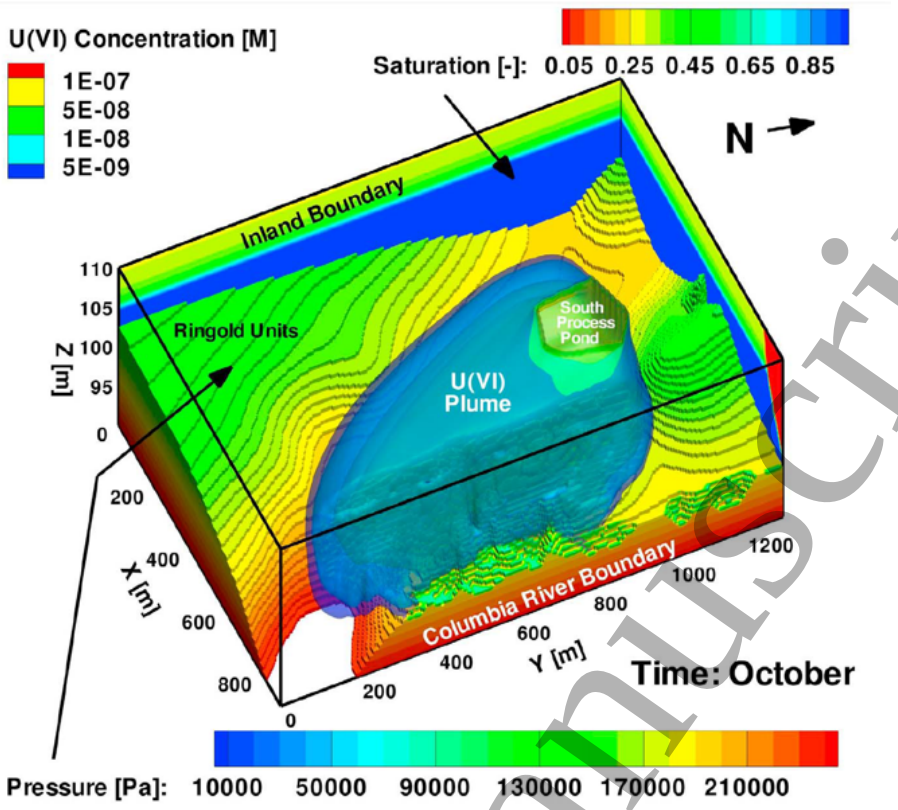

Figure 5: *Example of a 3D flow and reactive transport simulation of the Hanford 300 area, with hydrological and geochemical transients driven by changing water stages in the Columbia River (from Hammond and Lichtner, 2010).*

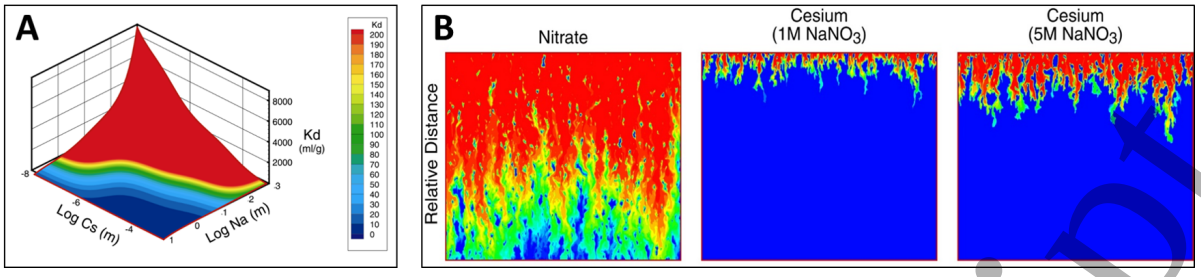

Figure 6: *Example of ^{137}Cs transport in the Hanford 200 Area tank farm. (A) Effective linear distribution coefficient (K_d) for Cs^+ (from Steefel et al., 2003). The K_d depends on both the competing cation concentration (Na^+ associated with $NaNO_3$ in the tank wastes), and on Cs^+ itself because of the presence of at least two sites with different selectivities for Cs^+ versus Na^+; (B) Relative migration of nitrate (nonreactive), and Cs^+ at 1 M $NaNO_3$ and 5 M $NaNO_3$. The high Na^+ concentrations in the tank leak explain the enhanced migration and thus weaker-than-expected retardation of ^{137}Cs at the Hanford 200 tanks (From Steefel et al., 2005).*

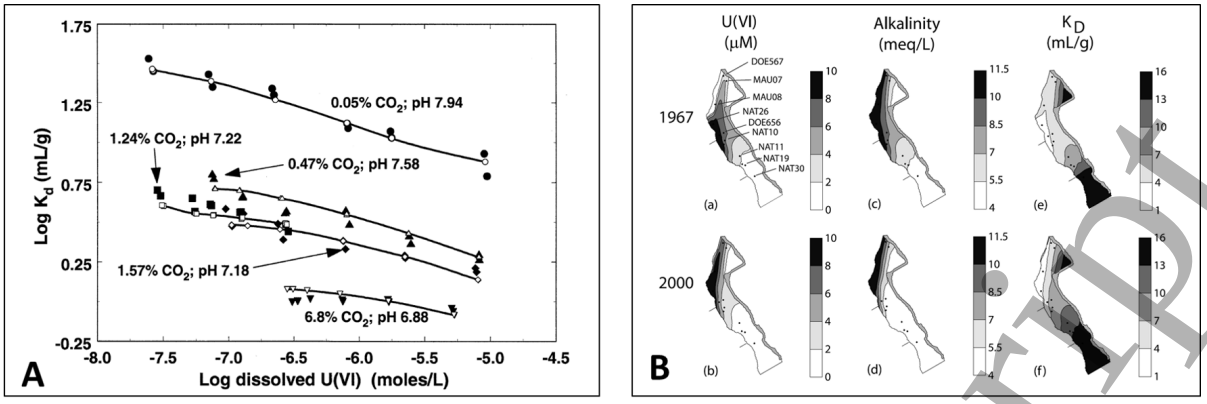

Figure 7: *Example demonstrating inadequacy of* K_d *(linear sorption) models to describe U transport. (A)* K_d *values for Naturita sediment as a function of partial pressure of* CO_2*, pH, and solid/liquid ratio (From Davis et al., 2004). (B) Simulated values of field scale dissolved U, alkalinity, and spatially variable* K_d *at the Naturita site (From Curtis et al., 2006).*

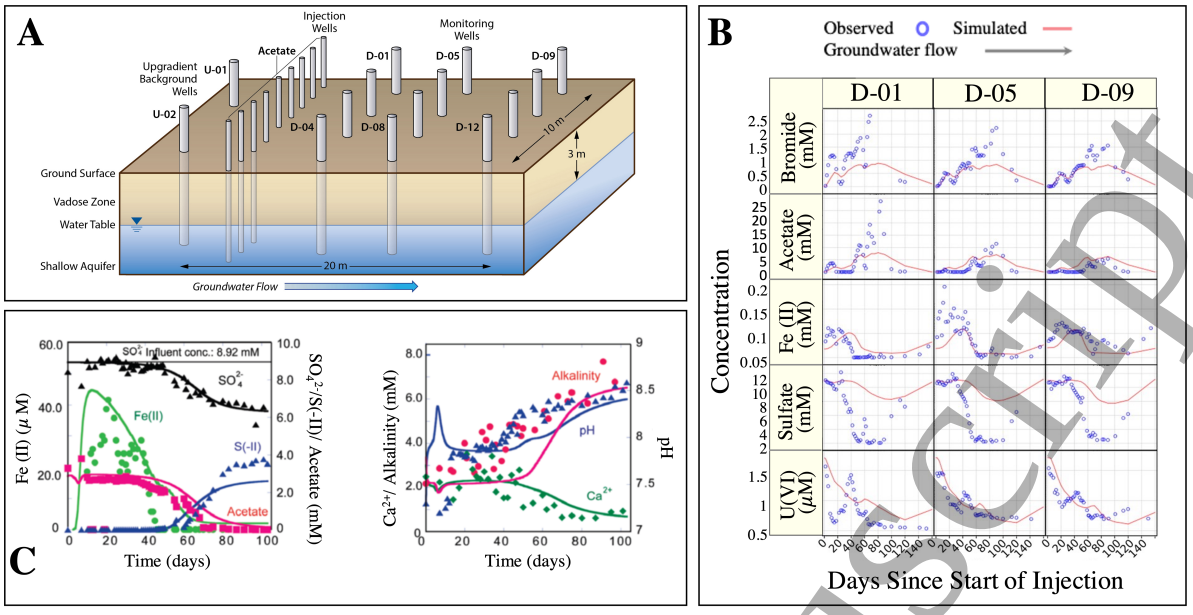

Figure 8: *Acetate injection-induced reduction and immobilization of U^{VI} at the Rifle site. (A) Well layout for the 2008 field experiment at the Rifle site (from Yabusaki et al., 2011). (B) Comparison of simulated (red solid line) and observed dissolved U^{VI} in groundwater as monitored during 2008 acetate injection experiment (from Yabusaki et al., 2011). (C) Comparison of column experimental data (symbols) and 1D reactive transport modeling (from Li et al., 2009).*

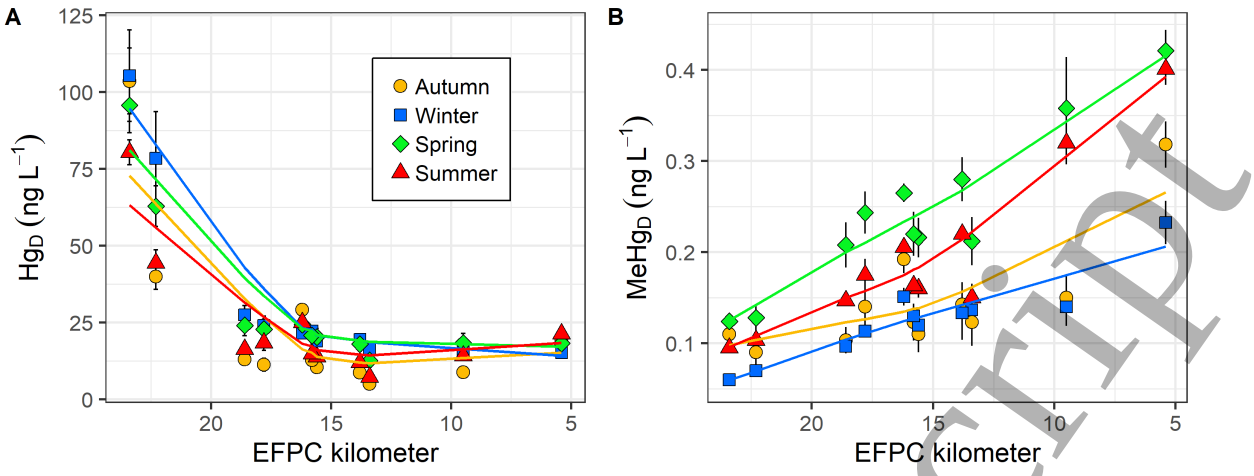

Figure 9: *Filter passing total Hg (A) and MeHg (B) along EFPC sampled under baseflow conditions as a function of season. Creek flow is from left to right. Smoothed curves are added to help visualize the data.*

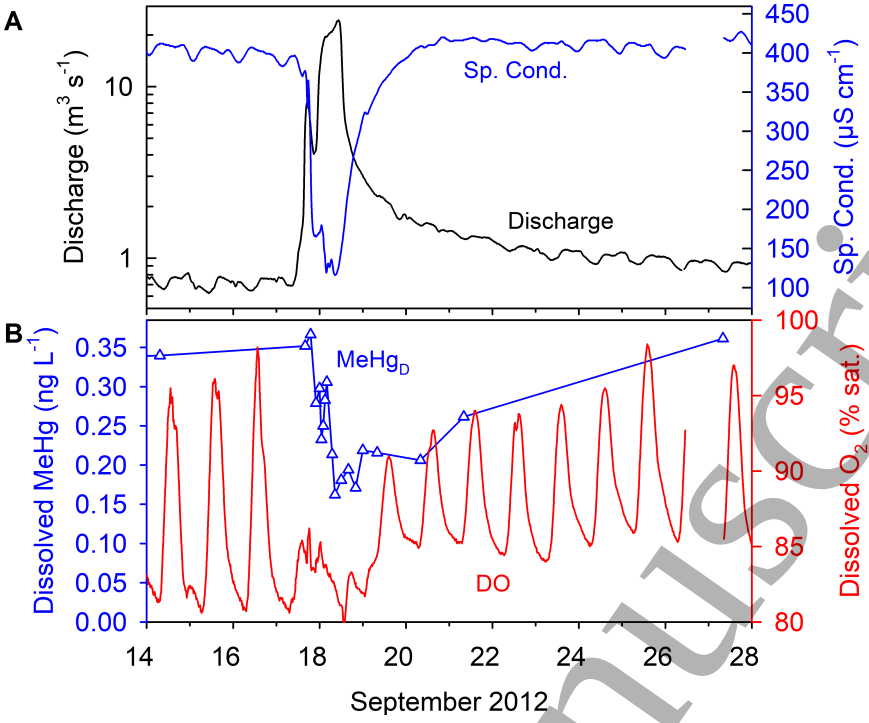

Figure 10: *Flood hydrograph from EFPC illustrating (A) creek discharge and specific conductance as a proxy measure of dissolved ions, and (B) dissolved MeHg and DO dynamics before, during, and after the storm event. The specific conductance mirrors the flood hydrograph diluting during higher flow and returning to pre-flood levels approximately one and a half days after the start of the flood. In contrast, DO and $MeHg_D$ do not return to pre-flood conditions until ten days after the flood start (from Riscassi et al., 2016).*

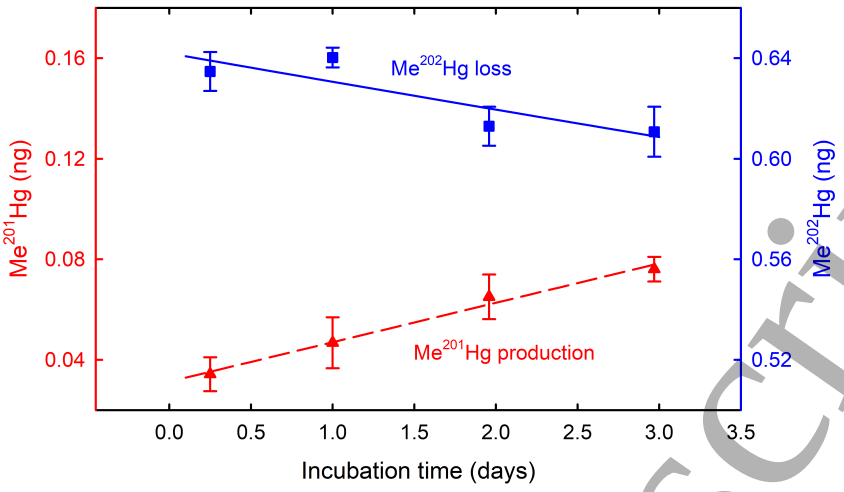

Figure 11: *Hg methylation (production of $Me^{201}Hg$) and MeHg demethylation (loss of $Me^{202}Hg$) by periphyton biofilms over time. Samples were grown in winter and incubated at ambient stream temperature. These biofilms are a net positive source of MeHg to the creek (from Olsen et al., 2016).*

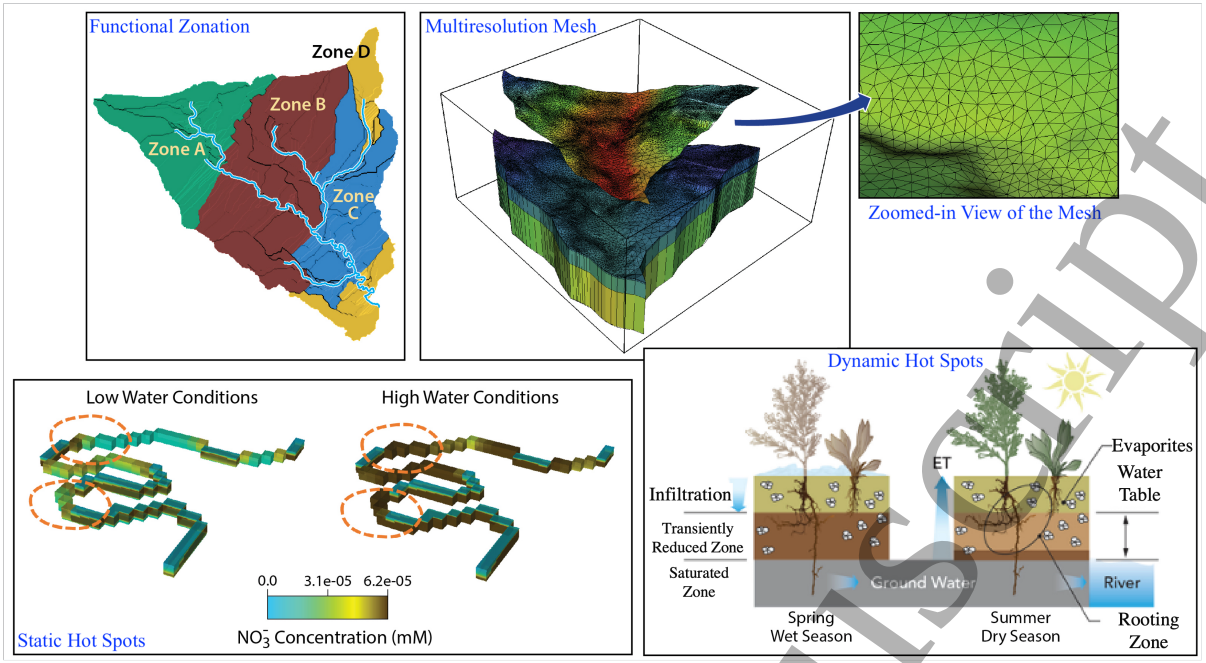

Figure 12: *Several scale-aware constructs have emerged over the years to tackle scale and complexity of ecosystem processes. Examples illustrate multiresolution mesh, HSHMs, and functional zonation. Zoomed-in view of the mesh figure courtesy of Ilhan Özgen-Xian (LBNL).*

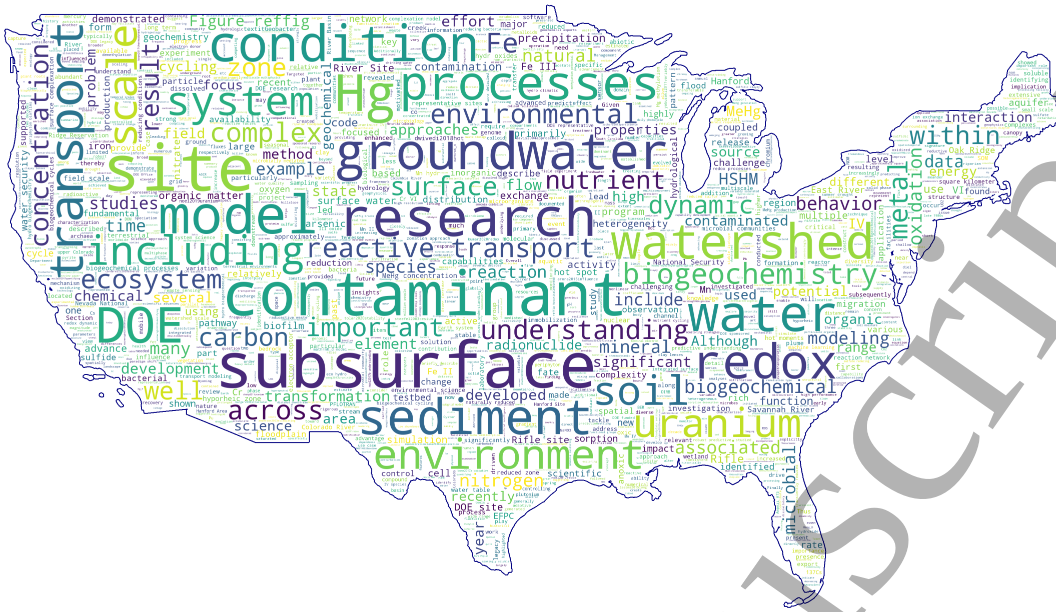

Figure 13: *Word cloud shows a spectrum of science topics covered through DOE research over the past two decades. Font sizes show topical importance.*